PHYSICAL REVIEW D **82,** 114511 (2010)

Perturbative and nonperturbative renormalization in lattice QCD

M. Göckeler,[1] R. Horsley,[2] Y. Nakamura,[1,*] H. Perlt,[3] D. Pleiter,[4] P. E. L. Rakow,[5] A. Schäfer,[1] G. Schierholz,[1,6] A. Schiller,[3] H. Stüben,[7] and J. M. Zanotti[2]

(QCDSF/UKQCD Collaborations)

[1]*Institut für Theoretische Physik, Universität Regensburg, 93040 Regensburg, Germany*
[2]*School of Physics and Astronomy, University of Edinburgh, Edinburgh EH9 3JZ, UK*
[3]*Institut für Theoretische Physik, Universität Leipzig, 04109 Leipzig, Germany*
[4]*Deutsches Elektronen-Synchrotron DESY and John von Neumann-Institut für Computing NIC, 15738 Zeuthen, Germany*
[5]*Theoretical Physics Division, Department of Mathematical Sciences, University of Liverpool, Liverpool L69 3BX, UK*
[6]*Deutsches Elektronen-Synchrotron DESY, 22603 Hamburg, Germany*
[7]*Konrad-Zuse-Zentrum für Informationstechnik Berlin, 14195 Berlin, Germany*

(Received 8 April 2010; revised manuscript received 16 August 2010; published 21 December 2010)

We investigate the perturbative and nonperturbative renormalization of composite operators in lattice QCD restricting ourselves to operators that are bilinear in the quark fields (quark-antiquark operators). These include operators which are relevant to the calculation of moments of hadronic structure functions. The nonperturbative computations are based on Monte Carlo simulations with two flavors of clover fermions and utilize the Rome-Southampton method also known as the regularization independent momentum or RI-MOM scheme. We compare the results of this approach with various estimates from lattice perturbation theory, in particular, with recent two-loop calculations.

DOI: 10.1103/PhysRevD.82.114511 PACS numbers: 12.38.Gc, 11.10.Gh

I. INTRODUCTION

The investigation of hadron structure has become a central topic of lattice QCD. In many cases this involves the evaluation of matrix elements of local operators between hadron states. For example, (moments of) generalized parton distributions can be extracted from matrix elements of quark-antiquark operators, i.e., operators composed of a quark field, its adjoint, and a number of gluon fields entering through covariant derivatives which act on the quark fields. In general such operators have to be renormalized. In this process the operator of interest may receive contributions also from other operators, i.e., it may mix with these additional operators. On the lattice, mixing occurs more frequently than in the continuum due to the restricted space-time symmetries. Since in the end one wants to make contact with phenomenological studies, which almost exclusively refer to operators renormalized in the $\overline{\text{MS}}$ scheme of dimensional regularization, one needs the renormalization factors leading from the bare operators on the lattice to the $\overline{\text{MS}}$ operators in the continuum.

The most straightforward approach toward the calculation of renormalization factors is based on lattice perturbation theory (for a review see Ref. [1]). Unfortunately, this method meets with some difficulties. First, perturbation theory on the lattice is computationally much more complex than in the continuum and therefore the calculations rarely extend beyond one-loop order (see, however, Refs. [2–4]). Second, lattice perturbation theory usually converges rather slowly so that the accuracy of perturbative renormalization factors is limited. Identifying one source of these poor convergence properties, Lepage and Mackenzie proposed as a remedy the so-called tadpole-improved perturbation theory [5]. Still, considerable uncertainty remains. Third, mixing with operators of lower dimension cannot be treated by perturbation theory.

In special cases, when the renormalization factors contain no ultraviolet divergences, a nonperturbative determination is possible with the help of Ward identities [6]. However, there are many interesting operators that cannot be renormalized by this method.

A general nonperturbative approach to renormalization has been developed within the Schrödinger functional scheme (see, e.g., Refs. [7,8]; reviews are given in Refs. [9,10]). In this method the finite size of the lattices employed in the simulations (along with appropriate boundary conditions in Euclidean time) is used to set the renormalization scale. In the end continuum perturbation theory is employed to convert the results from the Schrödinger functional scheme to the $\overline{\text{MS}}$ scheme. Though theoretically appealing the practical implementation of the procedure requires a lot of effort and has to be repeated for every new operator again from the very beginning.

Another nonperturbative method for computing renormalization coefficients of arbitrary quark-antiquark operators is the Rome-Southampton method (also known as the regularization independent momentum or RI-MOM

*Present address: Center for Computational Sciences, University of Tsukuba, Tsukuba, Ibaraki 305-8577, Japan

scheme) introduced in Ref. [11]. It mimics the procedure used in continuum perturbation theory. The basic objects are quark two-point functions with an insertion of the operator under consideration at momentum zero. These are computed in a suitable gauge, e.g., the Landau gauge. In continuum perturbation theory the two-point functions are calculated order by order in an expansion in powers of the strong coupling constant while in the Rome-Southampton method they are evaluated within a Monte Carlo simulation on the lattice. In order to extract from these data renormalization factors which yield renormalized operators in the $\overline{\mathrm{MS}}$ scheme in the continuum limit one needs a renormalization condition which is applicable to lattice data as well as to perturbative continuum results. A suitable condition has been given in Ref. [11].

Compared with the Schrödinger functional approach the Rome-Southampton method is distinguished by its relatively simple implementation. Furthermore, one can deal with all desired operators in a single simulation. On the other hand, the Schrödinger functional method is explicitly gauge invariant, while the Rome-Southampton method requires gauge fixing.

In a previous publication [12] we have performed an extensive study of nonperturbative renormalization for a variety of quark-antiquark operators using the Rome-Southampton method, motivated by our investigations of hadron structure functions. This was done with Wilson fermions in the quenched approximation for two values of the lattice spacing. Later on, these studies have been extended to improved Wilson fermions, based on quenched simulations at three values of the lattice spacing [13]. Meanwhile we are using gauge field configurations generated with two flavors of dynamical quarks, which has made a reconsideration of renormalization necessary.

In this paper we present results for renormalization factors obtained within the Rome-Southampton approach with $n_f = 2$ dynamical quarks. We work with nonperturbatively $O(a)$-improved Wilson fermions (clover fermions). The operators are, however, not (yet) improved. We continue to apply the momentum sources introduced in Ref. [12]. In addition, we have refined our approach, subtracting lattice artifacts through one-loop boosted perturbation theory. As in Ref. [12] we consider only flavor-nonsinglet quark-antiquark operators. For some thoughts concerning flavor-singlet operators see Refs. [14,15].

The paper is organized as follows: After introducing in Sec. II the operators to be studied we explain the method of nonperturbative renormalization in Sec. III. Our implementation of this method employing momentum sources is described in Sec. IV. After a brief overview of our gauge field configurations in Sec. V we discuss the chiral extrapolation of our data in Sec. VI. Section VII reviews formulas from continuum perturbation theory that will be needed in the analysis. Results from lattice perturbation theory are compiled in Sec. VIII. Section IX explains how we apply lattice perturbation theory in order to subtract lattice artifacts. In Sec. X we describe our method of extracting the renormalization factors from the Monte Carlo data. The results (perturbative as well as nonperturbative) are then presented and discussed in Sec. XI. Finally, we present our conclusions in Sec. XII. Some technical details are explained in the appendixes.

II. THE OPERATORS

In the Euclidean continuum we want to study the operators

$$\mathcal{O}_{\mu\mu_1\ldots\mu_n} = \bar{u}\gamma_\mu \overleftrightarrow{D}_{\mu_1}\ldots\overleftrightarrow{D}_{\mu_n} d, \tag{1}$$

$$\mathcal{O}^5_{\mu\mu_1\ldots\mu_n} = \bar{u}\gamma_\mu\gamma_5 \overleftrightarrow{D}_{\mu_1}\ldots\overleftrightarrow{D}_{\mu_n} d, \tag{2}$$

$$\mathcal{O}^T_{\mu\nu\mu_1\ldots\mu_n} = \bar{u}\sigma_{\mu\nu} \overleftrightarrow{D}_{\mu_1}\ldots\overleftrightarrow{D}_{\mu_n} d \tag{3}$$

(with $\sigma_{\mu\nu} = (\mathrm{i}/2)[\gamma_\mu, \gamma_\nu]$ and $\overleftrightarrow{D}_\mu = \overrightarrow{D}_\mu - \overleftarrow{D}_\mu$) or rather $O(4)$ irreducible multiplets with definite charge conjugation parity. In particular, we obtain twist-2 operators by symmetrizing the indices and subtracting the traces. We have given the quark fields definite flavors (assumed to be degenerate) in order to make apparent that we are considering the flavor-nonsinglet case. Hence the twist-2 operators do not mix and are multiplicatively renormalizable.

Working with Wilson fermions it is straightforward to write down lattice versions of the above operators. One simply replaces the continuum covariant derivative by its lattice analogue. However, $O(4)$ being restricted to its finite subgroup $H(4)$ (the hypercubic group) on the lattice, the constraints imposed by space-time symmetry are less stringent than in the continuum and the possibilities for mixing increase [16–19].

While the $H(4)$ classification for operators $\mathcal{O}_{\mu\mu_1\ldots\mu_n}$ and $\mathcal{O}^5_{\mu\mu_1\ldots\mu_n}$ with $n \leq 3$ has been treated in detail in Ref. [18], we have to refer to Ref. [20] for the operators $\mathcal{O}^T_{\mu\nu\mu_1\ldots\mu_n}$. Note however that the classification of the latter operators for $n \leq 2$ can be derived from the results presented in Ref. [18].

In our investigations of hadronic matrix elements we have considered the following operators whose renormalization factors have already been studied in Ref. [12]:

$$\mathcal{O}_{v_{2,a}} = \mathcal{O}_{\{14\}}, \tag{4}$$

$$\mathcal{O}_{v_{2,b}} = \mathcal{O}_{\{44\}} - \frac{1}{3}(\mathcal{O}_{\{11\}} + \mathcal{O}_{\{22\}} + \mathcal{O}_{\{33\}}), \tag{5}$$

$$\mathcal{O}_{v_3} = \mathcal{O}_{\{114\}} - \frac{1}{2}(\mathcal{O}_{\{224\}} + \mathcal{O}_{\{334\}}), \tag{6}$$

$$\mathcal{O}_{v_4} = \mathcal{O}_{\{1144\}} + \mathcal{O}_{\{2233\}} - \mathcal{O}_{\{1133\}} - \mathcal{O}_{\{2244\}}, \tag{7}$$

$$\mathcal{O}_{a_2} = \mathcal{O}^5_{\{124\}}, \tag{8}$$

$$\mathcal{O}_{r_{2,a}} = \mathcal{O}^5_{\{14\}}, \tag{9}$$

$$\mathcal{O}_{r_{2,b}} = \mathcal{O}^5_{\{44\}} - \frac{1}{3}(\mathcal{O}^5_{\{11\}} + \mathcal{O}^5_{\{22\}} + \mathcal{O}^5_{\{33\}}), \tag{10}$$

$$\mathcal{O}_{r_3} = \mathcal{O}^5_{\{114\}} - \frac{1}{2}(\mathcal{O}^5_{\{224\}} + \mathcal{O}^5_{\{334\}}). \tag{11}$$

Their labels refer to the structure function moments that they determine. These operators have been selected such that they have a definite transformation behavior under $H(4)$ (i.e., belong to an irreducible multiplet) with as little mixing as possible. Moreover we have tried to minimize the number of nonzero momentum components required in the evaluation of the hadronic matrix elements. Note, however, that in the numerical simulations reported in Ref. [13] different operators [though from the same $H(4)$ multiplets] have been used for the matrix elements v_3 and v_4.

The operators $\mathcal{O}_{v_{2,a}}$ and $\mathcal{O}_{v_{2,b}}$ transform according to inequivalent representations of $H(4)$, although they belong to the same irreducible $O(4)$ multiplet in the continuum. Therefore their renormalization factors calculated on the lattice need not coincide. The same remark applies to $\mathcal{O}_{r_{2,a}}$ and $\mathcal{O}_{r_{2,b}}$.

Since our matrix element calculations now involve additional operators, not considered in Ref. [12], we have extended the above list by the following operators, again guided by the $H(4)$ classification given in Refs. [18,20]:

$$\mathcal{O}_{v_{3,a}} = \mathcal{O}_{\{124\}}, \tag{12}$$

$$\mathcal{O}_{h_{1,a}} = \mathcal{O}^T_{1\{23\}}, \tag{13}$$

$$\mathcal{O}_{h_{1,b}} = \mathcal{O}^T_{122} - \mathcal{O}^T_{133}, \tag{14}$$

$$\mathcal{O}_{h_{2,a}} = \mathcal{O}^T_{4\{123\}}, \tag{15}$$

$$\mathcal{O}_{h_{2,b}} = \mathcal{O}^T_{1\{122\}} - \mathcal{O}^T_{1\{133\}} + \mathcal{O}^T_{2\{233\}}, \tag{16}$$

$$\mathcal{O}_{h_{2,c}} = \mathcal{O}^T_{13\{23\}} + \mathcal{O}^T_{23\{13\}} + \mathcal{O}^T_{41\{24\}} + \mathcal{O}^T_{42\{14\}}, \tag{17}$$

$$\mathcal{O}_{h_{2,d}} = \mathcal{O}^T_{1211} - \mathcal{O}^T_{1222} + \mathcal{O}^T_{13\{23\}} + \mathcal{O}^T_{23\{13\}} - \mathcal{O}^T_{41\{24\}} - \mathcal{O}^T_{42\{14\}}. \tag{18}$$

The operator $\mathcal{O}_{v_{3,a}}$ yields the same structure function moment as $\mathcal{O}_{v_3}$. However, in contrast to $\mathcal{O}_{v_3}$ it cannot mix with any operator of the same or lower dimension. On the other hand, it has the disadvantage that one needs spatial momenta with two nonvanishing components in order to extract the moment v_3 from its matrix elements. The latter fact is the reason why we did not employ it in our previous investigations of nucleon structure. The operators constructed from $\mathcal{O}^T_{\ldots}$ are relevant for transversity.

Furthermore, we have studied the following operators without derivatives ("currents"):

$$\mathcal{O}^S = \bar{u}d, \tag{19}$$

$$\mathcal{O}^P = \bar{u}\gamma_5 d, \tag{20}$$

$$\mathcal{O}^V_\mu = \bar{u}\gamma_\mu d, \tag{21}$$

$$\mathcal{O}^A_\mu = \bar{u}\gamma_\mu\gamma_5 d, \tag{22}$$

$$\mathcal{O}^T_{\mu\nu} = \bar{u}\sigma_{\mu\nu} d, \tag{23}$$

where all quark fields are taken at the same lattice point. Finally we have also considered the quark wave function renormalization constant Z_q.

In Table I we list all operators studied, along with the $H(4)$ representation they belong to and their charge conjugation parity C.

While in the evaluation of hadronic matrix elements the members of a given operator multiplet require different momentum components to be nonzero and hence are of different usefulness, such distinctions do not matter in our computation of renormalization factors. Therefore we consider not only individual operators but also complete operator bases for the representations under study. The representations studied and the chosen bases are given in Appendix A.

Concerning the mixing properties a few remarks are in order. Mixing with operators of equal or lower dimension is excluded for the operators $\mathcal{O}_{v_{2,a}}$, $\mathcal{O}_{v_{2,b}}$, $\mathcal{O}_{v_{3,a}}$, $\mathcal{O}_{a_2}$, $\mathcal{O}_{r_{2,a}}$, $\mathcal{O}_{r_{2,b}}$, $\mathcal{O}_{h_{1,a}}$, $\mathcal{O}_{h_{1,b}}$, $\mathcal{O}_{h_{2,a}}$, $\mathcal{O}_{h_{2,b}}$, $\mathcal{O}_{h_{2,c}}$ as well as for the currents.

TABLE I. Operators and their transformation behavior [18,20]. The charge conjugation parity is denoted by C.

Operator	Representation	C	Operator	Representation	C
$\mathcal{O}^S$	$\tau_1^{(1)}$	$+1$	$\mathcal{O}_{h_{1,b}}$	$\tau_1^{(8)}$	$+1$
$\mathcal{O}^P$	$\tau_4^{(1)}$	$+1$	$\mathcal{O}_{v_3}$	$\tau_1^{(8)}$	-1
$\mathcal{O}^V_\mu$	$\tau_1^{(4)}$	-1	$\mathcal{O}_{v_{3,a}}$	$\tau_2^{(4)}$	-1
$\mathcal{O}^A_\mu$	$\tau_4^{(4)}$	$+1$	$\mathcal{O}_{r_3}$	$\tau_2^{(8)}$	$+1$
$\mathcal{O}^T_{\mu\nu}$	$\tau_1^{(6)}$	-1	$\mathcal{O}_{a_2}$	$\tau_3^{(4)}$	$+1$
$\mathcal{O}_{v_{2,a}}$	$\tau_3^{(6)}$	$+1$	$\mathcal{O}_{h_{2,a}}$	$\tau_2^{(3)}$	-1
$\mathcal{O}_{v_{2,b}}$	$\tau_1^{(3)}$	$+1$	$\mathcal{O}_{h_{2,b}}$	$\tau_3^{(3)}$	-1
$\mathcal{O}_{r_{2,a}}$	$\tau_4^{(6)}$	-1	$\mathcal{O}_{h_{2,c}}$	$\tau_2^{(6)}$	-1
$\mathcal{O}_{r_{2,b}}$	$\tau_4^{(3)}$	-1	$\mathcal{O}_{h_{2,d}}$	$\tau_3^{(6)}$	-1
$\mathcal{O}_{h_{1,a}}$	$\tau_2^{(8)}$	$+1$	$\mathcal{O}_{v_4}$	$\tau_1^{(2)}$	$+1$

The case of the operator $\mathcal{O}_{v_3}$, for which there are two further operators with the same dimension and the same transformation behavior, is discussed in Refs. [18,19]. Similarly, $\mathcal{O}_{h_{2,d}}$ could mix with another operator of the same dimension. The operators $\mathcal{O}_{v_4}$, $\mathcal{O}_{r_3}$, on the other hand, could in principle mix not only with operators of the same dimension but also with an operator of one dimension less constructed from $\mathcal{O}^T_{\ldots}$. A few more details on the mixing issue can be found in Ref. [13], in particular in Appendix B.

Our analysis ignores mixing completely. This seems to be justified for $\mathcal{O}_{v_3}$. Here a perturbative calculation gives a rather small mixing coefficient for one of the mixing operators [17,19], whereas the other candidate for mixing does not appear at all in a one-loop calculation of quark matrix elements at momentum transfer zero, because its Born term vanishes in the forward direction. The same is true for all operators of dimension less or equal to 6 which transform identically to $\mathcal{O}_{v_4}$: Their Born terms vanish in forward matrix elements, hence they do not show up in a one-loop calculation at vanishing momentum transfer. In the case of $\mathcal{O}_{r_3}$, however, the mixing with an operator of lower dimension is already visible at the one-loop level even in forward direction. Nevertheless, the nucleon matrix elements of the operators mixing with $\mathcal{O}_{v_3}$ and $\mathcal{O}_{v_4}$ seem to be small, at least in the quenched approximation [13].

III. THE METHOD

We calculate our renormalization constants with the help of the procedure proposed by Martinelli *et al.* [11] (the Rome-Southampton approach). It follows closely the definitions used in (continuum) perturbation theory. We work on a lattice of spacing a and volume V in Euclidean space. For a fixed gauge let

$$G_{\alpha\beta}(p) = \frac{a^{12}}{V}\sum_{x,y,z} \mathrm{e}^{-\mathrm{i}p\cdot(x-y)}\langle u_\alpha(x)\mathcal{O}(z)\bar{d}_\beta(y)\rangle \tag{24}$$

denote the nonamputated quark-quark Green function with one insertion of the operator $\mathcal{O}$ at momentum zero. It is to be considered as a 12×12 matrix in the combined color and Dirac space. The corresponding vertex function (or amputated Green function) is given by

$$\Gamma(p) = S^{-1}(p)G(p)S^{-1}(p), \tag{25}$$

where for $q = u$ or $q = d$

$$S_{\alpha\beta}(p) = \frac{a^8}{V}\sum_{x,y} \mathrm{e}^{-\mathrm{i}p\cdot(x-y)}\langle q_\alpha(x)\bar{q}_\beta(y)\rangle \tag{26}$$

denotes the quark propagator. We define the renormalized vertex function by

$$\Gamma_{\mathrm{R}}(p) = Z_q^{-1}Z\Gamma(p) \tag{27}$$

and fix the renormalization constant Z by imposing the renormalization condition

$$\frac{1}{12}\,\mathrm{tr}(\Gamma_{\mathrm{R}}(p)\Gamma_{\mathrm{Born}}(p)^{-1}) = 1 \tag{28}$$

at $p^2 = \mu_p^2$, where μ_p is the renormalization scale. So Z can be calculated from the relation

$$Z_q^{-1}Z\frac{1}{12}\,\mathrm{tr}(\Gamma(p)\Gamma_{\mathrm{Born}}(p)^{-1}) = 1 \tag{29}$$

with $p^2 = \mu_p^2$. Here $\Gamma_{\mathrm{Born}}(p)$ is the Born term in the vertex function of $\mathcal{O}$ computed on the lattice, and Z_q denotes the quark field renormalization constant. The latter is taken as

$$Z_q(p) = \frac{\mathrm{tr}(-\mathrm{i}\sum_\lambda \gamma_\lambda \sin(ap_\lambda)aS^{-1}(p))}{12\sum_\lambda \sin^2(ap_\lambda)}, \tag{30}$$

again at $p^2 = \mu_p^2$. Aiming at a mass-independent renormalization scheme we finally have to extrapolate the resulting values of Z to the chiral limit.

Note that there will be no $O(a)$ lattice artifacts in Eq. (29), because they come with operators of opposite chirality in the vertex function, and these drop out when the trace is taken. Still, matrix elements of the renormalized operators will in general have $O(a)$ lattice artifacts because the operators are not improved. Once improved operators are available one can evaluate their renormalization factors using the methods described in this paper.

Equations (28) and (30) (in the chiral limit) together define a renormalization scheme of the momentum subtraction type which is called the RI′-MOM scheme [11]. RI stands for ''regularization independent.'' This nomenclature refers to the fact that the definition of the RI′-MOM scheme does not depend on a particular regularization—here we have used a lattice cutoff just for definiteness and because the lattice regularization will be the basis of our numerical investigations. The $\overline{\mathrm{MS}}$ scheme, on the other hand, can only be defined within dimensional regularization and is therefore restricted to perturbation theory.

The RI′-MOM scheme differs from the RI-MOM scheme only in the definition of the quark field renormalization constant, which in the RI′-MOM scheme is more suitable for the numerical evaluation.

In general, the RI′-MOM scheme will not agree with any of the momentum subtraction schemes used in continuum perturbation theory. It is therefore desirable to convert our results to a more popular scheme like the $\overline{\mathrm{MS}}$ scheme. Another reason for converting to the $\overline{\mathrm{MS}}$ scheme lies in the fact that many of the operators discussed in this paper appear in the operator product expansion along with the corresponding Wilson coefficients, which are generally given in the $\overline{\mathrm{MS}}$ scheme. Hence we have to perform a finite renormalization leading us from the RI′-MOM scheme to the $\overline{\mathrm{MS}}$ scheme if we want to use our renormalized operators together with the perturbative Wilson coefficients. This finite renormalization factor can be computed in continuum perturbation theory using, e.g., dimensional

regularization. The details needed for the evaluation of this factor will be discussed in Sec. VII.

If the operator under study belongs to an $O(4)$ multiplet of dimension greater than 1, i.e., if it carries at least one space-time index, the trace in Eq. (29) will in general depend on the direction of p. This has the immediate consequence that the renormalization condition (28) violates $O(4)$ covariance even in the continuum limit. In the continuum, one can restore $O(4)$ covariance by a summation over the members of the $O(4)$ multiplet. On the lattice, each operator when renormalized according to Eq. (29) has in general its own Z factor, and only after conversion to a covariant scheme all operators in an irreducible $H(4)$ multiplet will have the same renormalization factor. However, it is also possible to define a common Z factor for all members of such an $H(4)$ multiplet already in the RI-MOM framework by taking a suitable average. If $j = 1, 2, \ldots, N$ labels the members of the chosen basis of the multiplet we can average over this basis and calculate Z from

$$Z_q^{-1} Z \frac{1}{N} \sum_{j=1}^{N} \frac{1}{12} \operatorname{tr}(\Gamma_j(p) \Gamma_j^{\mathrm{Born}}(p)^{-1}) = 1 \tag{31}$$

with $p^2 = \mu_p^2$. This procedure has two advantages. It is simpler than working with a different renormalization factor for every single operator, and it leads to a smoother dependence of the results on p^2, because it reduces the amount of $O(4)$ violation.

The bases actually used in our calculations are given in Appendix A. Whenever we want to refer to this averaging procedure we shall write the respective operator with a bar on top, i.e., $\mathcal{O}_{v_{2,a}}$ means precisely the operator (4) while $\bar{\mathcal{O}}_{v_{2,a}}$ refers to a result for the operator multiplet (A1), and analogously for the currents.

Ideally, the scale μ_p at which our renormalization constants are defined should satisfy the conditions

$$1/L^2 \ll \Lambda_{\mathrm{QCD}}^2 \ll \mu_p^2 \ll 1/a^2 \tag{32}$$

on a lattice with linear extent L. The inequality $\Lambda_{\mathrm{QCD}}^2 \ll \mu_p^2$ should ensure that we can safely use (continuum) perturbation theory to transform our results from one scheme to another. The inequality $\mu_p^2 \ll 1/a^2$ is supposed to keep discretization effects small. So we have to find a way between the Scylla of difficult to control nonperturbative effects and the Charybdis of lattice artifacts. Whether in a concrete calculation the conditions (32) may be considered as fulfilled remains to be seen.

Let us finally comment on our notation for the renormalization scale. In the case of a general scheme $\mathcal{S}$ we use the letter M, in the case of the $\overline{\mathrm{MS}}$ scheme we use μ. We take μ_p when dealing with the RI′-MOM scheme and μ_M in the case of the MOM scheme to be defined below.

IV. NUMERICAL IMPLEMENTATION

Let us sketch the main ingredients of our calculational procedure [12]. To simplify the notation we set the lattice spacing $a = 1$ in this section. Moreover we suppress Dirac and color indices. In a first step the gauge field configurations are numerically fixed to some convenient gauge, the Landau gauge in our case [21]. Representing the operator under study in the form

$$\sum_z \mathcal{O}(z) = \sum_{z,z'} \bar{q}(z) J(z, z') q(z'), \tag{33}$$

we calculate the nonamputated Green function (24) as the gauge field average of the quantity

$$\hat{G}(p) = \frac{1}{V} \sum_{x,y,z,z'} \mathrm{e}^{-\mathrm{i}p\cdot(x-y)} \hat{S}(x, z) J(z, z') \hat{S}(z', y), \tag{34}$$

constructed from the quark propagator $\hat{S}$ on the same gauge field configuration. Working in the limit of exact isospin invariance we do not have to distinguish between u and d propagators. With the help of the relation

$$\hat{S}(x, y) = \gamma_5 \hat{S}(y, x)^+ \gamma_5, \tag{35}$$

we rewrite $\hat{G}(p)$ as

$$\hat{G}(p) = \frac{1}{V} \sum_{z,z'} \gamma_5 \Big(\sum_x \hat{S}(z, x) \mathrm{e}^{\mathrm{i}p\cdot x} \Big)^+ \gamma_5 J(z, z') \times \Big(\sum_y \hat{S}(z', y) \mathrm{e}^{\mathrm{i}p\cdot y} \Big). \tag{36}$$

The quantities

$$\sum_x \hat{S}(z, x) \mathrm{e}^{\mathrm{i}p\cdot x} \tag{37}$$

appearing in this expression can be calculated by solving the lattice Dirac equation with a momentum source:

$$\sum_z M(y, z) \Big(\sum_x \hat{S}(z, x) \mathrm{e}^{\mathrm{i}p\cdot x} \Big) = \mathrm{e}^{\mathrm{i}p\cdot y}. \tag{38}$$

Here $M(x, y)$ represents the fermion matrix. So the number of required matrix inversions is proportional to the number of momenta considered. But the quark propagators, which we need for the amputation and the computation of the quark wave function renormalization, are immediately obtained from the quantities already calculated.

Strictly speaking, one should evaluate the quark propagators going into the calculation of $S(p)$ in Eq. (26) on configurations that are statistically independent of those used for the computation of the Green functions (24) in order to avoid unwanted correlations [22]. If we calculate these expectation values on two independent ensembles, statistical fluctuations in the quark propagators and the Green functions (24) are uncorrelated, and (31) gives a good estimate of the true Z. If we calculate both expectation values on the same ensemble, the fluctuations will be

correlated, particularly if the configuration number N_{conf} is small. It can be shown [23] that this will give a bias proportional to $1/N_{\mathrm{conf}}$. In our case statistical fluctuations are very small, because of our use of momentum sources, so we do not expect a large problem. Indeed, estimating the bias introduced by our procedure (see, e.g., Refs. [23,24] for appropriate methods) we confirm this expectation. Note that such correlations exist also in the calculation of hadronic matrix elements from ratios of correlation functions. However, given the typical number of configurations used in these studies, the bias should be very small.

Another computational strategy would be to choose a particular location for the operator. Translational invariance ensures that this will give the same expectation value after averaging over all gauge field configurations. For this method we need to solve the Dirac equation with a point source at the location of the operator and (in the case of extended operators) for a small number of point sources in the immediate neighborhood. For operators with a small number of derivatives the point source method would require fewer inversions, but it turns out that relying on translational invariance increases the statistical errors.

The required gauge fixing necessarily raises the question of the influence of Gribov copies. Fortunately, investigations of this problem indicate that the fluctuations induced by the Gribov copies are not overwhelmingly large and may be less important than the ordinary statistical fluctuations [25,26] (see also Ref. [27]).

Since the numerical effort is proportional to the number of momenta, the proper choice of the momenta considered is of particular importance. In order to minimize cutoff effects we choose them close to the diagonal of the Brillouin zone and achieve for most operators an essentially smooth dependence on the renormalization scale μ_p^2. It goes without saying that in this way we cannot eliminate lattice artifacts completely. However, more sophisticated strategies for coping with the cutoff effects such as those suggested in Refs. [28,29] would require the use of far more momenta than we can afford when working with momentum sources. As the treatment of lattice artifacts is a subtle issue anyway we have decided to keep the advantage of small statistical errors provided by the above procedure and to deal with the discretization errors in a different manner.

A specific lattice artifact is caused by the $O(a)$ chiral symmetry breaking term of the quark propagator. In position space this term is concentrated at very short distances, for fermion actions obeying the Ginsparg-Wilson condition it is even exactly a delta function. In momentum space it gives rise to the Wilson mass term, $\sim a p^2$ in the inverse propagator. The authors of Ref. [30] discuss one method of suppressing this artifact (for an earlier treatment of the same effect see Ref. [31]). Here, our approach to this problem is to define Z_q from Eq. (30), in which the trace removes the Wilson mass term, and to suppress the remaining $O(a^2)$ lattice artifacts by using the perturbative subtraction scheme described in Sec. IX.

V. MONTE CARLO ENSEMBLES

We work with two degenerate flavors of nonperturbatively improved Wilson fermions (clover fermions). For the explicit form of the fermionic action see, e.g., Ref. [31]. As our gauge field action we take Wilson's plaquette action. In Table II we collect the parameters of our simulations, β, $\kappa = \kappa_{\mathrm{sea}}$, the clover coefficient c_{SW}, and the lattice volume along with am_π, the pion mass in lattice units. Table III contains the critical hopping parameters κ_c as well as the values of the Sommer parameter r_0/a and the average plaquette $P = \langle \frac{1}{3} \mathrm{tr} U_\Box \rangle$ in the chiral limit [32] which are employed in this paper. Note that the results for the chiral extrapolation of r_0/a given here are based on a larger set of data than that used in Ref. [32].

The statistical errors will be calculated by means of the jackknife procedure.

TABLE II. Simulation parameters β, $\kappa = \kappa_{\mathrm{sea}}$, clover coefficient c_{SW}, and lattice volume along with the corresponding values of the pion mass in lattice units.

β	κ	c_{SW}	V	am_π
5.20	0.1342	2.0171	$16^3 \times 32$	0.5847(12)
5.20	0.1350	2.0171	$16^3 \times 32$	0.4148(13)
5.20	0.1355	2.0171	$16^3 \times 32$	0.2907(15)
5.25	0.1346	1.9603	$16^3 \times 32$	0.4932(10)
5.25	0.1352	1.9603	$16^3 \times 32$	0.3821(13)
5.25	0.13575	1.9603	$24^3 \times 48$	0.25556(55)
5.25	0.1360	1.9603	$24^3 \times 48$	0.18396(56)
5.29	0.1340	1.9192	$16^3 \times 32$	0.5767(11)
5.29	0.1350	1.9192	$16^3 \times 32$	0.42057(92)
5.29	0.1355	1.9192	$24^3 \times 48$	0.32696(64)
5.29	0.1359	1.9192	$24^3 \times 48$	0.23997(47)
5.29	0.1362	1.9192	$24^3 \times 48$	0.15784(75)
5.40	0.1350	1.8228	$24^3 \times 48$	0.40301(43)
5.40	0.1356	1.8228	$24^3 \times 48$	0.31232(67)
5.40	0.1361	1.8228	$24^3 \times 48$	0.22081(72)
5.40	0.13625	1.8228	$24^3 \times 48$	0.19053(62)
5.40	0.1364	1.8228	$24^3 \times 48$	0.1535(13)

TABLE III. Critical hopping parameters κ_c along with chirally extrapolated values for the Sommer parameter r_0/a and the average plaquette P.

β	κ_c	r_0/a	P
5.20	0.136008(15)	5.454(59)	0.538608(49)
5.25	0.136250(7)	5.880(26)	0.544780(89)
5.29	0.136410(9)	6.201(25)	0.549877(109)
5.40	0.136690(22)	6.946(44)	0.562499(46)

VI. CHIRAL EXTRAPOLATION

As already mentioned in Sec. III we have to extrapolate our results obtained at nonvanishing quark masses to the chiral limit. This will be done for each β at fixed values of p^2. In the cases where the simulations for different values of κ have been performed on different volumes, i.e., for $\beta = 5.25$ and $\beta = 5.29$, the sets of momenta used depend on κ, and some kind of interpolation is required. For this purpose we fit the data on the larger lattices ($24^3 \times 48$) with cubic splines in $\ln(a^2 p^2)$. Except for very small momenta, which will not influence the final results, these fits yield a very good description of our data. An example is shown in Fig. 1.

Of course, "wiggles" in the data (caused by lattice artifacts) will be smoothed out by this interpolation. These wiggles are less pronounced on the larger lattices than on the smaller ones. That is why we have chosen to work with the momenta coming from the smaller lattices so that we can use the data on these lattices directly without any interpolation and have to interpolate only the results obtained on the larger lattices.

Alternatively, one could use the interpolation for all κ values. This however leads to negligible differences in the final results.

For the chosen momenta we can then extrapolate our data to the chiral limit. This is done linearly in $(r_0 m_\pi)^2$, i.e., by means of a fit of the form

$$Z = z_0 + z_1 (r_0 m_\pi)^2, \tag{39}$$

where the fit parameter z_0 is identified with the desired value of the renormalization factor in the chiral limit. Note that this is essentially a linear fit in the quark mass. The ansatz is motivated by the fact that in perturbation theory the leading quark mass dependence is linear as the chiral limit is approached (see, e.g., Ref. [31]).

With the possible exception of the smallest momenta these fits work well. Examples are shown in Figs. 2 and 3. Nevertheless, we have also performed quadratic extrapolations of the form

$$Z = z_0 + z_1 (r_0 m_\pi)^2 + z_2 (r_0 m_\pi)^4 \tag{40}$$

in order to get an idea of the impact of the chiral extrapolation on the final results. (Note that this corresponds to a three-parameter fit at three data points for $\beta = 5.20$.)

However, there is an exceptional case where these simple extrapolations are not trustworthy. This is the pseudoscalar density $\mathcal{O}^P$. In this case one expects that $Z = Z_P$ vanishes with the quark mass m_q, because Z_P^{-1} develops a pole in m_q. Therefore we follow Ref. [33] and try to subtract the pole contribution using a fit of the form

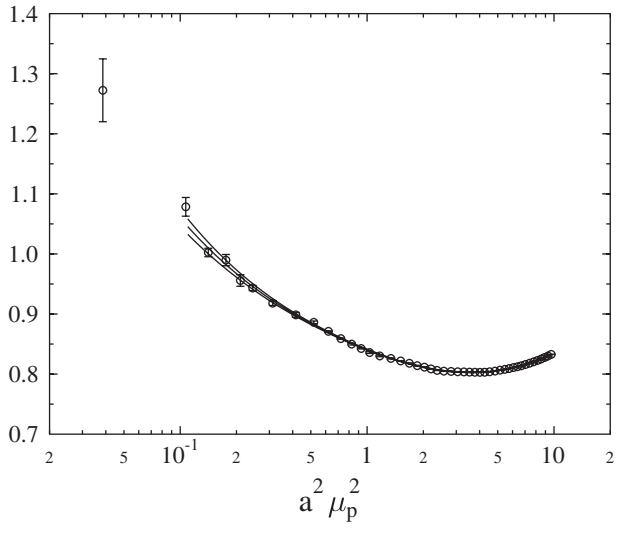

FIG. 1. $Z^{\mathrm{RI'\text{-}MOM}}$ for the operator $\bar{\mathcal{O}}_T$ at $\beta = 5.29$, $\kappa = 0.1362$ on a $24^3 \times 48$ lattice. The curves represent splines with two interior knots fitted to the data and to the data $\pm$ the statistical error.

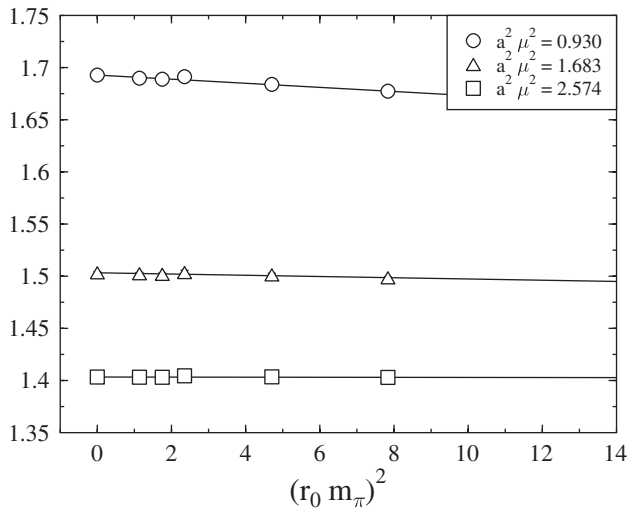

FIG. 2. Chiral extrapolation for $\mathcal{O}_{a_2}$ at $\beta = 5.40$.

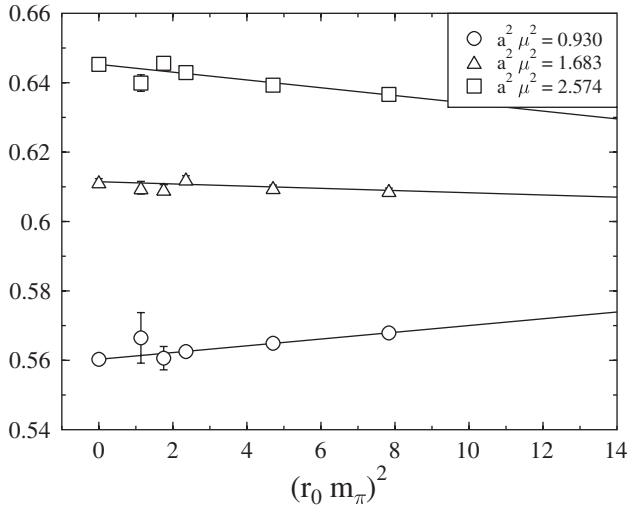

FIG. 3. Chiral extrapolation for $\mathcal{O}^S$ (subtracted data, as explained in Sec. IX) at $\beta = 5.40$.

$$\frac{1}{Z_P} = s_0 \frac{1}{am_q} + s_1 + s_2 am_q \tag{41}$$

with

$$am_q = \frac{1}{2}\left(\frac{1}{\kappa} - \frac{1}{\kappa_c}\right). \tag{42}$$

Here κ_c is the critical hopping parameter defined for fixed β by the vanishing of the pseudoscalar mass m_π. The values used in this paper can be found in Table III. The fit parameter s_1 is then identified with the inverse of Z_P in the chiral limit. Examples of such fits are shown in Fig. 4. The curvature in the data is clearly visible establishing the existence of the Goldstone pole.

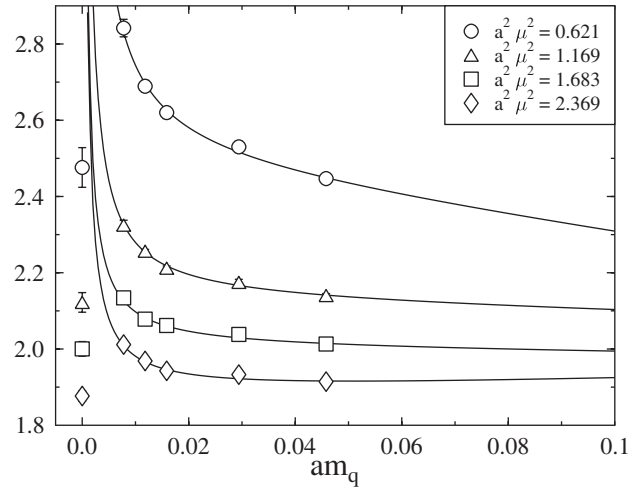

FIG. 4. Chiral extrapolation of $1/Z_P$ (subtracted data, as explained in Sec. IX) at $\beta = 5.40$. The symbols at $am = 0$ represent the chirally extrapolated values, i.e., the quantity s_1.

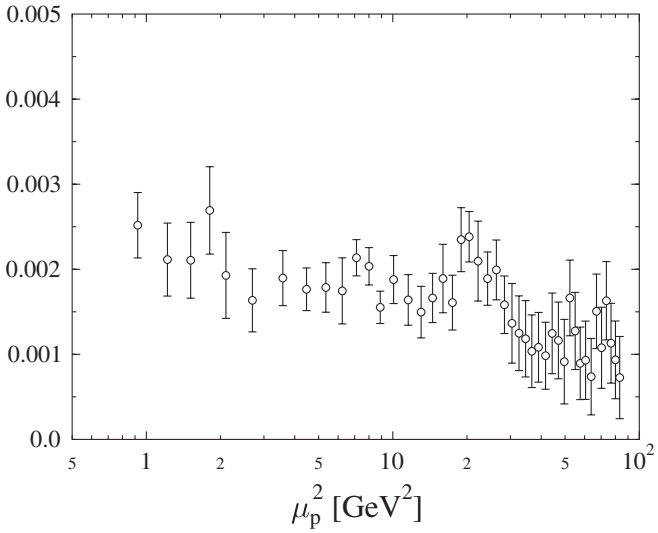

FIG. 5. $a^2\mu_p^2 s_0$ (from a fit to subtracted data, as explained in Sec. IX) as a function of μ_p^2 for the pseudoscalar density at $\beta = 5.40$.

How can we judge the reliability of the resulting numbers? From the operator product expansion [34,35] we expect that s_0 is inversely proportional to μ_p^2, i.e., $\mu_p^2 s_0$ should become independent of μ_p^2. Therefore we plot $a^2\mu_p^2 s_0$ versus μ_p^2 in Fig. 5. The μ_p^2 independence seems to be satisfied with reasonable accuracy. Thus we are confident that our extrapolation for Z_P works fairly well. Nevertheless, the results for Z_P must be considered with some caution.

VII. INPUT FROM CONTINUUM PERTURBATION THEORY

In Sec. III we have explained how one can compute nonperturbative renormalization factors leading us from the bare lattice operators (at lattice spacing a) to renormalized operators in the RI′-MOM scheme (renormalization scale μ_p). In this section we collect results from continuum perturbation theory which will be needed for the conversion to standard renormalization schemes such as the $\overline{\text{MS}}$ scheme.

If the operator $\mathcal{O}$ under study is multiplicatively renormalizable the operator renormalized in some scheme $\mathcal{S}$ at the scale M is related to the bare lattice operator $\mathcal{O}_{\text{bare}}$ by

$$\mathcal{O}^{\mathcal{S}}(M) = Z^{\mathcal{S}}_{\text{bare}}(M, a)\mathcal{O}_{\text{bare}}. \tag{43}$$

The scale dependence of the renormalized operator is determined by the anomalous dimension

$$\gamma^{\mathcal{S}} = -M\frac{\mathrm{d}}{\mathrm{d}M}\ln Z^{\mathcal{S}}_{\text{bare}}. \tag{44}$$

Here the derivative is to be taken at fixed bare parameters, and it is implicitly assumed that the cutoff has been removed in the end. In perturbation theory $\gamma^{\mathcal{S}}$ is expanded in powers of some renormalized coupling constant $g^{\mathcal{S}}(M)$:

$$\gamma^{\mathcal{S}} = \gamma_0 \frac{g^{\mathcal{S}}(M)^2}{16\pi^2} + \gamma_1^{\mathcal{S}}\left(\frac{g^{\mathcal{S}}(M)^2}{16\pi^2}\right)^2 + \gamma_2^{\mathcal{S}}\left(\frac{g^{\mathcal{S}}(M)^2}{16\pi^2}\right)^3 + \gamma_3^{\mathcal{S}}\left(\frac{g^{\mathcal{S}}(M)^2}{16\pi^2}\right)^4 + \cdots. \tag{45}$$

Note that the one-loop coefficient γ_0 is scheme independent.

Similarly we define the quark field renormalization constant $Z^{\mathcal{S}}_{q,\text{bare}}(M, a)$ in the scheme $\mathcal{S}$ so that the renormalized quark propagator is given by $Z^{\mathcal{S}}_{q,\text{bare}}(M, a)S_{\text{bare}}$. In the RI′-MOM scheme, $Z^{\text{RI}'\text{-MOM}}_{q,\text{bare}}$ is then specified by Eq. (30) or its continuum analogue. For the anomalous dimension of the quark field we adopt the definition

$$\gamma_q^{\mathcal{S}} = -M\frac{\mathrm{d}}{\mathrm{d}M}\ln Z^{\mathcal{S}}_{q,\text{bare}}. \tag{46}$$

The running of the coupling constant $g^{\mathcal{S}}(M)$ as the scale M is varied is controlled by the β function

$$\beta^{\mathcal{S}} = M\frac{\mathrm{d}}{\mathrm{d}M}g^{\mathcal{S}}(M). \tag{47}$$

Again, the derivative is to be taken at fixed bare parameters and it is implicitly assumed that the cutoff has been removed in the end. The perturbative expansion of the β function can be written as

$$\beta^{\mathcal{S}} = -\beta_0\frac{g^{\mathcal{S}}(M)^3}{16\pi^2} - \beta_1\frac{g^{\mathcal{S}}(M)^5}{(16\pi^2)^2} - \beta_2^{\mathcal{S}}\frac{g^{\mathcal{S}}(M)^7}{(16\pi^2)^3} - \beta_3^{\mathcal{S}}\frac{g^{\mathcal{S}}(M)^9}{(16\pi^2)^4} + \cdots. \tag{48}$$

In this case the first two coefficients β_0 and β_1 are scheme independent.

Integrating Eq. (47) we obtain

$$\frac{M}{\Lambda^{\mathcal{S}}} = \left(\frac{\beta_0}{16\pi^2}g^{\mathcal{S}}(M)^2\right)^{(\beta_1/2\beta_0^2)}\exp\left(\frac{1}{2\beta_0}\cdot\frac{16\pi^2}{g^{\mathcal{S}}(M)^2}\right) \times \exp\left\{\int_0^{g^{\mathcal{S}}(M)}\mathrm{d}g'\left(\frac{1}{\beta^{\mathcal{S}}(g')} + \frac{1}{\beta_0}\frac{16\pi^2}{g'^3} - \frac{\beta_1}{\beta_0^2}\frac{1}{g'}\right)\right\} \tag{49}$$

with the Λ parameter $\Lambda^{\mathcal{S}}$ appearing as an integration constant.

In the same spirit we define the so-called RGI (renormalization group invariant) operator, which is independent of scale and scheme, by

$$\mathcal{O}^{\mathrm{RGI}} = \Delta Z^{\mathcal{S}}(M)\mathcal{O}^{\mathcal{S}}(M) = Z^{\mathrm{RGI}}(a)\mathcal{O}_{\mathrm{bare}} \tag{50}$$

with

$$\Delta Z^{\mathcal{S}}(M) = \left(2\beta_0\frac{g^{\mathcal{S}}(M)^2}{16\pi^2}\right)^{-(\gamma_0/2\beta_0)} \times \exp\left\{\int_0^{g^{\mathcal{S}}(M)}\mathrm{d}g'\left(\frac{\gamma^{\mathcal{S}}(g')}{\beta^{\mathcal{S}}(g')} + \frac{\gamma_0}{\beta_0 g'}\right)\right\} \tag{51}$$

and

$$Z^{\mathrm{RGI}}(a) = \Delta Z^{\mathcal{S}}(M)Z^{\mathcal{S}}_{\mathrm{bare}}(M,a), \tag{52}$$

where Z^{RGI} depends only on a (or on the bare coupling parameter β). Once we know $\mathcal{O}^{\mathrm{RGI}}$ (or equivalently Z^{RGI}), multiplication with $\Delta Z^{\mathcal{S}}(M)^{-1}$ will allow us to evaluate $Z^{\mathcal{S}}_{\mathrm{bare}}(M,a)$ and hence the operator $\mathcal{O}$ (or rather its matrix elements) in any scheme and at any scale we like, provided we know the β and γ functions sufficiently well.

In the two-loop approximation, i.e., setting $\beta_n^{\mathcal{S}} = \gamma_n^{\mathcal{S}} = 0$ for $n \geq 2$, one can evaluate the integral in Eq. (51) easily:

$$\Delta Z^{\mathcal{S}}(M) = \left(2\beta_0\frac{g^{\mathcal{S}}(M)^2}{16\pi^2}\right)^{-(\gamma_0/2\beta_0)} \times \left(1 + \frac{\beta_1}{\beta_0}\frac{g^{\mathcal{S}}(M)^2}{16\pi^2}\right)^{(\gamma_0\beta_1 - \gamma_1^{\mathcal{S}}\beta_0)/2\beta_0\beta_1}. \tag{53}$$

Whenever we need them we evaluate the integrals in Eqs. (49) and (51) exactly (by numerical methods) and do not reexpand them in $g^{\mathcal{S}}(M)$.

With the help of the methods described in Secs. III and IV we can compute $Z^{\mathrm{RI'\text{-}MOM}}_{\mathrm{bare}}(\mu_p)$ numerically for some range of scales μ_p. Knowledge of $\Delta Z^{\mathrm{RI'\text{-}MOM}}(\mu_p)$ would then permit us to compute Z^{RGI}. However, being not covariant for most operators, the RI′-MOM scheme is not very suitable for evaluating anomalous dimensions. Therefore we will adopt a two-step procedure for computing Z^{RGI}. In the first step we transform the numerical results for $Z^{\mathrm{RI'\text{-}MOM}}_{\mathrm{bare}}$ to a covariant ''intermediate'' scheme $\mathcal{S}$, e.g., the $\overline{\mathrm{MS}}$ scheme, and in the second step we use the anomalous dimension and the β function in this scheme to compute $\Delta Z^{\mathcal{S}}$ and hence Z^{RGI}. Thus we could in principle compute $Z^{\mathrm{RGI}}(a)$ as

$$Z^{\mathrm{RGI}}(a) = \Delta Z^{\mathcal{S}}(M=\mu_p)Z^{\mathcal{S}}_{\mathrm{RI'\text{-}MOM}}(M=\mu_p) \times Z^{\mathrm{RI'\text{-}MOM}}_{\mathrm{bare}}(\mu_p,a), \tag{54}$$

where $Z^{\mathcal{S}}_{\mathrm{RI'\text{-}MOM}}$ denotes the finite renormalization factor leading from the RI′-MOM scheme to the scheme $\mathcal{S}$ and all the scales have been identified with the scale μ_p initially set in the RI′-MOM scheme.

The most obvious choice for $\mathcal{S}$ is of course the $\overline{\mathrm{MS}}$ scheme. However, it will turn out to be advantageous to consider also a kind of (perturbative) momentum subtraction scheme, which we call the MOM scheme. This is defined by requiring that in the renormalized vertex function the coefficient of the tree-level (or Born) term equals one at the renormalization scale μ_M. To make this definition unambiguous one has to specify in each case the basis used for the other contributions. The quark field renormalization constant is taken to be the same as in the RI′-MOM scheme:

$$Z^{\mathrm{MOM}}_{q,\mathrm{bare}}(\mu_M,a) = Z^{\mathrm{RI'\text{-}MOM}}_{q,\mathrm{bare}}(\mu_M,a). \tag{55}$$

The MOM scheme is covariant and rather ''close'' to the RI′-MOM scheme so that the conversion factor $Z^{\mathrm{MOM}}_{\mathrm{RI'\text{-}MOM}}$ from RI′-MOM to MOM usually differs less from one than the factor $Z^{\overline{\mathrm{MS}}}_{\mathrm{RI'\text{-}MOM}}$ leading from RI′-MOM to $\overline{\mathrm{MS}}$.

We can expand the conversion factor leading from RI′-MOM to $\overline{\mathrm{MS}}$ in powers of the $\overline{\mathrm{MS}}$ coupling constant:

$$Z^{\overline{\mathrm{MS}}}_{\mathrm{RI'\text{-}MOM}}(\mu) = 1 + c_1\frac{g^{\overline{\mathrm{MS}}}(\mu)^2}{16\pi^2} + c_2\left(\frac{g^{\overline{\mathrm{MS}}}(\mu)^2}{16\pi^2}\right)^2 + c_3\left(\frac{g^{\overline{\mathrm{MS}}}(\mu)^2}{16\pi^2}\right)^3 + \cdots. \tag{56}$$

Using

$$Z^{\overline{\mathrm{MS}}}_{\mathrm{MOM}}(\mu) = 1 + c_1'\frac{g^{\overline{\mathrm{MS}}}(\mu)^2}{16\pi^2} + c_2'\left(\frac{g^{\overline{\mathrm{MS}}}(\mu)^2}{16\pi^2}\right)^2 + c_3'\left(\frac{g^{\overline{\mathrm{MS}}}(\mu)^2}{16\pi^2}\right)^3 + \cdots, \tag{57}$$

we obtain for the conversion factor from RI′-MOM to MOM:

$$Z^{\mathrm{MOM}}_{\mathrm{RI'\text{-}MOM}}(\mu) = \frac{Z^{\overline{\mathrm{MS}}}_{\mathrm{RI'\text{-}MOM}}(\mu)}{Z^{\overline{\mathrm{MS}}}_{\mathrm{MOM}}(\mu)} = 1 + (c_1 - c_1')\frac{g^{\overline{\mathrm{MS}}}(\mu)^2}{16\pi^2} + (c_2 - c_1c_1' + c_1'^2 - c_2')\left(\frac{g^{\overline{\mathrm{MS}}}(\mu)^2}{16\pi^2}\right)^2 + (c_3 - c_2c_1' + c_1c_1'^2 - c_1c_2' - c_1'^3 + 2c_1'c_2' - c_3')\left(\frac{g^{\overline{\mathrm{MS}}}(\mu)^2}{16\pi^2}\right)^3 + \cdots. \quad (58)$$

If the vertex function $\Gamma(p)$ is proportional to the Born term $\Gamma_{\mathrm{Born}}(p)$ (as it happens in simple cases), the RI′-MOM scheme and the MOM scheme do not differ. So we have

$$Z^{\overline{\mathrm{MS}}}_{\mathrm{RI'\text{-}MOM}}(\mu) = Z^{\overline{\mathrm{MS}}}_{\mathrm{MOM}}(\mu) \quad (59)$$

and consequently $c_i = c_i'$. However, in the generic case the matrix $\Gamma(p)$ will contain also contributions that are not a multiple of $\Gamma_{\mathrm{Born}}(p)$. As we consider only operators which are multiplicatively renormalizable in the continuum these additional contributions are finite, but they make $Z^{\overline{\mathrm{MS}}}_{\mathrm{RI'\text{-}MOM}}$ different from $Z^{\overline{\mathrm{MS}}}_{\mathrm{MOM}}$ and are responsible for the dependence of $Z^{\overline{\mathrm{MS}}}_{\mathrm{RI'\text{-}MOM}}$ on the direction of the momentum p. An explicit example is discussed in Appendix B.

Working with the MOM scheme it is quite natural to expand in a coupling constant which is similarly defined through a momentum subtraction procedure. Therefore we have also considered the $\widetilde{\mathrm{MOM}}$gg scheme as defined in Ref. [36]. The corresponding coupling constant $g^{\widetilde{\mathrm{MOMgg}}}$ is related to the $\overline{\mathrm{MS}}$ coupling constant $g^{\overline{\mathrm{MS}}}$ by

$$\frac{g^{\widetilde{\mathrm{MOMgg}}}(\mu)^2}{16\pi^2} = \frac{g^{\overline{\mathrm{MS}}}(\mu)^2}{16\pi^2} + d_1\left(\frac{g^{\overline{\mathrm{MS}}}(\mu)^2}{16\pi^2}\right)^2 + d_2\left(\frac{g^{\overline{\mathrm{MS}}}(\mu)^2}{16\pi^2}\right)^3 + d_3\left(\frac{g^{\overline{\mathrm{MS}}}(\mu)^2}{16\pi^2}\right)^4 + \cdots, \quad (60)$$

where in the Landau gauge

$$d_1 = \frac{70}{3} - \frac{22}{9}n_f, \quad (61)$$

$$d_2 = \frac{516217}{576} - \frac{153}{4}\zeta_3 - \left(\frac{8125}{54} + \frac{4}{3}\zeta_3\right)n_f + \frac{376}{81}n_f^2, \quad (62)$$

$$d_3 = \frac{304676635}{6912} - \frac{299961}{64}\zeta_3 - \frac{81825}{64}\zeta_5 + \left(-\frac{13203725}{1296} + \frac{13339}{27}\zeta_3 + \frac{1885}{9}\zeta_5\right)n_f + \left(\frac{580495}{972} + \frac{40}{9}\zeta_3\right)n_f^2 - \frac{5680}{729}n_f^3. \quad (63)$$

As usual, ζ_n denotes the value of Riemann's ζ function at the argument n. Choosing $\mathcal{S} = \mathrm{MOM}$ in Eq. (51) we shall always work with the $\widetilde{\mathrm{MOM}}$gg coupling.

Using the above expressions, all expansions in the $\overline{\mathrm{MS}}$ coupling may be rewritten as expansions in powers of the $\widetilde{\mathrm{MOM}}$gg coupling. For example, the coefficients γ_i^{MOM} of the anomalous dimension in the MOM scheme expanded in powers of $g^{\widetilde{\mathrm{MOMgg}}}$ are related to the coefficients $\gamma_i^{\overline{\mathrm{MS}}}$ of the anomalous dimension in the $\overline{\mathrm{MS}}$ scheme expanded in powers of $g^{\overline{\mathrm{MS}}}$ by

$$\gamma_1^{\mathrm{MOM}} = \gamma_1^{\overline{\mathrm{MS}}} - 2\beta_0c_1' - d_1\gamma_0, \quad (64)$$

$$\gamma_2^{\mathrm{MOM}} = \gamma_2^{\overline{\mathrm{MS}}} - 2\beta_1c_1' - 2\beta_0(2c_2' - c_1'^2) - 2d_1(\gamma_1^{\overline{\mathrm{MS}}} - 2c_1'\beta_0) + \gamma_0(2d_1^2 - d_2), \quad (65)$$

$$\gamma_3^{\mathrm{MOM}} = \gamma_3^{\overline{\mathrm{MS}}} - 2\beta_2^{\overline{\mathrm{MS}}}c_1' - 3d_1[\gamma_2^{\overline{\mathrm{MS}}} - 2c_1'\beta_1 - 2\beta_0(2c_2' - c_1'^2)] + (\gamma_1^{\overline{\mathrm{MS}}} - 2\beta_0c_1')(5d_1^2 - 2d_2) - 2\beta_1(2c_2' - c_1'^2) - 2\beta_0(3c_3' - 3c_1'c_2' + c_1'^3) + \gamma_0(5d_1d_2 - 5d_1^3 - d_3). \quad (66)$$

For the actual evaluation of the expansion coefficients c_i and c_i' one starts from the bare vertex function for the operator under consideration computed in dimensional regularization and imposes the respective renormalization conditions yielding the renormalized vertex functions in the different schemes. These differ only by (scale-dependent) factors, from which the desired conversion factors can be derived immediately, once the quark field renormalization factor has been extracted from the quark propagator. The results for the coefficients c_1, c_2, c_3 and c_1', c_2', c_3' as well as the sources from which we have taken the required perturbative vertex functions are given in Appendix C.

VIII. LATTICE PERTURBATION THEORY

As long as no mixing with operators of lower dimension is involved it is possible to compute renormalization factors in lattice perturbation theory. Although straightforward in principle, the actual calculations tend to become rather cumbersome in practice. Hence they rarely extend beyond one-loop order (see, however, Refs. [2–4]). This is a severe limitation since lattice perturbation theory converges rather slowly in most cases of interest. Therefore various improvement schemes have been devised, such as boosted perturbation theory and tadpole improvement [5].

In spite of these problems we want to compare our nonperturbative results with the corresponding values obtained in (improved) lattice perturbation theory. For the renormalization factor $Z^{\overline{\mathrm{MS}}}_{\mathrm{bare}}(\mu, a)$ a straightforward application of one-loop lattice perturbation theory yields results of the form

$$Z^{\overline{\mathrm{MS}}}_{\mathrm{bare}}(\mu, a)_{\mathrm{pert}} = 1 - \frac{g^2}{16\pi^2}(\gamma_0 \ln(a\mu) + C_F\Delta), \quad (67)$$

where $\Delta = \Delta(c_{\mathrm{SW}})$ is a finite constant depending on the details of the lattice action and we have $C_F = 4/3$ for the gauge group SU(3). If mixing occurs, the single renormalization factor of a multiplicatively renormalizable operator is replaced by a matrix of Z factors. However, we shall neglect this complication and restrict ourselves to the matrix element on the diagonal corresponding to the operator under consideration. Working with an anticommuting γ_5 also in the continuum part of the calculation one obtains the values given in Table IV. They do not depend on the particular operator but only on the $H(4)$ multiplet to which the operator belongs. In the case $c_{\mathrm{SW}} = 0$ results for $\mathcal{O}_{v_4}$, $\mathcal{O}_{h_{1,b}}$, $\mathcal{O}_{h_{2,b}}$, and $\mathcal{O}^T_{\mu\nu}$ have already been obtained in Ref. [39]. Note that Δ is gauge invariant for our quark-antiquark operators, however, in the case of the quark wave function renormalization constant Z_q it is not. The result given in Table IV corresponds to the Landau gauge.

In order to obtain the corresponding results in tadpole-improved perturbation theory we write (with $\mu = 1/a$) for an operator with n_D covariant derivatives

TABLE IV. Finite contributions to the renormalization factors $Z^{\overline{\mathrm{MS}}}_{\mathrm{bare}}$ in lattice perturbation theory. The result for the quark field is given in the Landau gauge.

Operator	$\Delta(c_{\mathrm{SW}})$	Ref.
$\mathcal{O}^S$	$12.95241 + 7.73792c_{\mathrm{SW}} - 1.38038c^2_{\mathrm{SW}}$	[31]
$\mathcal{O}^P$	$22.59544 - 2.24887c_{\mathrm{SW}} + 2.03602c^2_{\mathrm{SW}}$	[31]
$\mathcal{O}^V_\mu$	$20.61780 - 4.74556c_{\mathrm{SW}} - 0.54317c^2_{\mathrm{SW}}$	[31]
$\mathcal{O}^A_\mu$	$15.79628 + 0.24783c_{\mathrm{SW}} - 2.25137c^2_{\mathrm{SW}}$	[31]
$\mathcal{O}^T_{\mu\nu}$	$17.01808 - 3.91333c_{\mathrm{SW}} - 1.97230c^2_{\mathrm{SW}}$	[31]
Z_q	$16.64441 - 2.24887c_{\mathrm{SW}} - 1.39727c^2_{\mathrm{SW}}$	[31]
$\mathcal{O}_{v_{2,a}}$	$1.27959 - 3.87297c_{\mathrm{SW}} - 0.67826c^2_{\mathrm{SW}}$	[31]
$\mathcal{O}_{v_{2,b}}$	$2.56184 - 3.96980c_{\mathrm{SW}} - 1.03973c^2_{\mathrm{SW}}$	[31]
$\mathcal{O}_{r_{2,a}}$	$0.34512 - 1.35931c_{\mathrm{SW}} - 1.89255c^2_{\mathrm{SW}}$	[31]
$\mathcal{O}_{r_{2,b}}$	$0.16738 - 1.24953c_{\mathrm{SW}} - 1.99804c^2_{\mathrm{SW}}$	[31]
$\mathcal{O}_{h_{1,a}}$	$1.25245 - 3.10180c_{\mathrm{SW}} - 1.59023c^2_{\mathrm{SW}}$	[37]
$\mathcal{O}_{h_{1,b}}$	$0.52246 - 2.99849c_{\mathrm{SW}} - 1.46224c^2_{\mathrm{SW}}$	[37]
$\mathcal{O}_{v_3}$	$-12.12740 - 2.92169c_{\mathrm{SW}} - 0.98166c^2_{\mathrm{SW}}$	[13,37,38]
$\mathcal{O}_{v_{3,a}}$	$-11.56318 - 2.89800c_{\mathrm{SW}} - 0.98387c^2_{\mathrm{SW}}$	[37]
$\mathcal{O}_{r_3}$	$-12.86094 - 1.49316c_{\mathrm{SW}} - 1.68673c^2_{\mathrm{SW}}$	[37]
$\mathcal{O}_{a_2}$	$-12.11715 - 1.51925c_{\mathrm{SW}} - 1.71846c^2_{\mathrm{SW}}$	[37]
$\mathcal{O}_{h_{2,a}}$	$-11.54826 - 2.41077c_{\mathrm{SW}} - 1.51175c^2_{\mathrm{SW}}$	[37]
$\mathcal{O}_{h_{2,b}}$	$-11.86877 - 2.30651c_{\mathrm{SW}} - 1.34908c^2_{\mathrm{SW}}$	[37]
$\mathcal{O}_{h_{2,c}}$	$-11.74773 - 2.36201c_{\mathrm{SW}} - 1.45084c^2_{\mathrm{SW}}$	[37]
$\mathcal{O}_{h_{2,d}}$	$-12.9268 - 2.38849c_{\mathrm{SW}} - 1.3900c^2_{\mathrm{SW}}$	this work
$\mathcal{O}_{v_4}$	$-25.50303 - 2.41788c_{\mathrm{SW}} - 1.12826c^2_{\mathrm{SW}}$	[13,38]

$$1 - \frac{g^2}{16\pi^2}C_F\Delta = \frac{u_0}{u_0^{n_D}}u_0^{n_D-1}\left(1 - \frac{g^2}{16\pi^2}C_F\Delta\right) = \frac{u_0}{u_0^{n_D}}\left(1 - \frac{g^2_{\mathrm{LAT}}}{16\pi^2}C_F\bar{\Delta}\right) + O(g^4_{\mathrm{LAT}}), \quad (68)$$

where

$$u_0 = \left\langle \frac{1}{3}\,\mathrm{tr}U_\Box \right\rangle^{1/4} = 1 - \frac{g^2}{16\pi^2}C_F\pi^2 + O(g^4) \quad (69)$$

and

$$\bar{\Delta} = \Delta + (n_D - 1)\pi^2. \quad (70)$$

This reflects the fact that one has n_D operator tadpole diagrams and one leg tadpole diagram, which are of the same magnitude but contribute with opposite sign. It remains to make a physically reasonable choice for the expansion parameter g_{LAT}. Here we identify g_{LAT} with the boosted coupling

$$g_\Box = \frac{g}{u_0^2}. \quad (71)$$

Now we have two options. Either we stay with the expression (67) and its tadpole-improved analogue

$$Z^{\overline{\mathrm{MS}}}_{\mathrm{bare}}(\mu, a)_{\mathrm{ti}} = u_0^{1-n_D}\left[1 - \frac{g^2_{\mathrm{LAT}}}{16\pi^2}(\gamma_0 \ln(a\mu) + C_F\bar{\Delta})\right] \quad (72)$$

or we apply these formulas only at a fixed scale $\mu = \mu_0$ (e.g., $\mu_0 = 1/a$) using the renormalization group to change μ:

$$Z^{\overline{\mathrm{MS}}}_{\mathrm{bare}}(\mu, a)^{\mathrm{RG}}_{\mathrm{pert}} = \Delta Z^{\overline{\mathrm{MS}}}(\mu)^{-1}\Delta Z^{\overline{\mathrm{MS}}}(\mu_0)Z^{\overline{\mathrm{MS}}}_{\mathrm{bare}}(\mu_0, a)_{\mathrm{pert}}, \quad (73)$$

$$Z^{\overline{\mathrm{MS}}}_{\mathrm{bare}}(\mu, a)^{\mathrm{RG}}_{\mathrm{ti}} = \Delta Z^{\overline{\mathrm{MS}}}(\mu)^{-1}\Delta Z^{\overline{\mathrm{MS}}}(\mu_0)Z^{\overline{\mathrm{MS}}}_{\mathrm{bare}}(\mu_0, a)_{\mathrm{ti}}. \quad (74)$$

The latter option seems preferable leading to the estimates $\Delta Z^{\overline{\mathrm{MS}}}(\mu_0)Z^{\overline{\mathrm{MS}}}_{\mathrm{bare}}(\mu_0, a)_{\mathrm{pert}}$ and $\Delta Z^{\overline{\mathrm{MS}}}(\mu_0)Z^{\overline{\mathrm{MS}}}_{\mathrm{bare}}(\mu_0, a)_{\mathrm{ti}}$ for Z^{RGI}. Working in the chiral limit we compute u_0 from the chirally extrapolated values for $P = u_0^4$ given in Table III. To be consistent with lowest order perturbation theory we set $c_{\mathrm{SW}} = 1$.

Further improvement can be attempted by tadpole-improved, renormalization-group-improved boosted perturbation theory or TRB perturbation theory [13,40]. This works as follows. In Eq. (44) we have defined the anomalous dimension $\gamma^{\mathcal{S}}$ by differentiating $Z^{\mathcal{S}}_{\mathrm{bare}}$ with respect to the renormalization scale M at fixed cutoff and bare parameters. Alternatively one can keep the renormalized quantities fixed and take the derivative with respect to the cutoff, the lattice spacing a in our case. Then one obtains

$$\gamma^{\mathrm{LAT}} = -a\frac{\mathrm{d}}{\mathrm{d}a}\ln Z^{\mathcal{S}}_{\mathrm{bare}}. \quad (75)$$

Note that the derivative with respect to a also acts on $c_{\rm SW}$, unless only the tree-level value $c_{\rm SW} = 1$ is used. The anomalous dimension $\gamma^{\rm LAT}$ is to be considered as a function of some bare coupling constant $g_{\rm LAT} = g_{\rm LAT}(a)$. This could be the usual bare coupling g, but for our purposes it will be more advantageous to work with the boosted coupling $g_{\Box}$. Expanding in $g_{\rm LAT}$ and recalling that the one-loop coefficient γ_0 is universal we can write

$$\gamma^{\rm LAT}(g_{\rm LAT}) = \gamma_0 \frac{g^2_{\rm LAT}}{16\pi^2} + \gamma_1^{\rm LAT}\left(\frac{g^2_{\rm LAT}}{16\pi^2}\right)^2 + \cdots. \quad (76)$$

Similarly we define

$$\begin{aligned}\beta^{\rm LAT}(g_{\rm LAT}) &= -a\frac{{\rm d}g_{\rm LAT}}{{\rm d}a} \\ &= -\beta_0\frac{g^3_{\rm LAT}}{16\pi^2} - \beta_1\frac{g^5_{\rm LAT}}{(16\pi^2)^2} + O(g^7_{\rm LAT}), \quad (77)\end{aligned}$$

where β_0 and β_1 have the same values as in the β function (47). Expressing $Z^{\rm RGI}(a) = \Delta Z^{\mathcal{S}}(M) Z^{\mathcal{S}}_{\rm bare}(M, a)$ in terms of $\gamma^{\rm LAT}$ and $\beta^{\rm LAT}$ we find

$$\begin{aligned}Z^{\rm RGI} &= \left(2\beta_0\frac{g^2_{\rm LAT}}{16\pi^2}\right)^{-(\gamma_0/2\beta_0)} \\ &\quad\times \exp\left\{\int_0^{g_{\rm LAT}} {\rm d}g_0\left(\frac{\gamma^{\rm LAT}(g_0)}{\beta^{\rm LAT}(g_0)} + \frac{\gamma_0}{\beta_0 g_0}\right)\right\}. \quad (78)\end{aligned}$$

In the two-loop approximation we obtain

$$\begin{aligned}Z^{\rm RGI} &= \left(2\beta_0\frac{g^2_{\rm LAT}}{16\pi^2}\right)^{-(\gamma_0/2\beta_0)} \\ &\quad\times\left(1 + \frac{\beta_1}{\beta_0}\frac{g^2_{\rm LAT}}{16\pi^2}\right)^{(\gamma_0\beta_1 - \gamma_1^{\rm LAT}\beta_0)/2\beta_0\beta_1}. \quad (79)\end{aligned}$$

Choosing $g_{\rm LAT} = g_{\Box}$ one has

$$\begin{aligned}\gamma_1^{\rm LAT} &= \gamma_1^{\Box} \\ &= \gamma_1^{\overline{\rm MS}} + 2\beta_0 C_F \Delta(c_{\rm SW}) + 16\pi^2\gamma_0\left(t_1 - \frac{1}{4}C_F\right), \quad (80)\end{aligned}$$

where [41–44]

$$\begin{aligned}t_1 &= 0.4682013 - (0.0066960 \\ &\quad - 0.0050467 c_{\rm SW} + 0.0298435 c^2_{\rm SW}) n_f. \quad (81)\end{aligned}$$

Tadpole improvement finally yields the result in TRB perturbation theory:

$$\begin{aligned}Z^{\rm RGI}_{\rm TRB} &= u_0^{1-n_D}\left(2\beta_0\frac{g^2_{\Box}}{16\pi^2}\right)^{-(\gamma_0/2\beta_0)} \\ &\quad\times\left(1 + \frac{\beta_1}{\beta_0}\frac{g^2_{\Box}}{16\pi^2}\right)^{((\gamma_0\beta_1 - \gamma_1^{\Box}\beta_0)/2\beta_0\beta_1) + \pi^2(1-n_D)C_F(\beta_0/\beta_1)}. \quad (82)\end{aligned}$$

Applying this formula we shall set again $c_{\rm SW} = 1$ to be consistent with lowest order perturbation theory.

For the operators $\mathcal{O}^S$, $\mathcal{O}^P$, $\mathcal{O}^V_\mu$, $\mathcal{O}^A_\mu$, and $\mathcal{O}^T_{\mu\nu}$ without derivatives two-loop calculations of the renormalization factors in lattice perturbation theory have recently appeared [3,4]. The various improvement schemes can be applied also to these two-loop expressions. However, the resulting formulas become considerably more complicated. Therefore we defer the corresponding discussion to Appendix D.

IX. PERTURBATIVE SUBTRACTION OF LATTICE ARTIFACTS

In the perturbative form (67) of the renormalization factors the lattice spacing a only appears in the logarithm (and implicitly in the bare gauge coupling g). In the remaining contributions the limit $a \to 0$ has been performed at fixed μ leading to the finite constant Δ. In this way all lattice artifacts vanishing like powers of a have been eliminated. However, there is no need to do so. In fact, $a\mu$ is not necessarily small in our Monte Carlo results. Hence it is worthwhile to keep a finite and to compare the lattice artifacts in the perturbative expressions with their nonperturbative counterparts.

To do this we simply write down the one-loop integrals for general external momentum p and perform the integrations numerically. The integrals can no longer be reduced to a small number of standard integrals, they have to be done independently at each value of p, and can only be obtained in numerical form. They will in general not only depend on p^2 but also on the direction of the momentum.

For general p we can write the one-loop expression for $Z^{\rm RI'\text{-}MOM}_{\rm bare}$ in the form

$$Z^{\rm RI'\text{-}MOM}_{\rm bare}(p, a) = 1 + \frac{g^2}{16\pi^2} C_F F(p, a) + O(g^4), \quad (83)$$

where the quark mass has been set equal to zero. Neglecting all contributions which vanish as $a \to 0$ we get from $F(p, a)$ the expression $\tilde{F}(p, a)$; e.g., for the scalar density $\mathcal{O}^S$ it is given by

$$\begin{aligned}\tilde{F}(p, a) &= 3\ln(a^2p^2) - 16.9524 - 7.73792 c_{\rm SW} \\ &\quad + 1.38038 c^2_{\rm SW} \quad (84)\end{aligned}$$

in the Landau gauge. The difference between F and $\tilde{F}$ represents the lattice artifacts in one-loop perturbation theory. Though being $O(a^2)$, $F - \tilde{F}$ can be fairly large for the momenta in the actual simulations. An example for the case of the scalar density $\mathcal{O}^S$ is shown in Fig. 6.

We can (and will) use this calculated difference to correct for the discretization errors in our lattice data (see also Ref. [45]). We take

$$D(p, a) = F(p, a) - \tilde{F}(p, a) \quad (85)$$

as an estimate of the perturbative discretization errors in our Monte Carlo renormalization constants $Z^{\rm RI'\text{-}MOM}_{\rm bare}(p, a)_{\rm MC}$ and define subtracted renormalization constants by

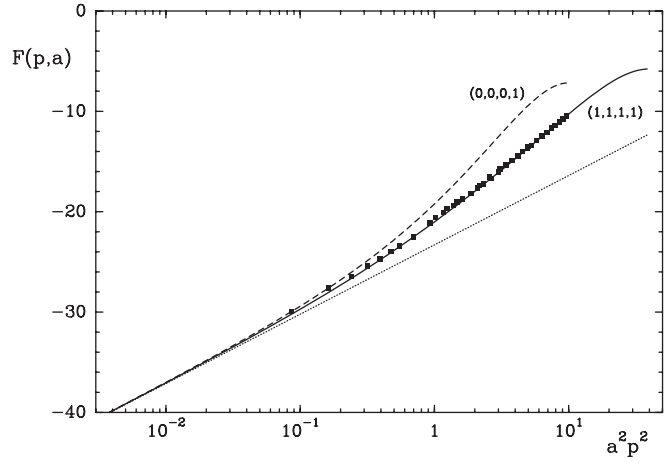

FIG. 6. Lattice artifacts for the scalar density. The dotted straight line shows $\tilde{F}(p, a)$, while the two other curves represent $F(p, a)$ for the momentum directions indicated in the plot. The black squares denote the values of $F(p, a)$ at the momenta used on the $16^3 \times 32$ lattices, which have been chosen close to the diagonal of the Brillouin zone.

$$Z_{\text{bare}}^{\text{RI}'\text{-MOM}}(p, a)_{\text{MC,sub}} = Z_{\text{bare}}^{\text{RI}'\text{-MOM}}(p, a)_{\text{MC}} - \frac{g_{\Box}^2}{16\pi^2} C_F D(p, a) \qquad (86)$$

employing boosted perturbation theory with u_0 in $g_{\Box}$ taken at the respective κ value, i.e., before the chiral extrapolation. Working consistently with one-loop perturbation theory we set $c_{\text{SW}} = 1$. This procedure removes all the g^2a^2 discretization terms in $Z_{\text{bare}}^{\text{RI}'\text{-MOM}}(p, a)_{\text{MC}}$, leaving lattice artifacts $O(g^4a^2)$. As we shall see, the use of the boosted coupling $g_{\Box}$ seems to do a reasonable job of estimating the higher-order discretization effects.

Unfortunately, this procedure becomes rather cumbersome for operators with more than one derivative. So we can use it only for the quark wave function renormalization, the currents, and the operators with one derivative.

X. EXTRACTING THE RENORMALIZATION FACTORS

The simplest procedure for obtaining a value of $Z^{\text{RGI}}(a)$ would be to plot the right-hand side of Eq. (54), i.e., of the relation

$$Z^{\text{RGI}}(a) = \Delta Z^{\mathcal{S}}(M = \mu_p) Z^{\mathcal{S}}_{\text{RI}'\text{-MOM}}(M = \mu_p) \times Z_{\text{bare}}^{\text{RI}'\text{-MOM}}(\mu_p, a), \qquad (87)$$

versus μ_p and to read off $Z^{\text{RGI}}(a)$ in an interval of μ_p where the inequalities (32) are satisfied. In this region the value of $Z^{\text{RGI}}(a)$ would be independent of μ_p, i.e., one would observe a plateau, and one could determine the final result by fitting a constant to the data for $Z^{\text{RGI}}(a)$. Examples of such plots before and after the perturbative subtraction of lattice artifacts are shown in Fig. 7, and in Fig. 8 subtracted and

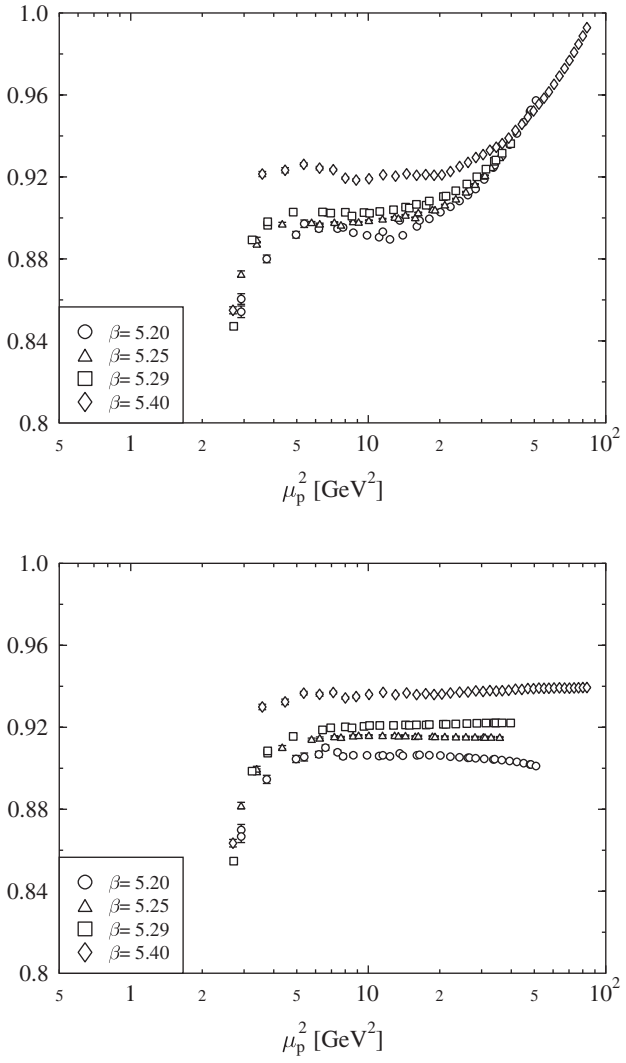

FIG. 7. Z^{RGI} for the operator $\bar{O}_T$ before (upper plot) and after (lower plot) the perturbative subtraction of lattice artifacts.

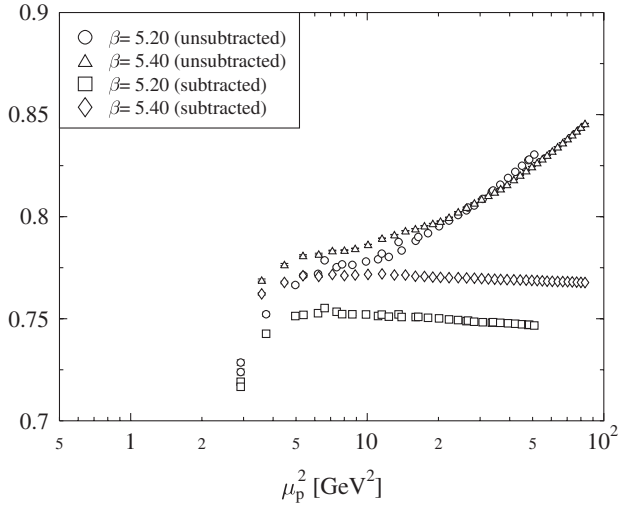

FIG. 8. Z^{RGI} for the quark field renormalization constant Z_q before and after the perturbative subtraction of lattice artifacts.

unsubtracted results for the quark field renormalization constant Z_q are directly compared at $\beta = 5.20$ and $\beta = 5.40$. Equivalently one could fit the values obtained for $Z^{\mathcal{S}}_{\mathrm{bare}}(\mu_p, a) = Z^{\mathcal{S}}_{\mathrm{RI'\text{-}MOM}}(\mu_p) Z^{\mathrm{RI'\text{-}MOM}}_{\mathrm{bare}}(\mu_p, a)$ in the plateau region by $\Delta Z^{\mathcal{S}}(\mu_p)^{-1} Z^{\mathrm{RGI}}(a)$ (with $Z^{\mathrm{RGI}}(a)$ as fit parameter) using the most accurate perturbative expressions for $Z^{\mathcal{S}}_{\mathrm{RI'\text{-}MOM}}$ and $\Delta Z^{\mathcal{S}}$.

However, in our actual simulations it is not so clear how well the inequalities (32) are fulfilled, and there are two effects to be considered that jeopardize the reliability of this approach. First, there will be lattice artifacts which vanish like powers (up to logarithms) of a for $a \to 0$ [28,29]. In order to reduce the corresponding contamination one would like to perform the fit at small values of μ_p. Second, the truncation of the perturbative expansions in $\Delta Z^{\mathcal{S}}$ and $Z^{\mathcal{S}}_{\mathrm{RI'\text{-}MOM}}$ will produce noticeable effects in the region of small μ_p leading, in particular, to a dependence of the results on the intermediate scheme $\mathcal{S}$. In order to minimize the related uncertainties one would like to move the fit interval to large values of μ_p. Because of these conflicting requirements it is a nontrivial matter to extract a final value for Z^{RGI} from the data.

Let us first investigate to which extent we can separate truncation effects from lattice artifacts. According to Eq. (54), $Z^{\mathcal{S}}_{\mathrm{bare}}(\mu_p, a) = Z^{\mathcal{S}}_{\mathrm{RI'\text{-}MOM}}(\mu_p) Z^{\mathrm{RI'\text{-}MOM}}_{\mathrm{bare}}(\mu_p, a)$ can be written as

$$Z^{\mathcal{S}}_{\mathrm{bare}}(\mu_p, a) = \Delta Z^{\mathcal{S}}(\mu_p)^{-1} Z^{\mathrm{RGI}}(a). \tag{88}$$

In this way, we have factorized the dependence of $Z^{\mathcal{S}}_{\mathrm{bare}}(\mu_p, a)$ on the renormalization scale μ_p and on the cutoff a. Consequently we can write

$$Z^{\mathcal{S}}_{\mathrm{bare}}(\mu_p, a) = \frac{Z^{\mathrm{RGI}}(a)}{Z^{\mathrm{RGI}}(a')} Z^{\mathcal{S}}_{\mathrm{bare}}(\mu_p, a'). \tag{89}$$

Hence multiplication by an appropriate (μ_p-independent) scaling factor should bring the values of $Z^{\mathcal{S}}_{\mathrm{bare}}(\mu_p, a)$ obtained for different values of a (or β) onto a single curve representing a function $f^{\mathcal{S}}(\mu_p)$ of μ_p only, provided μ_p is small enough so that lattice artifacts can be neglected. Note that the ratio $Z^{\mathcal{S}}_{\mathrm{bare}}(s\mu_p, a)/Z^{\mathcal{S}}_{\mathrm{bare}}(\mu_p, a)$ for some fixed value of s, the so-called step scaling function, has a decent continuum limit. This coincides with $f^{\mathcal{S}}(s\mu_p)/f^{\mathcal{S}}(\mu_p)$ in the region where $f^{\mathcal{S}}(\mu_p)$ is well defined.

In most cases, this collapse onto a single function works quite well for a reasonable range of renormalization scales, even if mixing is allowed. For an example see Fig. 9. So the factorization of μ_p dependence and a dependence seems to be possible (except for the highest values of μ_p).

However, the available perturbative results cannot describe the μ_p dependence below $\mu_p^2 \approx 5\ \mathrm{GeV}^2$, as exemplified by Fig. 7. It would be interesting to investigate whether this observation is related to the claim [46] that Dokshitzer-Gribov-Lipatov-Altarelli-Parisi (DGLAP) evolution cannot be used below $Q^2 = 5\ \mathrm{GeV}^2$ (at least in the region of larger values of Bjorken's variable x [47]). Note also that an even later onset of (three-loop) perturbative behavior has been found for the quenched gluon propagator [48,49].

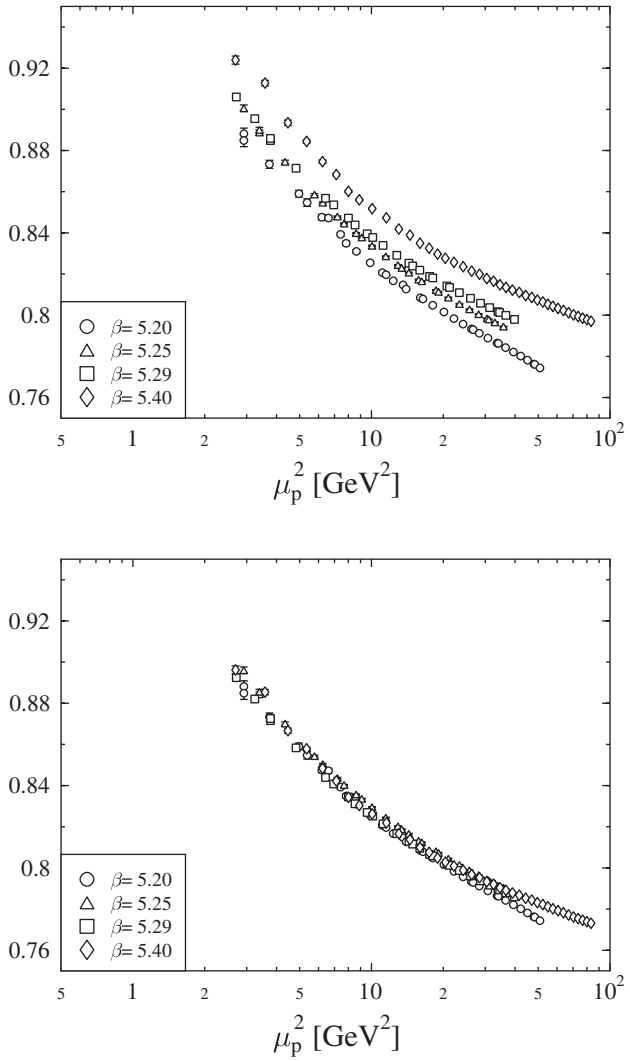

FIG. 9. $Z^{\mathrm{MOM}}_{\mathrm{bare}}$ (perturbatively subtracted) for the operator $\bar{\mathcal{O}}_T$ as a function of the renormalization scale μ_p. The upper plot shows the actual results. In the lower plot they have been multiplied by suitable (μ_p-independent) scaling factors.

In Fig. 7 we have taken $\mathcal{S} = \mathrm{MOM}$ and we have exploited the freedom to select the scheme $\mathcal{S}'$ for the coupling used in the perturbative expansion of $Z^{\mathcal{S}}_{\mathrm{RI'\text{-}MOM}}$ choosing $\mathcal{S}' = \widetilde{\mathrm{MOM}}\mathrm{gg}$. Generally, the plateaus in Z^{RGI} look better for $\mathcal{S} = \mathrm{MOM}$ than for $\mathcal{S} = \overline{\mathrm{MS}}$. This may be due to the fact that the perturbative expansion of $Z^{\mathcal{S}}_{\mathrm{RI'\text{-}MOM}}$ seems to be better behaved for $\mathcal{S} = \mathrm{MOM}$. For $\mathcal{S}'$, the choice $\mathcal{S}' = \widetilde{\mathrm{MOM}}\mathrm{gg}$ turns out to be preferable. An example comparing results obtained with $\mathcal{S} = \overline{\mathrm{MS}}$, $\mathcal{S}' = \overline{\mathrm{MS}}$ to results obtained with $\mathcal{S} = \mathrm{MOM}$, $\mathcal{S}' = \widetilde{\mathrm{MOM}}\mathrm{gg}$ is

shown in Fig. 10. Note that the difference between the two sets of results is caused by the different truncation errors of the respective perturbative expansions.

In order to account for the deviations of the data from a perfect plateau, e.g., due to lattice artifacts and the truncation of the perturbative expansions, we have then applied a more complicated procedure than a simple fit with a constant. In particular, one should take into account that residual lattice artifacts and truncation errors might conspire to produce a fake plateau. Therefore we consider it important to include correction terms for both types of errors. We have tried to incorporate higher terms in the perturbative expansions of $\Delta Z^{\mathcal{S}}(\mu_p)$ and $Z^{\mathcal{S}}_{\mathrm{RI}'\text{-MOM}}(\mu_p)$ treating the corresponding coefficients as additional fit parameters. Similarly we have attempted to correct for discretization effects by including a simple ansatz for lattice artifacts. Again, the parameters in this ansatz have to be fitted. Nevertheless, the number of fit parameters will not get too large because we fit the data for all four β values simultaneously. Only the quantities $Z^{\mathrm{RGI}}(a)$, our final results, depend on β; the other parameters do not.

When we perform the fits we make the following choices. In the expansions for $Z^{\mathcal{S}}_{\mathrm{RI}'\text{-MOM}}(\mu_p)$ and $\Delta Z^{\mathcal{S}}(\mu_p)$ originating from continuum perturbation theory we use as many terms as are available. The same applies to the β function used when computing the running coupling $g^{\mathcal{S}}(\mu_p)$. We choose the MOM scheme as the intermediate scheme $\mathcal{S}$ and expand $Z^{\mathcal{S}}_{\mathrm{RI}'\text{-MOM}}$ in the $\widetilde{\mathrm{MOM}}$gg coupling. All data for $\mu_p^2 \geq 10\ \mathrm{GeV}^2$ are included in the fit. The correlations between the data at different momenta but the same β are not taken into account. Two examples of such fits are shown in Fig. 11. More details concerning the fit procedure can be found in Appendix E.

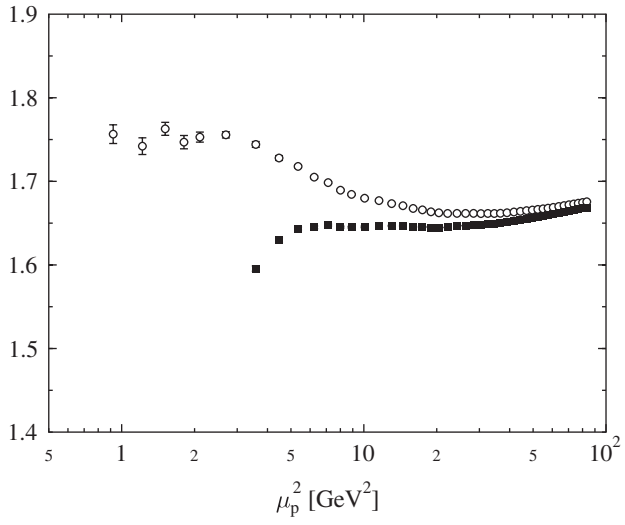

FIG. 10. Z^{RGI} (perturbatively subtracted) for the operator $\bar{\mathcal{O}}_{h_{1,a}}$ at $\beta = 5.40$ as a function of the renormalization scale μ_p. The open circles (filled squares) have been obtained with $\mathcal{S} = \mathcal{S}' = \overline{\mathrm{MS}}$ ($\mathcal{S} = \mathrm{MOM}$, $\mathcal{S}' = \widetilde{\mathrm{MOM}}$gg).

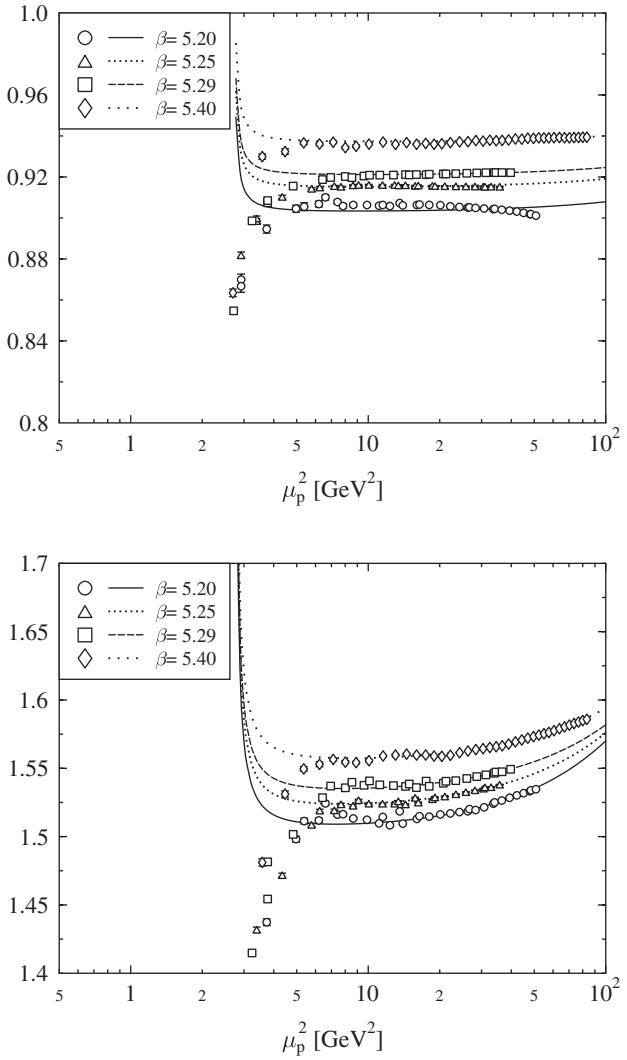

FIG. 11. Z^{RGI} (perturbatively subtracted) for the operators $\bar{\mathcal{O}}_T$ (upper plot) and $\bar{\mathcal{O}}_{v_{2,a}}$ (lower plot) as a function of the renormalization scale. Also shown are the fit curves used for the determination of Z^{RGI}.

In some cases, the data on our coarsest lattice ($\beta = 5.20$) are not very well reproduced by the fit; see, e.g., the upper plot in Fig. 11. Excluding these data would, however, lead only to tiny changes in the results. Therefore we have kept $\beta = 5.20$ in the fit for all operators. Note that the ''divergence'' of the fit curves (and the data) in the vicinity of $\mu_p^2 = 3\ \mathrm{GeV}^2$ is mainly caused by the Landau pole in the renormalized coupling constant in the $\widetilde{\mathrm{MOM}}$gg scheme.

While the fits for the subtracted data are reasonable it was hardly possible to obtain a satisfactory fit for the unsubtracted numbers. Although plots of unsubtracted data do not differ dramatically from plots of subtracted data (see Fig. 12 for results for an operator where no subtracted data are available), the fit curves look quite strange. Therefore we have to conclude that our fit

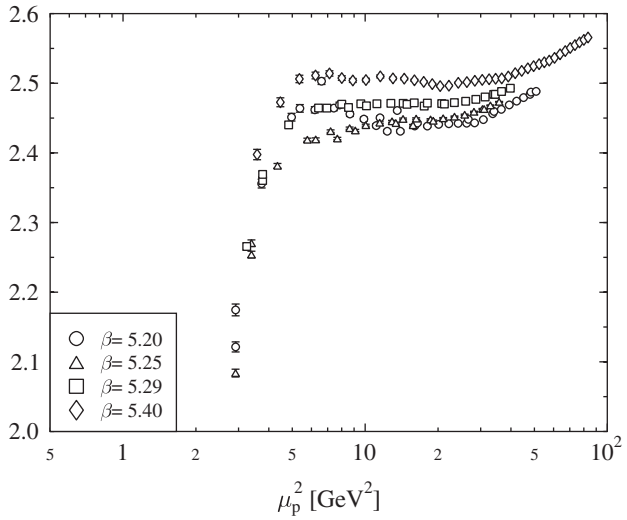

FIG. 12. Z^{RGI} for the operator $\bar{\mathcal{O}}_{h_{2,b}}$ as a function of the renormalization scale.

procedure is applicable only to perturbatively subtracted data and we must apply a different procedure to unsubtracted data. So we choose the following method. We read off Z^{RGI} at a reasonable value of μ_p^2 and take as the error the maximum of the differences with the results at one lower and one higher value of the scale. The choice of these three scales is to some extent dictated by the necessity to avoid large lattice artifacts as well as large truncation errors in the perturbative expansions. We take the values $\mu_p^2 = 10$ GeV^2, 20 GeV^2, and 30 GeV^2.

XI. RESULTS

Before we present and discuss our results we have to consider the influence of the two parameters that enter our analysis: the physical value of r_0 and $r_0\Lambda_{\overline{\mathrm{MS}}}$. The perturbative expressions which are needed in the evaluation of Z^{RGI} are functions of $\mu_p^2/\Lambda_{\overline{\mathrm{MS}}}^2$, where μ_p^2 is related to the momenta in lattice units q^2 by $a^2\mu_p^2 = q^2$. Since we use r_0 to set the scale we write

$$\mu_p^2 = \frac{(r_0/a)^2 q^2}{r_0^2} \tag{90}$$

so that

$$\frac{\mu_p^2}{\Lambda_{\overline{\mathrm{MS}}}^2} = \frac{(r_0/a)^2 q^2}{(r_0\Lambda_{\overline{\mathrm{MS}}})^2}. \tag{91}$$

This shows that the physical value of r_0 has an influence only on the scale μ_p to which a particular Z value is associated. As the question of the scale at which perturbation theory becomes applicable is not completely immaterial we shall set r_0 to a reasonable value, for which we take 0.467 fm [50,51] (see also Ref. [52]). However, the precise number does not matter too much because r_0 enters only logarithmically.

The value chosen for $r_0\Lambda_{\overline{\mathrm{MS}}}$, on the other hand, has an impact on the results for the renormalization factors. In particular, varying $r_0\Lambda_{\overline{\mathrm{MS}}}$ modifies the scale dependence of the right-hand side of Eq. (54) and improves or deteriorates the appearance of the plateau. We take $r_0\Lambda_{\overline{\mathrm{MS}}} = 0.617$ from Ref. [32], which is consistent with the value found in Ref. [53].

In order to estimate the systematic errors due to the uncertainties in the values of r_0 and $r_0\Lambda_{\overline{\mathrm{MS}}}$ we have repeated our analysis using $r_0 = 0.467$ fm, $r_0\Lambda_{\overline{\mathrm{MS}}} = 0.662$ and $r_0 = 0.5$ fm, $r_0\Lambda_{\overline{\mathrm{MS}}} = 0.617$ instead of our standard values $r_0 = 0.467$ fm, $r_0\Lambda_{\overline{\mathrm{MS}}} = 0.617$. Note that $r_0\Lambda_{\overline{\mathrm{MS}}} = 0.662$ results from $r_0\Lambda_{\overline{\mathrm{MS}}} = 0.617(40)(21)$ as given in Ref. [32] by adding the errors in quadrature. The ensuing differences will be shown in the same format as the (statistical) errors, however with the sign information included. For reasons of better readability they are given below the results themselves. The first (second) number corresponds to the difference caused by the variation of $r_0\Lambda_{\overline{\mathrm{MS}}}$ (r_0). For example, the entry

$$\begin{matrix} 0.45155(80) \\ (568)(15) \end{matrix}$$

means that the analysis with $r_0 = 0.467$ fm and $r_0\Lambda_{\overline{\mathrm{MS}}} = 0.617$ produced the result 0.45155 ± 0.00080 while using $r_0 = 0.467$ fm along with $r_0\Lambda_{\overline{\mathrm{MS}}} = 0.662$ led to 0.45723 and working with $r_0 = 0.5$ fm, $r_0\Lambda_{\overline{\mathrm{MS}}} = 0.617$ gave 0.45170. Note that the first error [(80) in the example] is determined from the deviation of the Z^{RGI} data from a perfect plateau as explained in more detail below, where also further sources of systematic errors will be discussed.

In the cases where lattice artifacts have been subtracted perturbatively as explained in Sec. IX we have determined values for Z^{RGI} by means of the fit procedure described in the previous section. The corresponding results will be called the fit results.

For unsubtracted data we apply the alternative method mentioned at the end of Sec. X. We evaluate Z^{RGI} at the scales $\mu_p^2 = 10$ GeV^2, 20 GeV^2, and 30 GeV^2, interpolating linearly in μ_p^2 between adjacent data points. We take the value at 20 GeV^2 as our central value and estimate the error from the maximum of the deviations of the values at the other two scales. This error is always larger (in most cases considerably larger) than the statistical error. These results will be called the interpolation results.

Of course, the same method can also be applied to the subtracted data. Except for $\mathcal{O}^S$ at $\beta = 5.20$, the error of the interpolation results is again larger than the statistical error. So, for the operators for which perturbatively subtracted data exist we have interpolation results and fit results, both based on the subtracted numbers, as well as interpolation results extracted from the unsubtracted data. For the operators for which no subtracted data are available we have only the interpolation results. Note that the v_4 operators are particularly difficult: $\Gamma_{\mathrm{Born}}(p)$ vanishes on the diagonal of

the Brillouin zone close to which all our momenta lie, and large lattice artifacts are obvious in the Monte Carlo data. So the corresponding nonperturbative results should be considered with caution.

Finally, we have to decide which numbers we want to consider as the most reliable results to be used in the applications. It is clear that we make use of the perturbatively subtracted data whenever they are available. In these cases our fits seem to exploit the Monte Carlo data in an optimal manner, and therefore we take the fit results as our final numbers. However, the errors computed by the MINUIT program [54] appear to be seriously underestimated as they are mainly determined by the statistical uncertainties. Hence we adopt a kind of hybrid approach taking the errors from the interpolation results (based on the subtracted numbers) because they take into account the deviation of our Z^{RGI} data from a perfect plateau. The uncertainties due to the scale setting and the value of $\Lambda_{\overline{\mathrm{MS}}}$ are again taken from the fit results.

For the operators with two or more derivatives we do not have much choice. So we take the interpolation results (including the systematic uncertainties) as our final numbers. All our final results are collected in Tables V (operators with at most one derivative, based on perturbatively subtracted data) and VI (operators with more than one derivative, based on unsubtracted data).

The impact of an uncertainty in r_0 or $r_0\Lambda_{\overline{\mathrm{MS}}}$ is easy to quantify and therefore given in Tables V and VI. Further systematic errors are more difficult to control. In particular, the error caused by gauge fixing is hard to estimate reliably. However, as already remarked above, the existing investigations indicate that the ''Gribov noise'' does not exceed the present statistical errors [25–27]. Since they are not the dominating uncertainty it seems justified to neglect the influence of Gribov copies although a more detailed study would clearly be desirable.

The necessity of gauge fixing in the Rome-Southampton approach has also another consequence: The operators of interest, though of course gauge invariant, can mix with non-gauge-invariant (NGI) operators. However, in perturbation theory this effect shows up only in two-loop order and can thus reasonably be expected to be small. NGI improvement terms for the quark propagator were discussed at some length in Refs. [55,56]. While $O(g^2)$ perturbation theory cannot distinguish between the gauge-invariant and NGI improvement terms, in an $O(g^3)$ calculation of the qqg vertex [57], we could calculate the NGI improvement coefficient, and found it indeed to be numerically small. Mixing with gauge-invariant operators, on the other hand, can in most cases be excluded by means of symmetry arguments (see Sec. II).

TABLE V. Final nonperturbative results for operators with at most one derivative obtained with $r_0 = 0.467$ fm and $r_0\Lambda_{\overline{\mathrm{MS}}} = 0.617$ from perturbatively subtracted data. Estimates of systematic errors have been included.

Operator	$Z^{\mathrm{RGI}}\|_{\beta=5.20}$	$Z^{\mathrm{RGI}}\|_{\beta=5.25}$	$Z^{\mathrm{RGI}}\|_{\beta=5.29}$	$Z^{\mathrm{RGI}}\|_{\beta=5.40}$
$\mathcal{O}^S$	0.45061(28)	0.44990(65)	0.44880(72)	0.45155(80)
	(608)(21)	(593)(18)	(584)(17)	(568)(15)
$\mathcal{O}^P$	0.3376(95)	0.3422(95)	0.347(11)	0.367(11)
	(43)(−5)	(42)(−6)	(4)(−1)	(4)(−1)
$\bar{\mathcal{O}}_V$	0.7228(35)	0.7323(28)	0.7373(37)	0.7513(25)
	(−3)(1)	(−3)(1)	(−3)(2)	(−3)(1)
$\bar{\mathcal{O}}_A$	0.7527(21)	0.76024(78)	0.76439(30)	0.77682(54)
	(1)(−8)	(6)(−70)	(6)(−62)	(6)(−60)
$\bar{\mathcal{O}}_T$	0.9027(16)	0.91453(58)	0.92055(68)	0.9368(14)
	(−40)(−1)	(−390)(−6)	(−389)(1)	(−39)(0)
Z_q	0.7501(18)	0.7557(12)	0.75958(80)	0.7703(14)
	(−7)(−6)	(−7)(−6)	(−66)(−49)	(−7)(−5)
$\bar{\mathcal{O}}_{v_{2,a}}$	1.5028(47)	1.5182(58)	1.5298(61)	1.5526(54)
	(−164)(8)	(−162)(7)	(−161)(6)	(−159)(6)
$\bar{\mathcal{O}}_{v_{2,b}}$	1.5089(56)	1.5233(81)	1.5336(96)	1.5555(28)
	(−159)(−7)	(−156)(−5)	(−157)(−5)	(−155)(−6)
$\bar{\mathcal{O}}_{r_{2,a}}$	1.4920(17)	1.5071(38)	1.5194(55)	1.5430(34)
	(−159)(0)	(−156)(1)	(−156)(−1)	(−154)(0)
$\bar{\mathcal{O}}_{r_{2,b}}$	1.5382(23)	1.5514(67)	1.5614(92)	1.5822(15)
	(−159)(−15)	(−158)(−14)	(−158)(−13)	(−155)(−12)
$\bar{\mathcal{O}}_{h_{1,a}}$	1.5791(39)	1.5963(58)	1.6096(41)	1.6363(37)
	(−187)(0)	(−185)(1)	(−185)(0)	(−184)(−1)
$\bar{\mathcal{O}}_{h_{1,b}}$	1.5989(43)	1.6155(63)	1.6282(47)	1.6541(44)
	(−191)(−1)	(−189)(0)	(−188)(0)	(−186)(−1)

TABLE VI. Final nonperturbative results for operators with two and three derivatives obtained with $r_0 = 0.467$ fm and $r_0\Lambda_{\overline{\rm MS}} = 0.617$ from unsubtracted data. Estimates of systematic errors have been included.

Operator	$Z^{\rm RGI}\|_{\beta=5.20}$	$Z^{\rm RGI}\|_{\beta=5.25}$	$Z^{\rm RGI}\|_{\beta=5.29}$	$Z^{\rm RGI}\|_{\beta=5.40}$
$\bar{\mathcal{O}}_{v_3}$	2.3796(97)	2.385(23)	2.410(30)	2.4337(69)
	(−481)(17)	(−48)(5)	(−49)(−2)	(−489)(18)
$\bar{\mathcal{O}}_{v_{3,a}}$	2.3586(70)	2.365(13)	2.385(18)	2.4084(98)
	(−501)(0)	(−50)(4)	(−51)(3)	(−515)(13)
$\bar{\mathcal{O}}_{r_3}$	2.3979(67)	2.401(25)	2.426(32)	2.4488(59)
	(−485)(7)	(−49)(4)	(−49)(−3)	(−492)(14)
$\bar{\mathcal{O}}_{a_2}$	2.357(14)	2.360(11)	2.383(24)	2.4084(94)
	(−50)(−2)	(−50)(3)	(−51)(2)	(−515)(4)
$\bar{\mathcal{O}}_{h_{2,a}}$	2.4265(77)	2.435(14)	2.4588(69)	2.486(10)
	(−518)(10)	(−52)(4)	(−525)(6)	(−53)(1)
$\bar{\mathcal{O}}_{h_{2,b}}$	2.4408(68)	2.448(14)	2.4710(76)	2.4967(79)
	(−521)(13)	(−52)(4)	(−528)(8)	(−533)(13)
$\bar{\mathcal{O}}_{h_{2,c}}$	2.4363(72)	2.444(14)	2.4680(68)	2.494(10)
	(−520)(4)	(−52)(4)	(−527)(4)	(−53)(1)
$\bar{\mathcal{O}}_{h_{2,d}}$	2.420(10)	2.427(19)	2.450(12)	2.475(11)
	(−52)(2)	(−52)(5)	(−52)(2)	(−53)(2)
$\bar{\mathcal{O}}_{v_4}$	3.59(25)	3.60(12)	3.631(47)	3.720(87)
	(−9)(−1)	(−9)(−5)	(−93)(−11)	(−95)(−141)

A few further systematic uncertainties can be estimated more easily. We have tested the sensitivity to the chiral extrapolation by repeating the analysis employing a quadratic chiral extrapolation [see Eq. (40)]. This changed the results by less than 1%, except for the case of $\bar{\mathcal{O}}_{v_4}$ at $\beta = 5.20$, where a change of 1.8% was observed. In order to estimate the error caused by the truncation of the perturbative series we have reduced the order of all perturbative expressions involved by one compared to the maximal value available. This led to changes of at most 1%. Finally, we have considered the uncertainty related to the chiral extrapolation of r_0/a. Since little is known about the quark mass dependence of r_0, we had to rely on some phenomenological ansatz [32] leading to chirally extrapolated values of r_0/a with errors of the order of 1% (see Table III). Varying the values of r_0/a used in the analysis by 1% produced changes of at most 0.5% in the results for $Z^{\rm RGI}$. Thus it seems justified to assign an additional uncertainty of about 2% to our results.

In the case of the perturbative estimates we consider the choices "bare PT," "TI PT," and "TRB PT". Here bare PT and TI PT refer to the expressions $\Delta Z^{\overline{\rm MS}}(\mu_0) Z^{\overline{\rm MS}}_{\rm bare}(\mu_0, a)_{\rm pert}$ and $\Delta Z^{\overline{\rm MS}}(\mu_0) Z^{\overline{\rm MS}}_{\rm bare}(\mu_0, a)_{\rm ti}$, respectively, both evaluated at $\mu_0 = 1/a$ [see Eqs. (73) and (74)]; TRB PT corresponds to the estimate by tadpole-improved, renormalization-group-improved boosted perturbation theory in Eq. (82). Because of our choice $\mu_0 = 1/a$ the perturbative estimates do not depend on r_0. The bare PT and TI PT values do however depend on $r_0\Lambda_{\overline{\rm MS}}$ as well as on the intermediate scheme $\mathcal{S}$, which was taken to be the $\overline{\rm MS}$ scheme in Eqs. (73) and (74). We stick to this choice and set $r_0\Lambda_{\overline{\rm MS}} = 0.617$. The TRB PT value, on the other hand, is independent of these choices. Note, however, that all three perturbative estimates depend on the chosen value of $c_{\rm SW}$. As remarked above, we have set $c_{\rm SW} = 1$. For the operators without derivatives we give the resulting numbers in Table VII. The analogous results obtained from the two-loop calculations as described in Appendix D are given in Table VIII. All these perturbative numbers apply to any member of the $H(4)$ multiplet to which the operator listed belongs.

TABLE VII. Perturbative estimates for $Z^{\rm RGI}$ based on one-loop lattice perturbation theory. The intermediate scheme $\mathcal{S}$ is taken to be the $\overline{\rm MS}$ scheme and $r_0\Lambda_{\overline{\rm MS}} = 0.617$. In all cases $c_{\rm SW} = 1$ is used.

Operator		$Z^{\rm RGI}\|_{\beta=5.20}$	$Z^{\rm RGI}\|_{\beta=5.25}$	$Z^{\rm RGI}\|_{\beta=5.29}$	$Z^{\rm RGI}\|_{\beta=5.40}$
$\mathcal{O}^S$	bare PT	0.5602	0.5532	0.5486	0.5399
	TI PT	0.4902	0.4865	0.4843	0.4811
	TRB PT	0.4637	0.4615	0.4598	0.4553
$\mathcal{O}^P$	bare PT	0.5396	0.5331	0.5288	0.5209
	TI PT	0.4573	0.4547	0.4533	0.4519
	TRB PT	0.4398	0.4382	0.4370	0.4336
$\mathcal{O}^V_\mu$	bare PT	0.8507	0.8521	0.8532	0.8562
	TI PT	0.7721	0.7760	0.7792	0.7872
	TRB PT	0.7800	0.7837	0.7866	0.7940
$\mathcal{O}^A_\mu$	bare PT	0.8656	0.8669	0.8679	0.8706
	TI PT	0.7959	0.7994	0.8023	0.8094
	TRB PT	0.8008	0.8042	0.8069	0.8136
$\mathcal{O}^T_{\mu\nu}$	bare PT	0.9811	0.9878	0.9926	1.0029
	TI PT	0.9212	0.9296	0.9357	0.9494
	TRB PT	0.9547	0.9617	0.9673	0.9815

TABLE VIII. Perturbative estimates for Z^{RGI} based on two-loop lattice perturbation theory. The intermediate scheme $\mathcal{S}$ is taken to be the $\overline{\mathrm{MS}}$ scheme and $r_0\Lambda_{\overline{\mathrm{MS}}} = 0.617$. In all cases the one-loop value for c_{SW} is used.

Operator		$Z^{\mathrm{RGI}}\|_{\beta=5.20}$	$Z^{\mathrm{RGI}}\|_{\beta=5.25}$	$Z^{\mathrm{RGI}}\|_{\beta=5.29}$	$Z^{\mathrm{RGI}}\|_{\beta=5.40}$
$\mathcal{O}^S$	bare PT	0.5165	0.5110	0.5074	0.5012
	TI PT	0.4618	0.4596	0.4585	0.4578
	TRB PT	0.4577	0.4558	0.4543	0.4503
$\mathcal{O}^P$	bare PT	0.4860	0.4813	0.4784	0.4735
	TI PT	0.4175	0.4170	0.4171	0.4192
	TRB PT	0.4201	0.4194	0.4188	0.4170
$\mathcal{O}^V_\mu$	bare PT	0.7861	0.7887	0.7908	0.7963
	TI PT	0.6943	0.7013	0.7068	0.7204
	TRB PT	0.7067	0.7129	0.7179	0.7301
$\mathcal{O}^A_\mu$	bare PT	0.8101	0.8124	0.8142	0.8191
	TI PT	0.7320	0.7380	0.7428	0.7545
	TRB PT	0.7401	0.7456	0.7500	0.7608
$\mathcal{O}^T_{\mu\nu}$	bare PT	0.9789	0.9857	0.9905	1.0009
	TI PT	1.0007	1.0064	1.0105	1.0190
	TRB PT	1.0085	1.0136	1.0178	1.0285

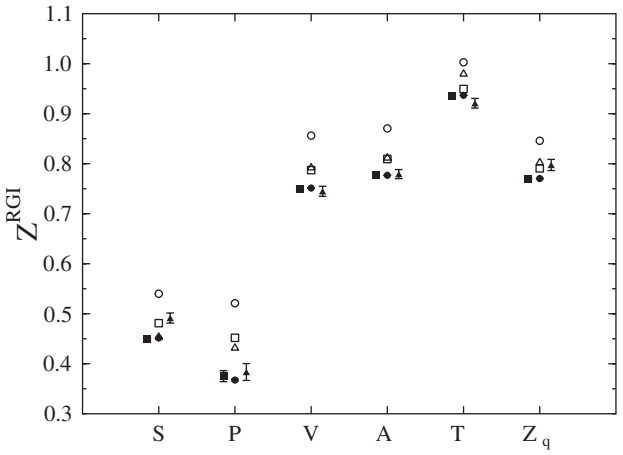

FIG. 13. Results for operators without derivatives at $\beta = 5.40$. The filled symbols correspond to our fit results (circles), interpolation results based on subtracted (squares), and unsubtracted (triangles) data. Our final numbers are the fit results with the errors taken from the interpolation results based on the subtracted data. The open symbols represent estimates from bare perturbation theory (circles), tadpole-improved perturbation theory (squares), and TRB perturbation theory (triangles) based on one-loop calculations.

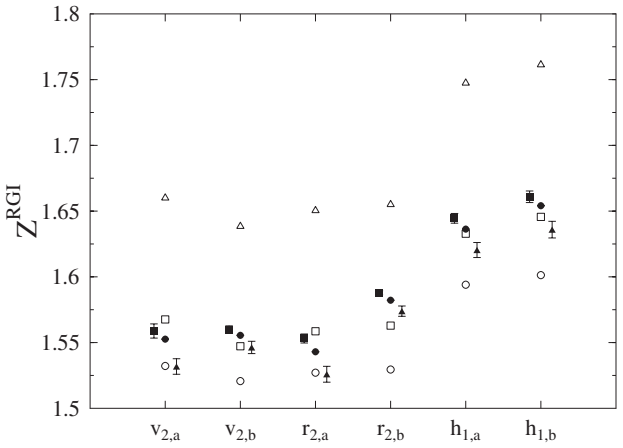

FIG. 14. Results for operators with one derivative at $\beta = 5.40$. The filled symbols correspond to our fit results (circles), interpolation results based on subtracted (squares), and unsubtracted (triangles) data. Our final numbers are the fit results with the errors taken from the interpolation results based on the subtracted data. The open symbols represent estimates from bare perturbation theory (circles), tadpole-improved perturbation theory (squares), and TRB perturbation theory (triangles) based on one-loop calculations.

Let us now compare the results obtained by the various methods, i.e., by the different procedures of extracting Z^{RGI} from the Monte Carlo data and by the different versions of lattice perturbation theory. In particular, for the operators for which perturbatively subtracted data exist we can compare the results extracted from the perturbatively subtracted data, both by interpolation and by means of the fit procedure, and the interpolation results based on the unsubtracted numbers. Of course, ideally they should agree within the errors. In reality, this is not always true. Note, however, that the errors of the fit results only account for the (rather small) statistical uncertainties of the raw data while the errors of the interpolation results are dominated by systematic effects.

Figures 13–15 give an overview of our results for $\beta = 5.40$. The corresponding plots for the other β values look similar. For the operators without derivatives (see Fig. 13) the nonperturbative results obtained with the different methods (with and without perturbative subtraction of lattice artifacts) are well consistent in most cases. The one-loop perturbative estimates are larger, but tadpole improvement works. TRB perturbation theory, on the other hand, leads to further improvement only in a few cases, for some operators it is even worse than ordinary tadpole-improved perturbation theory.

In the case of the operators with one derivative (see Fig. 14) the agreement between the different methods for the nonperturbative results is less convincing, in particular, the interpolation results obtained without perturbative subtraction of lattice artifacts lie about 1–2% lower. Also the numbers from bare perturbation theory are smaller than the nonperturbative results. Again, tadpole improvement moves the perturbative estimates in the right direction, though too far in some cases. However, TRB perturbation theory leads to a significant overestimation.

For operators with two derivatives (see Fig. 15) the only nonperturbative numbers we have at our disposal are those obtained without perturbative subtraction of lattice artifacts. Since the corresponding results for operators with one derivative lie consistently below those coming from

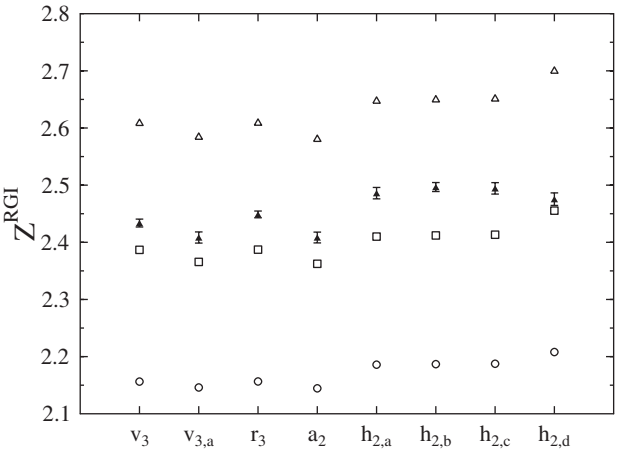

FIG. 15. Results for operators with two derivatives at $\beta = 5.40$. The filled triangles correspond to our nonperturbative results obtained by the interpolation method. The open symbols represent estimates from bare perturbation theory (circles), tadpole-improved perturbation theory (squares), and TRB perturbation theory (triangles) based on one-loop calculations.

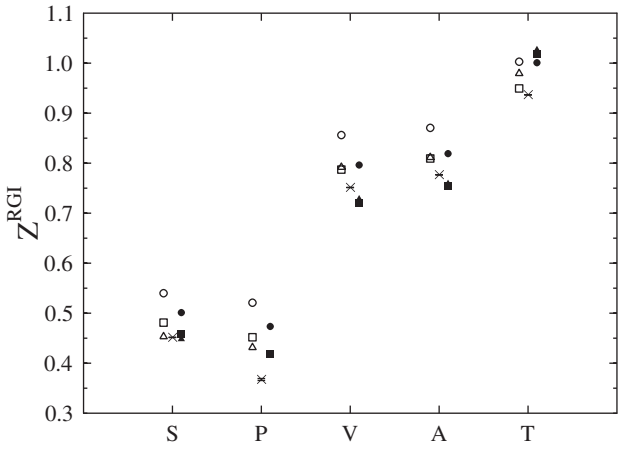

FIG. 16. Results for operators without derivatives at $\beta = 5.40$. The crosses correspond to our nonperturbative results obtained by fits of the subtracted data. The open symbols represent estimates from bare perturbation theory (circles), tadpole-improved perturbation theory (squares), and TRB perturbation theory (triangles) in the one-loop approximation. The corresponding estimates based on two-loop calculations are shown by the filled symbols.

the perturbatively subtracted data, it is tempting to guess that this is also the case for operators with two derivatives though we cannot quantify the difference. The behavior of the perturbative estimates is similar to that observed for operators with one derivative. Bare perturbation theory underestimates the results considerably, while tadpole-improved perturbation theory comes much closer to the nonperturbative numbers. The results from TRB perturbation theory lie too high again. It should however be noted that the relative positions of the nonperturbative renormalization factors for almost all operators considered are surprisingly well reproduced by any of the perturbative estimates.

In Fig. 16 we plot our fit results for the operators without derivatives together with the one-loop and two-loop perturbative estimates, again for $\beta = 5.40$. Let us comment on the numbers from bare lattice perturbation theory first, represented by circles in the figure. They exhibit the expected behavior: The two-loop results come closer to the nonperturbative numbers than the one-loop estimates, though only slightly in the case of the tensor current $\mathcal{O}^T_{\mu\nu}$. Except for the tensor current, tadpole improvement works also in the two-loop approximation moving the perturbative values, indicated by squares, closer to the nonperturbative numbers. However, the results from TRB perturbation theory, shown by triangles, do not differ much from the values found by tadpole-improved two-loop perturbation theory. At the moment it is unclear why the tensor current shows such a peculiar behavior.

The perturbative estimates can easily be calculated at arbitrary values of the bare coupling constant g. However, for tadpole improvement one also needs nonperturbative values for u_0 (or for the average plaquette $P = u_0^4$) at these couplings. Such values can (approximately) be obtained from the results for P given in Table III by a simple Padé fit taking into account the known two-loop expression for P [58]. In Fig. 17 we plot the tadpole-improved perturbative results for the renormalization factor of the local axial current $\mathcal{O}^A_\mu$ in the one- and two-loop aproximation along with our nonperturbative numbers and those from the ALPHA Collaboration [59].

In a few cases we can compare our nonperturbative renormalization factors with results obtained by other methods. The renormalization factor of the local vector

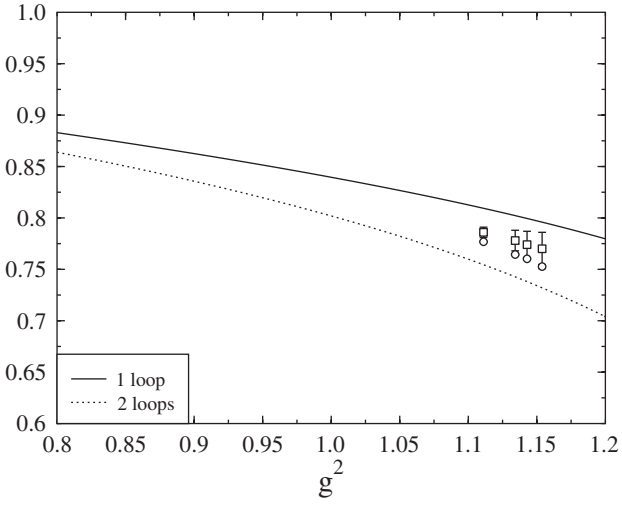

FIG. 17. Renormalization factor of the local axial current as a function of g^2. The curves represent one- and two-loop tadpole-improved perturbation theory. The circles are our nonperturbative results from Table V. The squares are numbers obtained by the ALPHA Collaboration [59].

TABLE IX. Results from alternative approaches. See Table 3 in Ref. [60] for Z_V, Eq. (3.7) in Ref. [61] for Z_V (ALPHA), and Eq. (4.10) in Ref. [59] for Z_A (ALPHA). The numbers for Z_m in Ref. [62] are taken from Table III in that reference.

	$Z^{\mathrm{RGI}}\|_{\beta=5.20}$	$Z^{\mathrm{RGI}}\|_{\beta=5.25}$	$Z^{\mathrm{RGI}}\|_{\beta=5.29}$	$Z^{\mathrm{RGI}}\|_{\beta=5.40}$
Z_V	0.7304(18)	0.7357(13)	0.7420(7)	
Z_V (ALPHA)	0.739(5)	0.744(5)	0.749(5)	0.759(5)
Z_A (ALPHA)	0.770(16)	0.774(13)	0.778(11)	0.786(5)
Z_m [62]	2.270(12)	2.191(24)	2.177(14)	2.124(6)
Z_m (this work)	2.230(63)	2.222(62)	2.203(70)	2.117(63)

current $\mathcal{O}^V_\mu$, usually called Z_V, can also be extracted from hadron three-point functions by considering the time component of the current and imposing charge conservation. Some time ago we have employed this approach in the case of the nucleon [60] on a subset of the gauge field ensembles used in the present work. The results are given in Table IX along with the renormalization factor of the local axial current $\mathcal{O}^A_\mu$, usually called Z_A, obtained by the ALPHA Collaboration by means of the Schrödinger functional method [59]. We also include the results for Z_V from the ALPHA Collaboration [61]. Note that in these determinations no gauge fixing is required. Hence the reasonable agreement of the numbers in Table IX with those found in the present work indicates that the Gribov noise is small.

In addition, we give in this table values for $Z_m^{\mathrm{RGI}} = (Z_A/Z_P)^{\mathrm{RGI}}$, where Z_P is the renormalization factor of the pseudoscalar density $\mathcal{O}^P$. The factor Z_m^{RGI} renormalizes the quark mass as determined from the lattice axial Ward identity. In Ref. [62] we have calculated it by a method similar to that used in the present paper and applied the results in an evaluation of the strange quark mass. For easier comparison we also give the numbers following from Table V. They differ from the older results by at most 2%.

Factors for converting Z^{RGI} to the $\overline{\mathrm{MS}}$ scheme, i.e., $\Delta Z^{\overline{\mathrm{MS}}}(\mu)^{-1}$ evaluated for our standard values of r_0 and $r_0\Lambda_{\overline{\mathrm{MS}}}$ can be found in Appendix F.

XII. CONCLUSIONS

As more and more detailed questions about hadron structure are treated in lattice QCD the renormalization of composite operators has become an important issue and perturbative as well as nonperturbative methods have been developed. In this paper we have presented results of a nonperturbative study in the RI-MOM scheme for a large variety of quark-antiquark operators, based on simulations with $n_f = 2$ dynamical clover fermions. The results for the renormalization constants will be applied in the evaluation of phenomenologically relevant hadron matrix elements. Apart from these numbers, there are also a few lessons of a more general nature to be learned from our investigation.

The renormalization factors connecting the bare operators on the lattice with their renormalized counterparts in some renormalization scheme, e.g., the $\overline{\mathrm{MS}}$ scheme, depend on the cutoff used, the lattice spacing a in our case, and the renormalization scale M. The dependence on these two quantities should factorize, and this is indeed observed in a broad range of M. However, the available results from continuum perturbation theory for the anomalous dimensions and the β function can describe the M dependence only for relatively large values of the scale, above $M^2 \approx 5\ \mathrm{GeV}^2$.

Only in the region where the scale dependence is well described by continuum perturbation theory is it possible to extract reliable values for the renormalization factors. On the other hand, for large values of the renormalization scale lattice artifacts may jeopardize the whole approach. It is therefore important to keep discretization effects under control, and we have seen that this purpose can be achieved (at least approximately) by subtracting lattice artifacts with the help of lattice perturbation theory. We did this at the one-loop level, but to all orders in a. Unfortunately, our procedure turned out to be too complicated for operators with more than one covariant derivative. Alternatively, one can calculate the lattice artifacts proportional to a^2 in one-loop lattice perturbation theory. This has recently been done for operators without derivatives [63]. Since it should be possible to extend such calculations to more complicated operators, it would be interesting to see if subtraction of the a^2 contributions is already sufficient for our purposes.

With the help of lattice perturbation theory one can not only calculate lattice artifacts, but also the renormalization factors themselves. However, due to the notoriously poor convergence properties of bare lattice perturbation theory some kind of improvement is mandatory, at least if only one-loop calculations are available. Indeed, we have found that tadpole improvement does quite a good job, although it is hard to predict how good the results actually are. For operators without derivatives, there are now even two-loop results. In bare perturbation theory they lead to a reduction of the difference with our nonperturbative renormalization factors, but the situation is less clear when tadpole improvement is included. Perhaps the ideal perturbative scheme is still to be found.

Let us finally mention a few possible directions for future research. The RI-MOM scheme has the disadvantage that it requires gauge fixing. In principle, this problem

could be overcome by working with correlation functions in coordinate space, and a first implementation of this idea has been published [64]. It seems, however, that very fine lattices are necessary for this method.

Another possible modification concerns the choice of the momenta. In our application we have followed the original RI-MOM scheme, where the momentum transfer at the operator insertion vanishes. However, a generalization to nonexceptional momenta is possible [65–67].

A third variant of nonperturbative renormalization is motivated by the fact that the renormalization condition (28) involves only a particular trace of the vertex function $\Gamma(p)$. On the other hand, we have the complete vertex functions (as 4×4 matrices after averaging over color) at our disposal, the bare ones computed nonperturbatively on the lattice as well as the renormalized ones calculated perturbatively in the $\overline{\text{MS}}$ scheme. So instead of introducing the intermediate RI′-MOM scheme by imposing (28) one could directly compare the bare nonperturbative vertex function $\Gamma(p)$ with the renormalized perturbative vertex function $\Gamma^{\overline{\text{MS}}}(p)$ in the $\overline{\text{MS}}$ scheme. Up to lattice artifacts we should have

$$\Gamma^{\overline{\text{MS}}}(p) = (Z^{\overline{\text{MS}}}_{q,\text{bare}})^{-1} Z^{\overline{\text{MS}}}_{\text{bare}} \Gamma(p), \tag{92}$$

where $\Gamma^{\overline{\text{MS}}}(p)$ as well as the renormalization factors $Z^{\overline{\text{MS}}}_{q,\text{bare}}$ and $Z^{\overline{\text{MS}}}_{\text{bare}}$ also depend on the renormalization scale μ. An analogous relation should hold for the quark propagator and $Z^{\overline{\text{MS}}}_{q,\text{bare}}$.

Of course, it is not to be expected that (92) is satisfied exactly: Not only lattice artifacts would spoil the identity, but also the truncation of the perturbative expansion. So one would have to develop some kind of fit procedure for extracting $Z^{\overline{\text{MS}}}_{\text{bare}}$ from (92). In any case, it might be an interesting exercise to see how well (92) is fulfilled for our data.

ACKNOWLEDGMENTS

The numerical calculations have been performed on the apeNEXT and APEmille at NIC/DESY (Zeuthen). This work has been supported in part by the EU Integrated Infrastructure Initiative HadronPhysics2 and by the DFG under Contract No. SFB/TR55 (Hadron Physics from Lattice QCD).

APPENDIX A: OPERATOR BASES

In this appendix we list the operator bases we used when calculating the renormalization factors with the help of Eq. (31).

For $v_{2,a}$ (representation $\tau_3^{(6)}$, $C = +1$):

$$\mathcal{O}_{\{\mu\nu\}}, \qquad 1 \le \mu < \nu \le 4. \tag{A1}$$

For $v_{2,b}$ (representation $\tau_1^{(3)}$, $C = +1$):

$$\mathcal{O}_{11} + \mathcal{O}_{22} - \mathcal{O}_{33} - \mathcal{O}_{44}, \quad \mathcal{O}_{33} - \mathcal{O}_{44}, \quad \mathcal{O}_{11} - \mathcal{O}_{22}. \tag{A2}$$

For $r_{2,a}$ (representation $\tau_4^{(6)}$, $C = -1$):

$$\mathcal{O}^5_{\{\mu\nu\}}, \qquad 1 \le \mu < \nu \le 4. \tag{A3}$$

For $r_{2,b}$ (representation $\tau_4^{(3)}$, $C = -1$):

$$\mathcal{O}^5_{11} + \mathcal{O}^5_{22} - \mathcal{O}^5_{33} - \mathcal{O}^5_{44}, \quad \mathcal{O}^5_{33} - \mathcal{O}^5_{44}, \quad \mathcal{O}^5_{11} - \mathcal{O}^5_{22}. \tag{A4}$$

For $h_{1,a}$ (representation $\tau_2^{(8)}$, $C = +1$):

$$\begin{aligned} &2\mathcal{O}^T_{\nu_1\{\nu_2\nu_3\}} + \mathcal{O}^T_{\nu_2\{\nu_1\nu_3\}}, \qquad \mathcal{O}^T_{\nu_2\{\nu_1\nu_3\}}, \\ &1 \le \nu_1 < \nu_2 < \nu_3 \le 4. \end{aligned} \tag{A5}$$

For $h_{1,b}$ (representation $\tau_1^{(8)}$, $C = +1$):

$$\begin{aligned} &\mathcal{O}^T_{122} - \mathcal{O}^T_{133}, \qquad \mathcal{O}^T_{122} + \mathcal{O}^T_{133} - 2\mathcal{O}^T_{144}, \\ &\mathcal{O}^T_{211} - \mathcal{O}^T_{233}, \qquad \mathcal{O}^T_{211} + \mathcal{O}^T_{233} - 2\mathcal{O}^T_{244}, \\ &\mathcal{O}^T_{311} - \mathcal{O}^T_{322}, \qquad \mathcal{O}^T_{311} + \mathcal{O}^T_{322} - 2\mathcal{O}^T_{344}, \\ &\mathcal{O}^T_{411} - \mathcal{O}^T_{422}, \qquad \mathcal{O}^T_{411} + \mathcal{O}^T_{422} - 2\mathcal{O}^T_{433}. \end{aligned} \tag{A6}$$

For v_3 (representation $\tau_1^{(8)}$, $C = -1$):

$$\begin{aligned} &\mathcal{O}_{\{122\}} - \mathcal{O}_{\{133\}}, \qquad \mathcal{O}_{\{122\}} + \mathcal{O}_{\{133\}} - 2\mathcal{O}_{\{144\}}, \\ &\mathcal{O}_{\{211\}} - \mathcal{O}_{\{233\}}, \qquad \mathcal{O}_{\{211\}} + \mathcal{O}_{\{233\}} - 2\mathcal{O}_{\{244\}}, \\ &\mathcal{O}_{\{311\}} - \mathcal{O}_{\{322\}}, \qquad \mathcal{O}_{\{311\}} + \mathcal{O}_{\{322\}} - 2\mathcal{O}_{\{344\}}, \\ &\mathcal{O}_{\{411\}} - \mathcal{O}_{\{422\}}, \qquad \mathcal{O}_{\{411\}} + \mathcal{O}_{\{422\}} - 2\mathcal{O}_{\{433\}}. \end{aligned} \tag{A7}$$

For $v_{3,a}$ (representation $\tau_2^{(4)}$, $C = -1$):

$$\mathcal{O}_{\{234\}}, \qquad \mathcal{O}_{\{134\}}, \qquad \mathcal{O}_{\{124\}}, \qquad \mathcal{O}_{\{123\}}. \tag{A8}$$

For r_3 (representation $\tau_2^{(8)}$, $C = +1$):

$$\begin{aligned} &\mathcal{O}^5_{\{122\}} - \mathcal{O}^5_{\{133\}}, \qquad \mathcal{O}^5_{\{122\}} + \mathcal{O}^5_{\{133\}} - 2\mathcal{O}^5_{\{144\}}, \\ &\mathcal{O}^5_{\{211\}} - \mathcal{O}^5_{\{233\}}, \qquad \mathcal{O}^5_{\{211\}} + \mathcal{O}^5_{\{233\}} - 2\mathcal{O}^5_{\{244\}}, \\ &\mathcal{O}^5_{\{311\}} - \mathcal{O}^5_{\{322\}}, \qquad \mathcal{O}^5_{\{311\}} + \mathcal{O}^5_{\{322\}} - 2\mathcal{O}^5_{\{344\}}, \\ &\mathcal{O}^5_{\{411\}} - \mathcal{O}^5_{\{422\}}, \qquad \mathcal{O}^5_{\{411\}} + \mathcal{O}^5_{\{422\}} - 2\mathcal{O}^5_{\{433\}}. \end{aligned} \tag{A9}$$

For a_2 (representation $\tau_3^{(4)}$, $C = +1$):

$$\mathcal{O}^5_{\{234\}}, \qquad \mathcal{O}^5_{\{134\}}, \qquad \mathcal{O}^5_{\{124\}}, \qquad \mathcal{O}^5_{\{123\}}. \tag{A10}$$

For v_4 (representation $\tau_1^{(2)}$, $C = +1$):

$$\begin{aligned} &\mathcal{O}_{\{1122\}} + \mathcal{O}_{\{3344\}} - \mathcal{O}_{\{1133\}} - \mathcal{O}_{\{2244\}}, \\ &\mathcal{O}_{\{1122\}} + \mathcal{O}_{\{3344\}} + \mathcal{O}_{\{1133\}} + \mathcal{O}_{\{2244\}} \\ &\quad - 2\mathcal{O}_{\{1144\}} - 2\mathcal{O}_{\{2233\}}. \end{aligned} \tag{A11}$$

For $h_{2,a}$ (representation $\tau_2^{(3)}$, $C=-1$):

$$\begin{aligned}
&\mathcal{O}^T_{14\{23\}} + \mathcal{O}^T_{24\{13\}} + \mathcal{O}^T_{34\{12\}} = -3\mathcal{O}^T_{4\{123\}},\\
&3\mathcal{O}^T_{13\{24\}} + \mathcal{O}^T_{14\{23\}} + 3\mathcal{O}^T_{23\{14\}} + \mathcal{O}^T_{24\{13\}} - 2\mathcal{O}^T_{34\{12\}}\\
&\quad = -9\mathcal{O}^T_{3\{124\}} - 3\mathcal{O}^T_{4\{123\}},\\
&2\mathcal{O}^T_{12\{34\}} + \mathcal{O}^T_{13\{24\}} + \mathcal{O}^T_{14\{23\}} - \mathcal{O}^T_{23\{14\}} - \mathcal{O}^T_{24\{13\}}\\
&\quad = 3\mathcal{O}^T_{1\{234\}} - 3\mathcal{O}^T_{2\{134\}}.
\end{aligned} \tag{A12}$$

For $h_{2,b}$ (representation $\tau_3^{(3)}$, $C=-1$):

$$\begin{aligned}
&\mathcal{O}^T_{1\{122\}} - \mathcal{O}^T_{1\{133\}} + \mathcal{O}^T_{2\{233\}},\\
&-2\mathcal{O}^T_{1\{122\}} - \mathcal{O}^T_{1\{133\}} + 3\mathcal{O}^T_{1\{144\}} + \mathcal{O}^T_{2\{233\}} - 3\mathcal{O}^T_{2\{244\}},\\
&-\mathcal{O}^T_{1\{133\}} + \mathcal{O}^T_{1\{144\}} - \mathcal{O}^T_{2\{233\}} + \mathcal{O}^T_{2\{244\}} - 2\mathcal{O}^T_{3\{344\}}.
\end{aligned} \tag{A13}$$

For $h_{2,c}$ (representation $\tau_2^{(6)}$, $C=-1$):

$$\begin{aligned}
&\mathcal{O}^T_{13\{32\}} + \mathcal{O}^T_{23\{31\}} - \mathcal{O}^T_{14\{42\}} - \mathcal{O}^T_{24\{41\}},\\
&\mathcal{O}^T_{12\{23\}} + \mathcal{O}^T_{32\{21\}} - \mathcal{O}^T_{14\{43\}} - \mathcal{O}^T_{34\{41\}},\\
&\mathcal{O}^T_{12\{24\}} + \mathcal{O}^T_{42\{21\}} - \mathcal{O}^T_{13\{34\}} - \mathcal{O}^T_{43\{31\}},\\
&\mathcal{O}^T_{21\{13\}} + \mathcal{O}^T_{31\{12\}} - \mathcal{O}^T_{24\{43\}} - \mathcal{O}^T_{34\{42\}},\\
&\mathcal{O}^T_{21\{14\}} + \mathcal{O}^T_{41\{12\}} - \mathcal{O}^T_{23\{34\}} - \mathcal{O}^T_{43\{32\}},\\
&\mathcal{O}^T_{31\{14\}} + \mathcal{O}^T_{41\{13\}} - \mathcal{O}^T_{32\{24\}} - \mathcal{O}^T_{42\{23\}}.
\end{aligned} \tag{A14}$$

For $h_{2,d}$ (representation $\tau_3^{(6)}$, $C=-1$):

$$\begin{aligned}
&\mathcal{O}^T_{1211} - \mathcal{O}^T_{1222} + \mathcal{O}^T_{13\{32\}} + \mathcal{O}^T_{23\{31\}} + \mathcal{O}^T_{14\{42\}} + \mathcal{O}^T_{24\{41\}},\\
&\mathcal{O}^T_{1311} - \mathcal{O}^T_{1333} + \mathcal{O}^T_{12\{23\}} + \mathcal{O}^T_{32\{21\}} + \mathcal{O}^T_{14\{43\}} + \mathcal{O}^T_{34\{41\}},\\
&\mathcal{O}^T_{1411} - \mathcal{O}^T_{1444} + \mathcal{O}^T_{12\{24\}} + \mathcal{O}^T_{42\{21\}} + \mathcal{O}^T_{13\{34\}} + \mathcal{O}^T_{43\{31\}},\\
&\mathcal{O}^T_{2322} - \mathcal{O}^T_{2333} + \mathcal{O}^T_{21\{13\}} + \mathcal{O}^T_{31\{12\}} + \mathcal{O}^T_{24\{43\}} + \mathcal{O}^T_{34\{42\}},\\
&\mathcal{O}^T_{2422} - \mathcal{O}^T_{2444} + \mathcal{O}^T_{21\{14\}} + \mathcal{O}^T_{41\{12\}} + \mathcal{O}^T_{23\{34\}} + \mathcal{O}^T_{43\{32\}},\\
&\mathcal{O}^T_{3433} - \mathcal{O}^T_{3444} + \mathcal{O}^T_{31\{14\}} + \mathcal{O}^T_{41\{13\}} + \mathcal{O}^T_{32\{24\}} + \mathcal{O}^T_{42\{23\}}.
\end{aligned} \tag{A15}$$

For the vector current (representation $\tau_1^{(4)}$, $C=-1$):

$$\mathcal{O}^V_\mu, \qquad 1 \le \mu \le 4. \tag{A16}$$

For the axial-vector current (representation $\tau_4^{(4)}$, $C=+1$):

$$\mathcal{O}^A_\mu, \qquad 1 \le \mu \le 4. \tag{A17}$$

For the tensor current (representation $\tau_1^{(6)}$, $C=-1$):

$$\mathcal{O}^T_{\mu\nu}, \qquad 1 \le \mu < \nu \le 4. \tag{A18}$$

APPENDIX B: EXAMPLE FOR CONVERSION FACTORS

We want to explain in detail how the difference between $Z^{\overline{\rm MS}}_{\rm RI'\text{-}MOM}$ and $Z^{\overline{\rm MS}}_{\rm MOM}$ arises, considering the operator

$$\mathcal{O}_{\{\mu\nu\}} = \frac{1}{2}\bar{u}(\gamma_\mu \overleftrightarrow{D}_\nu + \gamma_\nu \overleftrightarrow{D}_\mu)d \tag{B1}$$

for $\mu \neq \nu$ as an instructive example. The operator $\mathcal{O}_{v_{2,a}}$ belongs to this multiplet of operators.

Using dimensional regularization, straightforward perturbation theory in $4-\epsilon$ dimensions yields in the Landau gauge

$$\begin{aligned}
\Gamma(p) = {}& \mathrm{i}(\gamma_\mu p_\nu + \gamma_\nu p_\mu) + \frac{g^2}{16\pi^2} C_F \Big\{ \mathrm{i}(\gamma_\mu p_\nu + \gamma_\nu p_\mu)\\
&\times \Big[-\frac{8}{3}\Big(\frac{2}{\epsilon} + \ln(4\pi) - \gamma_{\rm E} - \ln(p^2/\mu^2)\Big) - \frac{31}{9}\Big]\\
&- \frac{2}{3} p_\mu p_\nu \frac{\mathrm{i}\not{p}}{p^2}\Big\} + O(g^4)
\end{aligned} \tag{B2}$$

up to terms which vanish for $\epsilon \to 0$. For QCD we have $C_F = 4/3$. In this appendix we restrict ourselves to one-loop order. Hence the coupling constant g can be identified with the bare coupling or with some renormalized coupling. Moreover, to this order and in the Landau gauge the quark wave function renormalization constant Z_q is equal to one in all schemes of interest to us (RI′-MOM, $\overline{\rm MS}$, and MOM); see also Eq. (C33). So we can ignore it in the following.

For the operator (B1) we have

$$\Gamma_{\rm Born}(p) = \mathrm{i}(\gamma_\mu p_\nu + \gamma_\nu p_\mu) \tag{B3}$$

and the term proportional to $\not{p}$ represents an additional structure which is not a multiple of the Born term. The renormalized vertex function in the $\overline{\rm MS}$ scheme reads

$$\begin{aligned}
\Gamma_{\overline{\rm MS}}(p) = {}& \Gamma_{\rm Born}(p) + \frac{g^2}{16\pi^2} C_F \Big\{ \Gamma_{\rm Born}(p) \Big[\frac{8}{3}\ln(p^2/\mu^2) - \frac{31}{9}\Big]\\
&- \frac{2}{3} p_\mu p_\nu \frac{\mathrm{i}\not{p}}{p^2}\Big\} + O(g^4)
\end{aligned} \tag{B4}$$

and we get

$$Z^{\overline{\rm MS}}_{\rm dimreg} = 1 + \frac{g^2}{16\pi^2} C_F \cdot \frac{8}{3}\Big(\frac{2}{\epsilon} + \ln(4\pi) - \gamma_{\rm E}\Big) + O(g^4). \tag{B5}$$

On the other hand, we can represent $\Gamma(p)$ as a linear combination of $\Gamma_{\rm Born}(p)$ and $p_\mu p_\nu(\mathrm{i}\not{p}/p^2)$. Requiring that in the MOM scheme the coefficient of $\Gamma_{\rm Born}(p)$ be unity for $p^2 = \mu^2$ we find

$$Z^{\rm MOM}_{\rm dimreg} = 1 + \frac{g^2}{16\pi^2} C_F \Big[\frac{8}{3}\Big(\frac{2}{\epsilon} + \ln(4\pi) - \gamma_{\rm E}\Big) + \frac{31}{9}\Big] + O(g^4), \tag{B6}$$

such that

$$\Gamma_{\mathrm{MOM}}(p) = \Gamma_{\mathrm{Born}}(p) + \frac{g^2}{16\pi^2} C_F \Big\{ \Gamma_{\mathrm{Born}}(p) \cdot \frac{8}{3} \ln(p^2/\mu^2) - \frac{2}{3} p_\mu p_\nu \frac{\mathrm{i}p}{p^2} \Big\} + O(g^4). \tag{B7}$$

Finally we obtain from Eq. (29)

$$Z^{\mathrm{RI'\text{-}MOM}}_{\mathrm{dimreg}} = 1 + \frac{g^2}{16\pi^2} C_F \Big[\frac{8}{3} \Big(\frac{2}{\epsilon} + \ln(4\pi) - \gamma_{\mathrm{E}} \Big) + \frac{31}{9} + \frac{4}{3} \frac{p_\mu^2 p_\nu^2}{p^2 (p_\mu^2 + p_\nu^2)} \Big] + O(g^4). \tag{B8}$$

Now we can calculate

$$Z^{\overline{\mathrm{MS}}}_{\mathrm{RI'\text{-}MOM}}(\mu) = \frac{Z^{\overline{\mathrm{MS}}}_{\mathrm{dimreg}}}{Z^{\mathrm{RI'\text{-}MOM}}_{\mathrm{dimreg}}} = 1 + \frac{g^2}{16\pi^2} C_F \Big(-\frac{31}{9} - \frac{4}{3} \frac{p_\mu^2 p_\nu^2}{p^2 (p_\mu^2 + p_\nu^2)} \Big) + O(g^4) \tag{B9}$$

and

$$Z^{\overline{\mathrm{MS}}}_{\mathrm{MOM}}(\mu) = \frac{Z^{\overline{\mathrm{MS}}}_{\mathrm{dimreg}}}{Z^{\mathrm{MOM}}_{\mathrm{dimreg}}} = 1 + \frac{g^2}{16\pi^2} C_F \Big(-\frac{31}{9} \Big) + O(g^4), \tag{B10}$$

in agreement with the results given in Appendix C.

APPENDIX C: RESULTS FROM CONTINUUM PERTURBATION THEORY

In this appendix we collect the results from continuum perturbation theory that go into our computations. They all refer to $n_c = 3$ colors and Landau gauge, but the number of flavors n_f is left free. Note that we quote only the papers which give the results with the largest number of loops.

We begin with the coefficients of the β function [see Eq. (48)]. In the $\overline{\mathrm{MS}}$ scheme they are given by (see Ref. [68])

$$\beta_0 = 11 - \frac{2}{3} n_f, \tag{C1}$$

$$\beta_1 = 102 - \frac{38}{3} n_f, \tag{C2}$$

$$\beta_2 = \frac{2857}{2} - \frac{5033}{18} n_f + \frac{325}{54} n_f^2, \tag{C3}$$

$$\beta_3 = \frac{149753}{6} + 3564\zeta_3 - \Big(\frac{1078361}{162} + \frac{6508}{27} \zeta_3 \Big) n_f + \Big(\frac{50065}{162} + \frac{6472}{81} \zeta_3 \Big) n_f^2 + \frac{1093}{729} n_f^3. \tag{C4}$$

In the $\widetilde{\mathrm{MOM}}$gg scheme one finds [36]

$$\beta_2 = \frac{186747}{64} - \frac{1683}{4} \zeta_3 - \Big(\frac{35473}{96} - \frac{65}{6} \zeta_3 \Big) n_f - \Big(\frac{829}{54} - \frac{8}{9} \zeta_3 \Big) n_f^2 + \frac{8}{9} n_f^3, \tag{C5}$$

$$\beta_3 = \frac{20783939}{128} - \frac{1300563}{32} \zeta_3 - \frac{900075}{32} \zeta_5 - \Big(\frac{2410799}{64} - \frac{1323259}{144} \zeta_3 - \frac{908995}{144} \zeta_5 \Big) n_f + \Big(\frac{1464379}{648} - \frac{12058}{27} \zeta_3 - \frac{7540}{27} \zeta_5 \Big) n_f^2 - \Big(\frac{3164}{27} - \frac{64}{9} \zeta_3 \Big) n_f^3 + \frac{320}{81} n_f^4, \tag{C6}$$

while β_0 and β_1 are scheme independent in the Landau gauge.

We now turn to the coefficients of the anomalous dimension in the $\overline{\mathrm{MS}}$ scheme. Our conventions have been given in Sec. VII; see, in particular, Eqs. (44) and (45). For notational simplicity the superscript $\overline{\mathrm{MS}}$ will be omitted. Note that we assume an anticommuting γ_5, so the coefficients γ_i correspond more precisely to the so-called naive dimensional regularization.

While $\mathcal{O}^V_\mu$ and $\mathcal{O}^A_\mu$ have of course vanishing anomalous dimension, we find for $\mathcal{O}^S$ and $\mathcal{O}^P$ (see Refs. [69,70])

$$\gamma_0 = -8, \tag{C7}$$

$$\gamma_1 = -\frac{404}{3} + \frac{40}{9} n_f, \tag{C8}$$

$$\gamma_2 = -2498 + \Big(\frac{4432}{27} + \frac{320}{3} \zeta_3 \Big) n_f + \frac{280}{81} n_f^2, \tag{C9}$$

$$\gamma_3 = -\frac{4603055}{81} - \frac{271360}{27} \zeta_3 + 17600\zeta_5 + \Big(\frac{183446}{27} + \frac{68384}{9} \zeta_3 - 1760\zeta_4 - \frac{36800}{9} \zeta_5 \Big) n_f + \Big(-\frac{10484}{243} - \frac{1600}{9} \zeta_3 + \frac{320}{3} \zeta_4 \Big) n_f^2 + \Big(\frac{664}{243} - \frac{128}{27} \zeta_3 \Big) n_f^3. \tag{C10}$$

For $\mathcal{O}^T_{\mu\nu}$ we have [71]

$$\gamma_0 = \frac{8}{3}, \tag{C11}$$

$$\gamma_1 = \frac{724}{9} - \frac{104}{27} n_f, \tag{C12}$$

$$\gamma_2 = \frac{105110}{81} - \frac{1856}{27}\zeta_3 - \left(\frac{10480}{81} + \frac{320}{9}\zeta_3\right)n_f - \frac{8}{9}n_f^2. \tag{C13}$$

The operators $\mathcal{O}_{v_{2,a}}$, $\mathcal{O}_{v_{2,b}}$, $\mathcal{O}_{r_{2,a}}$, and $\mathcal{O}_{r_{2,b}}$ have the same anomalous dimension. From Ref. [72] we get

$$\gamma_0 = \frac{64}{9}, \tag{C14}$$

$$\gamma_1 = \frac{23488}{243} - \frac{512}{81}n_f, \tag{C15}$$

$$\gamma_2 = \frac{11028416}{6561} + \frac{2560}{81}\zeta_3 - \left(\frac{334400}{2187} + \frac{2560}{27}\zeta_3\right)n_f - \frac{1792}{729}n_f^2. \tag{C16}$$

For $\mathcal{O}_{v_3}$, $\mathcal{O}_{v_{3,a}}$, $\mathcal{O}_{a_2}$, and $\mathcal{O}_{r_3}$ we extract from Ref. [73]

$$\gamma_0 = \frac{100}{9}, \tag{C17}$$

$$\gamma_1 = \frac{34450}{243} - \frac{830}{81}n_f, \tag{C18}$$

$$\gamma_2 = \frac{64486199}{26244} + \frac{2200}{81}\zeta_3 - \left(\frac{469910}{2187} + \frac{4000}{27}\zeta_3\right)n_f - \frac{2569}{729}n_f^2. \tag{C19}$$

The anomalous dimension of $\mathcal{O}_{v_4}$ can be found in Ref. [72]:

$$\gamma_0 = \frac{628}{45}, \tag{C20}$$

$$\gamma_1 = \frac{5241914}{30375} - \frac{26542}{2025}n_f, \tag{C21}$$

$$\gamma_2 = \frac{245787905651}{82012500} + \frac{11512}{405}\zeta_3 - \left(\frac{726591271}{2733750} + \frac{5024}{27}\zeta_3\right)n_f - \frac{384277}{91125}n_f^2. \tag{C22}$$

The three-loop anomalous dimension of transversity operators has been calculated by Gracey. For $\mathcal{O}_{h_{1,a}}$ and $\mathcal{O}_{h_{1,b}}$ we get from Ref. [74]

$$\gamma_0 = 8, \tag{C23}$$

$$\gamma_1 = 124 - 8n_f, \tag{C24}$$

$$\gamma_2 = \frac{19162}{9} - \left(\frac{5608}{27} + \frac{320}{3}\zeta_3\right)n_f - \frac{184}{81}n_f^2. \tag{C25}$$

In Ref. [75] we find for $\mathcal{O}_{h_{2,a}}$, $\mathcal{O}_{h_{2,b}}$, $\mathcal{O}_{h_{2,c}}$, and $\mathcal{O}_{h_{2,d}}$:

$$\gamma_0 = \frac{104}{9}, \tag{C26}$$

$$\gamma_1 = \frac{38044}{243} - \frac{904}{81}n_f, \tag{C27}$$

$$\gamma_2 = \frac{17770162}{6561} + \frac{1280}{81}\zeta_3 - \left(\frac{552308}{2187} + \frac{4160}{27}\zeta_3\right)n_f - \frac{2408}{729}n_f^2. \tag{C28}$$

Finally, we can take the anomalous dimension of the quark field to four loops from Ref. [76]:

$$\gamma_0 = 0, \tag{C29}$$

$$\gamma_1 = \frac{134}{3} - \frac{8}{3}n_f, \tag{C30}$$

$$\gamma_2 = \frac{20729}{18} - 79\zeta_3 - \frac{1100}{9}n_f + \frac{40}{27}n_f^2, \tag{C31}$$

$$\gamma_3 = \frac{2109389}{81} - \frac{565939}{162}\zeta_3 + \frac{2607}{2}\zeta_4 - \frac{761525}{648}\zeta_5 - \left(\frac{324206}{81} + \frac{4582}{27}\zeta_3 + 79\zeta_4 + \frac{320}{3}\zeta_5\right)n_f + \left(\frac{7706}{81} + \frac{320}{9}\zeta_3\right)n_f^2 + \frac{280}{243}n_f^3. \tag{C32}$$

Let us now consider the coefficients needed for the conversion from the RI′-MOM scheme and the MOM scheme to the $\overline{\text{MS}}$ scheme, as defined in Eqs. (56) and (57), respectively. Since the RI′-MOM scheme is in general not covariant, these coefficients may depend on the direction of the momentum p. In order to keep the paper at a reasonable length we refrain from giving the bases that are used in the representation of the vertex functions and enter the precise definition of the MOM scheme. The calculation makes use of the perturbative expressions for the vertex functions and of the ratio $Z^{\text{MOM}}_{q,\text{bare}}/Z^{\overline{\text{MS}}}_{q,\text{bare}} = Z^{\text{RI}'\text{-MOM}}_{q,\text{bare}}/Z^{\overline{\text{MS}}}_{q,\text{bare}}$. This ratio coincides with the quantity $C_2^{\text{RI}'}$ in Ref. [76], where we can read off the expansion

$$\frac{Z_q^{\text{MOM}}}{Z_q^{\overline{\text{MS}}}} = 1 + b_2\left(\frac{g^{\overline{\text{MS}}}(\mu)^2}{16\pi^2}\right)^2 + b_3\left(\frac{g^{\overline{\text{MS}}}(\mu)^2}{16\pi^2}\right)^3 + \cdots, \tag{C33}$$

with

$$b_2 = -\frac{359}{9} + 12\zeta_3 + \frac{7}{3}n_f, \tag{C34}$$

$$b_3 = -\frac{439543}{162} + \frac{8009}{6}\zeta_3 + \frac{79}{4}\zeta_4 - \frac{1165}{3}\zeta_5 + \left(\frac{24722}{81} - \frac{440}{9}\zeta_3\right)n_f - \frac{1570}{243}n_f^2. \tag{C35}$$

From Ref. [76] we get for $\mathcal{O}^S$ and $\mathcal{O}^P$

$$c_1 = \frac{16}{3}, \tag{C36}$$

$$c_2 = \frac{4291}{18} - \frac{152}{3}\zeta_3 - \frac{83}{9}n_f, \tag{C37}$$

$$c_3 = \frac{3890527}{324} - \frac{224993}{54}\zeta_3 + \frac{2960}{9}\zeta_5 - \left(\frac{241294}{243} - \frac{4720}{27}\zeta_3 + \frac{80}{3}\zeta_4\right)n_f + \left(\frac{7514}{729} + \frac{32}{27}\zeta_3\right)n_f^2. \tag{C38}$$

With the help of Ref. [77] we find for $\mathcal{O}^T_{\mu\nu}$

$$c_1 = 0, \tag{C39}$$

$$c_2 = -\frac{3847}{54} + \frac{184}{9}\zeta_3 + \frac{313}{81}n_f, \tag{C40}$$

$$c_3 = -\frac{9858659}{2916} + \frac{678473}{486}\zeta_3 + \frac{1072}{81}\zeta_4 - \frac{10040}{27}\zeta_5 + \left(\frac{286262}{729} - \frac{2096}{27}\zeta_3 + \frac{80}{9}\zeta_4\right)n_f - \left(\frac{13754}{2187} + \frac{32}{81}\zeta_3\right)n_f^2. \tag{C41}$$

For the vector and axial-vector currents $\mathcal{O}^V_\mu$ and $\mathcal{O}^A_\mu$ one finds from Ref. [77]

$$c_1 = 0, \tag{C42}$$

$$c_2 = \left(-\frac{134}{3} + \frac{8}{3}n_f\right)R, \tag{C43}$$

$$c_3 = \left(-\frac{52321}{18} + 607\zeta_3 + \left(\frac{8944}{27} - 32\zeta_3\right)n_f - \frac{208}{27}n_f^2\right)R, \tag{C44}$$

with $R = p_\mu^2/p^2$. If the index μ is averaged over in the renormalization condition [see Eq. (31)], R takes the value $1/4$.

Why do c_2 and c_3 not vanish although the vector current is conserved in the continuum? In the continuum the quark propagator $S(p)$ and the vertex function $\Gamma_\mu(p)$ of the vector current are linked by the Ward identity

$$\mathrm{i}\,\Gamma_\mu(p) = \frac{\partial}{\partial p_\mu} S^{-1}(p). \tag{C45}$$

By Lorentz symmetry the massless inverse propagator must have the form

$$S^{-1}(p) = \mathrm{i}A(p^2)\not{p}, \tag{C46}$$

where we expect A to depend logarithmically on p^2/μ^2. Therefore the vertex function has the form

$$\Gamma_\mu(p) = A(p^2)\gamma_\mu + \frac{\mathrm{d}A}{\mathrm{d}p^2}2p_\mu\not{p}, \tag{C47}$$

and the trace with the Born term gives

$$\frac{1}{12}\,\mathrm{tr}(\gamma_\mu\Gamma_\mu(p)) = A(p^2) + 2p^2\frac{\mathrm{d}A}{\mathrm{d}p^2}\frac{p_\mu^2}{p^2} = A(p^2) + 2p^2\frac{\mathrm{d}A}{\mathrm{d}p^2}R. \tag{C48}$$

The vector Ward identity therefore requires the existence of terms proportional to R in the trace, with a coefficient given by the logarithmic derivative of A. The coefficient c_1 vanishes because in the Landau gauge there is no term in the propagator of the form $g^2\ln(p^2/\mu^2)$, but in most other gauges c_1 is nonzero and we already have a term proportional to R at one loop.

In the following cases we express the coefficients c_1, c_2, and c_3 in the form

$$c_1 = c_1^{(1)} + c_1^{(2)}R, \tag{C49}$$

$$c_2 = c_2^{(1)} + b_2 + c_2^{(2)}R, \tag{C50}$$

$$c_3 = c_3^{(1)} + b_2c_1^{(1)} + b_3 + (c_3^{(2)} + b_2c_1^{(2)})R, \tag{C51}$$

where R contains the momentum dependence and is given in Table X. The expressions $R^{(j)}(p)$ for $j = 1, 2, 3, 4$ read

$$R^{(1)}_{\mu\nu\lambda\rho}(p) = \frac{p_\mu^2(p_\nu^2 - p_\lambda^2)^2}{(p_\nu^2 - p_\lambda^2)^2 + 4p_\mu^2(p_\nu^2 + p_\lambda^2)} + \frac{p_\mu^2(p_\nu^2 + p_\lambda^2 - 2p_\rho^2)^2}{(p_\nu^2 + p_\lambda^2 - 2p_\rho^2)^2 + 4p_\mu^2(p_\nu^2 + p_\lambda^2 + 4p_\rho^2)}, \tag{C52}$$

$$R^{(2)}_{\mu\nu\lambda}(p) = \frac{p_\mu^2p_\nu^2p_\lambda^2}{p_\mu^2p_\nu^2 + p_\mu^2p_\lambda^2 + p_\nu^2p_\lambda^2}, \tag{C53}$$

$$R^{(3)}(p) = \frac{(p_1^2 - p_4^2)^2(p_2^2 - p_3^2)^2}{(p_1^2 + p_4^2)(p_2^2 - p_3^2)^2 + (p_2^2 + p_3^2)(p_1^2 - p_4^2)^2}, \tag{C54}$$

$$R^{(4)}(p) = \frac{((p_1^2 + p_4^2)(p_2^2 + p_3^2) - 2p_1^2p_4^2 - 2p_2^2p_3^2)^2}{p_1^2(p_2^2 + p_3^2 - 2p_4^2)^2 + p_2^2(p_1^2 + p_4^2 - 2p_3^2)^2 + p_3^2(p_1^2 + p_4^2 - 2p_2^2)^2 + p_4^2(p_2^2 + p_3^2 - 2p_1^2)^2}. \tag{C55}$$

TABLE X. Momentum dependent factors R. For the definitions of the lengthier expressions $R^{(j)}(p)$, see Eqs. (C52)–(C55).

Operators	R
$\mathcal{O}_{v_{2,a}}$, $\mathcal{O}_{r_{2,a}}$	$\frac{2p_1^2p_4^2}{p^2(p_1^2+p_4^2)}$
$\mathcal{O}_{v_{2,b}}$, $\mathcal{O}_{r_{2,b}}$	$\frac{(p_4^2-(p_1^2+p_2^2+p_3^2)/3)^2}{2p^2(p_4^2+(p_1^2+p_2^2+p_3^2)/9)}$
$\mathcal{O}_{v_3}$, $\mathcal{O}_{r_3}$	$\frac{-9p_4^2(p_1^2-(p_2^2+p_3^2)/2)^2}{p^2((4p_1^2+p_2^2+p_3^2)p_4^2+(p_1^2-(p_2^2+p_3^2)/2)^2)}$
$\mathcal{O}_{v_{3,a}}$, $\mathcal{O}_{a_2}$	$\frac{-9p_1^2p_2^2p_4^2}{p^2((p_1p_4)^2+(p_2p_4)^2+(p_1p_2)^2)}$
$\mathcal{O}_{v_4}$	$\frac{64(p_1^2-p_2^2)^2(p_4^2-p_3^2)^2}{p^2((p_1^2+p_2^2)(p_4^2-p_3^2)^2+(p_3^2+p_4^2)(p_2^2-p_1^2)^2)}$
$\bar{\mathcal{O}}_{v_{2,a}}$, $\bar{\mathcal{O}}_{r_{2,a}}$	$\frac{1}{3p^2}\sum_{\mu<\nu}\frac{p_\mu^2p_\nu^2}{p_\mu^2+p_\nu^2}$
$\bar{\mathcal{O}}_{v_{2,b}}$, $\bar{\mathcal{O}}_{r_{2,b}}$	$\frac{1}{6p^2}\left[\frac{(p_1^2+p_2^2-p_3^2-p_4^2)^2}{p^2}+\frac{(p_3^2-p_4^2)^2}{p_3^2+p_4^2}+\frac{(p_1^2-p_2^2)^2}{p_1^2+p_2^2}\right]$
$\bar{\mathcal{O}}_{v_3}$, $\bar{\mathcal{O}}_{r_3}$	$-\frac{9}{8p^2}(R^{(1)}_{1234}(p)+R^{(1)}_{2134}(p)+R^{(1)}_{3124}(p)+R^{(1)}_{4123}(p))$
$\bar{\mathcal{O}}_{v_{3,a}}$, $\bar{\mathcal{O}}_{a_2}$	$-\frac{9}{4p^2}(R^{(2)}_{123}(p)+R^{(2)}_{124}(p)+R^{(2)}_{134}(p)+R^{(2)}_{234}(p))$
$\bar{\mathcal{O}}_{v_4}$	$\frac{32}{p^2}(R^{(3)}(p)+R^{(4)}(p))$

For $\mathcal{O}_{v_{2,a}}$, $\mathcal{O}_{v_{2,b}}$, $\mathcal{O}_{r_{2,a}}$, and $\mathcal{O}_{r_{2,b}}$ one extracts from Ref. [74]

$$c_1^{(1)} = -\frac{124}{27}, \tag{C56}$$

$$c_2^{(1)} = -\frac{68993}{729}+\frac{160}{9}\zeta_3+\frac{2101}{243}n_f, \tag{C57}$$

$$c_3^{(1)} = -\frac{451293899}{157464}+\frac{1105768}{2187}\zeta_3-\frac{8959}{324}\zeta_4-\frac{4955}{81}\zeta_5 + \left(\frac{8636998}{19683}-\frac{224}{81}\zeta_3+\frac{640}{27}\zeta_4\right)n_f - \left(\frac{63602}{6561}+\frac{256}{243}\zeta_3\right)n_f^2, \tag{C58}$$

$$c_1^{(2)} = -\frac{8}{9}, \tag{C59}$$

$$c_2^{(2)} = -\frac{2224}{27}-\frac{40}{9}\zeta_3+\frac{40}{9}n_f, \tag{C60}$$

$$c_3^{(2)} = -\frac{136281133}{26244}+\frac{376841}{243}\zeta_3-\frac{43700}{81}\zeta_5 + \left(\frac{15184}{27}-\frac{1232}{81}\zeta_3\right)n_f-\frac{9680}{729}n_f^2. \tag{C61}$$

In the case of the operators $\mathcal{O}_{h_{1,a}}$ and $\mathcal{O}_{h_{1,b}}$ one obtains from Ref. [74]

$$c_1^{(1)} = -\frac{14}{3}, \tag{C62}$$

$$c_2^{(1)} = -\frac{2237}{18}+\frac{62}{3}\zeta_3+\frac{32}{3}n_f, \tag{C63}$$

$$c_3^{(1)} = -\frac{1852993}{432}+\frac{97391}{108}\zeta_3-\frac{79}{4}\zeta_4-\frac{7060}{27}\zeta_5 + \left(\frac{306881}{486}-\frac{122}{9}\zeta_3+\frac{80}{3}\zeta_4\right)n_f-\left(\frac{1160}{81}+\frac{32}{27}\zeta_3\right)n_f^2, \tag{C64}$$

$$c_1^{(2)} = c_2^{(2)} = c_3^{(2)} = 0. \tag{C65}$$

Similarly, Ref. [75] yields for $\mathcal{O}_{h_{2,a}}$, $\mathcal{O}_{h_{2,b}}$, $\mathcal{O}_{h_{2,c}}$, and $\mathcal{O}_{h_{2,d}}$

$$c_1^{(1)} = -\frac{218}{27}, \tag{C66}$$

$$c_2^{(1)} = -\frac{669202}{3645}+\frac{452}{15}\zeta_3+\frac{4394}{243}n_f, \tag{C67}$$

$$c_3^{(1)} = -\frac{1020141085}{157464} + \frac{59050063}{43740}\zeta_3 - \frac{7679}{324}\zeta_4 - \frac{12434}{27}\zeta_5 + \left(\frac{98639141}{98415} + \frac{12712}{1215}\zeta_3 + \frac{1040}{27}\zeta_4\right)n_f - \left(\frac{177970}{6561} + \frac{416}{243}\zeta_3\right)n_f^2, \tag{C68}$$

$$c_1^{(2)} = c_2^{(2)} = c_3^{(2)} = 0. \tag{C69}$$

The operators $\mathcal{O}_{v_3}$, $\mathcal{O}_{v_{3,a}}$, $\mathcal{O}_{r_3}$, and $\mathcal{O}_{a_2}$ require the coefficients

$$c_1^{(1)} = -\frac{214}{27}, \tag{C70}$$

$$c_2^{(1)} = -\frac{4763093}{29160} + \frac{152}{5}\zeta_3 + \frac{32363}{1944}n_f, \tag{C71}$$

$$c_3^{(1)} = -\frac{8619089351}{1574640} + \frac{12125507}{10935}\zeta_3 - \frac{8599}{324}\zeta_4 - \frac{2525}{9}\zeta_5 + \left(\frac{1364405723}{1574640} + \frac{814}{135}\zeta_3 + \frac{1000}{27}\zeta_4\right)n_f - \left(\frac{1227463}{52488} + \frac{400}{243}\zeta_3\right)n_f^2, \tag{C72}$$

$$c_1^{(2)} = \frac{4}{9}, \tag{C73}$$

$$c_2^{(2)} = \frac{4432}{135} + \frac{56}{15}\zeta_3 - \frac{50}{27}n_f, \tag{C74}$$

$$c_3^{(2)} = \frac{279011797}{131220} - \frac{1717789}{2430}\zeta_3 + \frac{9370}{27}\zeta_5 - \left(\frac{1665047}{7290} + \frac{28}{5}\zeta_3\right)n_f + \frac{4210}{729}n_f^2, \tag{C75}$$

extracted from Ref. [75]. For $\mathcal{O}_{v_4}$ we find

$$c_1^{(1)} = -\frac{7214}{675}, \tag{C76}$$

$$c_2^{(1)} = -\frac{764724499}{3645000} + \frac{1756}{45}\zeta_3 + \frac{5655503}{243000}n_f, \tag{C77}$$

$$c_3^{(1)} = -\frac{282373048664443}{39366000000} + \frac{796627067}{546750}\zeta_3 - \frac{43507}{1620}\zeta_4 - \frac{38398}{81}\zeta_5 + \left(\frac{1160956742099}{984150000} + \frac{3208}{135}\zeta_3 + \frac{1256}{27}\zeta_4\right)n_f - \left(\frac{1167227687}{32805000} + \frac{2512}{1215}\zeta_3\right)n_f^2, \tag{C78}$$

$$c_1^{(2)} = -\frac{1}{40}, \tag{C79}$$

$$c_2^{(2)} = -\frac{731129}{432000} - \frac{23}{90}\zeta_3 + \frac{119}{1200}n_f, \tag{C80}$$

$$c_3^{(2)} = -\frac{1047728166241}{9331200000} + \frac{109467991}{2916000}\zeta_3 - \frac{13111}{648}\zeta_5 + \left(\frac{232632277}{19440000} + \frac{755}{972}\zeta_3\right)n_f - \frac{51959}{162000}n_f^2, \tag{C81}$$

from Ref. [75]. When using Gracey's results given in Refs. [74,75,77] it is important to note that Gracey's RI′-MOM scheme is not the same as ours. Furthermore, Eqs. (A.1) and (A.9) in Ref. [75] are not quite correct, but we hope that we have worked with properly rectified versions. Another correction concerns Eq. (4.4) in Ref. [74], where the coefficient of $T_F N_f$ in the a^2 contribution should be 468 and not 486.

The corresponding coefficients c_1', c_2', and c_3' in Eq. (57) for the conversion from MOM to $\overline{\text{MS}}$ are obtained by setting $R = 0$. So in the cases where the coefficients c_i are independent of R we have $c_i' = c_i$ and the RI′-MOM scheme can be identified with the MOM scheme, at least to the order considered.

APPENDIX D: LATTICE PERTURBATION THEORY TO TWO LOOPS

In the two-loop approximation of bare lattice perturbation theory we have

$$Z_{\text{bare}}^{\overline{\text{MS}}}(\mu, a)_{\text{pert}} = 1 + \frac{g^2}{16\pi^2}(-\gamma_0 \ln(a\mu) + z_1) + \left(\frac{g^2}{16\pi^2}\right)^2 (l_1 \ln^2(a\mu) + l_2 \ln(a\mu) + z_2). \tag{D1}$$

For the currents the coefficients l_1, l_2, z_1, z_2 can be read off from Refs. [3,4] as functions of c_{SW}. Note that $z_1 = -C_F\Delta$ in the notation of Sec. VIII.

Anticipating that we may want to expand in a coupling g_{LAT} different from the bare lattice coupling g, e.g., the boosted coupling $g_\Box$ [see Eq. (71)], we express the $\overline{\text{MS}}$ coupling $g_{\overline{\text{MS}}}$ as a function of g_{LAT}:

$$\frac{1}{g_{\overline{\text{MS}}}^2} = \frac{1}{g_{\text{LAT}}^2} + 2\frac{\beta_0}{16\pi^2}\ln(a\mu) - t_1^{\text{LAT}} + \left(2\frac{\beta_1}{(16\pi^2)^2}\ln(a\mu) - t_2^{\text{LAT}}\right)g_{\text{LAT}}^2 + O(g_{\text{LAT}}^4). \tag{D2}$$

Here $t_i^{\text{LAT}} = t_i - p_i$ $(i = 1, 2)$, where the constants p_i encode the relation between g and g_{LAT}:

$$\frac{1}{g_{\text{LAT}}^2} = \frac{1}{g^2} - p_1 - p_2 g^2 + O(g^4). \tag{D3}$$

For $g_{\text{LAT}} = g$ one has $p_i = 0$, hence $t_i^{\text{LAT}} = t_i$, and the relation between $g_{\overline{\text{MS}}}$ and g takes the usual form [41–44].

For setting up tadpole improvement we need the expansion

$$u_0 = 1 + r_1 \frac{g^2}{16\pi^2} + r_2 \left(\frac{g^2}{16\pi^2}\right)^2 + O(g^6) \tag{D4}$$

$$= 1 + r_1 \frac{g^2_{\rm LAT}}{16\pi^2} + r_2^{\rm LAT} \left(\frac{g^2_{\rm LAT}}{16\pi^2}\right)^2 + O(g^6_{\rm LAT}), \tag{D5}$$

where $r_2^{\rm LAT} = r_2 - 16\pi^2 r_1 p_1$. The coefficients r_1 and r_2 can be found from Ref. [58]. For an operator with n_D covariant derivatives the tadpole-improved two-loop expression for the renormalization factor then takes the form

$$\begin{aligned} Z^{\overline{\rm MS}}_{\rm bare}(\mu, a)_{\rm ti} = u_0^{1-n_D} \Big[& 1 + \frac{g^2_{\rm LAT}}{16\pi^2}(-\gamma_0 \ln(a\mu) + z_1 \\ & + (n_D - 1) r_1) + \left(\frac{g^2_{\rm LAT}}{16\pi^2}\right)^2 (l_1 \ln^2(a\mu) \\ & + (l_2 + 16\pi^2 p_1 \gamma_0 - (n_D - 1) r_1 \gamma_0) \ln(a\mu) + z_2^{\rm LAT} \\ & + (n_D - 1) r_2^{\rm LAT} + \frac{1}{2}(n_D - 1)(n_D - 2) r_1^2 \\ & + (n_D - 1) r_1 z_1) + O(g^6_{\rm LAT}) \Big], \end{aligned} \tag{D6}$$

where $z_2^{\rm LAT} = z_2 - 16\pi^2 p_1 z_1$. Of course, for the currents we have $n_D = 0$. As in Sec. VIII, the corresponding estimates for $Z^{\rm RGI}$ are finally given by $\Delta Z^{\overline{\rm MS}}(\mu_0) \times Z^{\overline{\rm MS}}_{\rm bare}(\mu_0, a)_{\rm pert}$ and $\Delta Z^{\overline{\rm MS}}(\mu_0) Z^{\overline{\rm MS}}_{\rm bare}(\mu_0, a)_{\rm ti}$ with $\mu_0 = 1/a$. For the expansion parameter we take $g_{\rm LAT} = g_\Box = g/u_0^2$. Therefore we have

$$p_1 = -\frac{r_1}{4\pi^2} = \frac{1}{4} C_F = \frac{1}{3}, \tag{D7}$$

$$p_2 = -\frac{2r_2 + 3r_1^2}{128\pi^4}. \tag{D8}$$

In order to implement TRB perturbation theory at the two-loop level we start from Eq. (78). Using the three-loop expressions for $\gamma^{\rm LAT}$ and $\beta^{\rm LAT}$ we obtain

$$Z^{\rm RGI} = \left(2\beta_0 \frac{g^2_{\rm LAT}}{16\pi^2}\right)^{-(\gamma_0/2\beta_0)} \exp\{F(g^2_{\rm LAT}/(16\pi^2))\}, \tag{D9}$$

with

$$\begin{aligned} F(x) = & \frac{\beta_2^{\rm LAT}\gamma_0 - \beta_0 \gamma_2^{\rm LAT}}{4\beta_0 \beta_2^{\rm LAT}} f_1(x) \\ & + \frac{\beta_1 \beta_2^{\rm LAT} \gamma_0 + \beta_0 \beta_1 \gamma_2^{\rm LAT} - 2\beta_0 \beta_2^{\rm LAT} \gamma_1^{\rm LAT}}{2\beta_0^2 \beta_2^{\rm LAT}} f_2(x), \end{aligned} \tag{D10}$$

where

$$f_1(x) = \ln\left(1 + \frac{\beta_1}{\beta_0} x + \frac{\beta_2^{\rm LAT}}{\beta_0} x^2\right) \tag{D11}$$

and

$$\begin{aligned} f_2(x) = & \frac{1}{\sqrt{4\beta_2^{\rm LAT}/\beta_0 - (\beta_1/\beta_0)^2}} \\ & \times \arctan\left(\frac{\sqrt{4\beta_2^{\rm LAT}/\beta_0 - (\beta_1/\beta_0)^2}\, x}{2 + (\beta_1/\beta_0) x}\right). \end{aligned} \tag{D12}$$

The explicit expression for $\gamma_1^{\rm LAT}$ has been given in Eq. (80). For the tadpole-improvement factor we make the ansatz

$$u_0^{1-n_D} \exp(c_1 f_1(g^2_{\rm LAT}/(16\pi^2)) + c_2 f_2(g^2_{\rm LAT}/(16\pi^2))) \tag{D13}$$

determining the coefficients c_1 and c_2 such that

$$\begin{aligned} & \exp(c_1 f_1(g^2_{\rm LAT}/(16\pi^2)) + c_2 f_2(g^2_{\rm LAT}/(16\pi^2))) \\ & \quad = u_0^{n_D - 1} + O(g^6_{\rm LAT}). \end{aligned} \tag{D14}$$

Then the final result in TRB perturbation theory reads

$$\begin{aligned} Z^{\rm RGI}_{\rm TRB} = & u_0^{1-n_D} \left(2\beta_0 \frac{g^2_{\rm LAT}}{16\pi^2}\right)^{-(\gamma_0/2\beta_0)} \exp\{\tilde{c}_1 f_1(g^2_{\rm LAT}/(16\pi^2)) \\ & + \tilde{c}_2 f_2(g^2_{\rm LAT}/(16\pi^2))\}, \end{aligned} \tag{D15}$$

with

$$\begin{aligned} \tilde{c}_1 = & \frac{\beta_2^{\rm LAT}\gamma_0 - \beta_0 \gamma_2^{\rm LAT}}{4\beta_0 \beta_2^{\rm LAT}} \\ & + (n_D - 1) \frac{\beta_0}{\beta_2^{\rm LAT}} \left(r_2^{\rm LAT} + \frac{r_1}{2}\frac{\beta_1}{\beta_0} - \frac{r_1^2}{2}\right), \end{aligned} \tag{D16}$$

$$\begin{aligned} \tilde{c}_2 = & \frac{\beta_1 \beta_2^{\rm LAT} \gamma_0 + \beta_0 \beta_1 \gamma_2^{\rm LAT} - 2\beta_0 \beta_2^{\rm LAT} \gamma_1^{\rm LAT}}{2\beta_0^2 \beta_2^{\rm LAT}} \\ & + 2(n_D - 1)\left(r_1 - \frac{\beta_1}{\beta_2^{\rm LAT}}\left(r_2^{\rm LAT} + \frac{r_1}{2}\frac{\beta_1}{\beta_0} - \frac{r_1^2}{2}\right)\right). \end{aligned} \tag{D17}$$

Finally we have to decide how to deal with $c_{\rm SW}$. We insert the one-loop expression [57,78,79]

$$c_{\rm SW} = 1 + 0.268588 g^2 + O(g^4) \tag{D18}$$

in the above expansions and reexpand the result in the coupling constant. This means that we set $c_{\rm SW} = 1$ in the one-loop coefficients and the two-loop coefficients get additional contributions proportional to the one-loop coefficient in the expansion of $c_{\rm SW}$.

APPENDIX E: FIT DETAILS

In this appendix we give the details of the fits applied in the cases where perturbatively subtracted data are available.

Working with the ℓ-loop approximation of the conversion factor $Z^{\mathcal{S}}_{\mathrm{RI}'\text{-MOM}}(M)$ we write generically

$$Z^{\mathcal{S}}_{\mathrm{RI}'\text{-MOM}}(M) = 1 + \sum_{i=1}^{\ell} c_i^{\mathcal{S}\mathcal{S}'} \left(\frac{g^{\mathcal{S}'}(M)^2}{16\pi^2}\right)^i + R^c_\ell(M)^{\mathcal{S}\mathcal{S}'} = Z^c_\ell(M)^{\mathcal{S}\mathcal{S}'} + R^c_\ell(M)^{\mathcal{S}\mathcal{S}'} \quad \text{(E1)}$$

with the remainder $R^c_\ell(M)^{\mathcal{S}\mathcal{S}'} = O(g^{\mathcal{S}'}(M)^{2\ell+2})$. The scheme $\mathcal{S}'$ chosen for the coupling in which $Z^{\mathcal{S}}_{\mathrm{RI}'\text{-MOM}}$ is expanded could be the $\overline{\mathrm{MS}}$ scheme as in Eqs. (56)–(58), but another option would be the $\widetilde{\mathrm{MOM}}$gg scheme.

Unfortunately, in many cases the perturbative expansion of $Z^{\mathcal{S}}_{\mathrm{RI}'\text{-MOM}}$ is not very well convergent, in particular, for $\mathcal{S} = \mathcal{S}' = \overline{\mathrm{MS}}$. However, if one chooses $\mathcal{S} = \mathrm{MOM}$, Z^c_3 turns out to be equal to 1 for $\mathcal{O}^S$, $\mathcal{O}^P$, $\mathcal{O}^T_{\mu\nu}$, $\mathcal{O}_{h_{1,a}}$, $\mathcal{O}_{h_{1,b}}$, $\mathcal{O}_{h_{2,a}}$, $\mathcal{O}_{h_{2,b}}$, $\mathcal{O}_{h_{2,c}}$, $\mathcal{O}_{h_{2,d}}$. Generally, the use of the $\widetilde{\mathrm{MOM}}$gg coupling seems to improve the convergence for $\mathcal{S} = \overline{\mathrm{MS}}$ as well as for $\mathcal{S} = \mathrm{MOM}$. Working with $\mathcal{S} = \mathrm{MOM}$ instead of $\mathcal{S} = \overline{\mathrm{MS}}$ seems to have the additional advantage that at least some of the effects of $Z^{\mathcal{S}}_{\mathrm{RI}'\text{-MOM}}$ are shifted to the factor $\Delta Z^{\mathcal{S}}$ via the anomalous dimension. In $\Delta Z^{\mathcal{S}}$ we can then exploit renormalization group improvement.

Similarly, using the n-loop approximation of the β function and the anomalous dimension we express $\Delta Z^{\mathcal{S}}(M)$ as

$$\Delta Z^{\mathcal{S}}(M) = \left(2\beta_0 \frac{g^{\mathcal{S}}(M)^2}{16\pi^2}\right)^{-(\gamma_0/2\beta_0)} \times \exp\left\{\int_0^{g^{\mathcal{S}}(M)^2/16\pi^2} \mathrm{d}x \times \frac{\sum_{i=0}^{n-2}(\beta_0\gamma^{\mathcal{S}}_{i+1} - \gamma_0\beta^{\mathcal{S}}_{i+1})x^i}{2\beta_0\sum_{i=0}^{n-1}\beta^{\mathcal{S}}_i x^i} + R^{\mathcal{S}}_n(M)\right\} = \Delta^{\mathcal{S}}_n(M)\mathrm{e}^{R^{\mathcal{S}}_n(M)} \quad \text{(E2)}$$

with $R^{\mathcal{S}}_n(M) = O(g^{\mathcal{S}}(M)^{2n})$. From the $\overline{\mathrm{MS}}$ anomalous dimension one can compute the anomalous dimension in the scheme $\mathcal{S}$ to n loops, provided the conversion factor $Z^{\overline{\mathrm{MS}}}_{\mathcal{S}}$ (and the β function) is known to $n-1$ loops; see Eqs. (64)–(66) for $\mathcal{S} = \mathrm{MOM}$.

With the help of the above representations of $Z^{\mathcal{S}}_{\mathrm{RI}'\text{-MOM}}$ and $\Delta Z^{\mathcal{S}}$ we get from Eq. (88)

$$(Z^c_\ell(\mu_p)^{\mathcal{S}\mathcal{S}'} + R^c_\ell(\mu_p)^{\mathcal{S}\mathcal{S}'}) Z^{\mathrm{RI}'\text{-MOM}}_{\mathrm{bare}}(\mu_p, a) = Z^{\mathrm{RGI}}(a)\Delta^{\mathcal{S}}_n(\mu_p)^{-1}\mathrm{e}^{-R^{\mathcal{S}}_n(\mu_p)}. \quad \text{(E3)}$$

In this relation as well as in Eq. (88) lattice artifacts vanishing like a power of a have been neglected. For larger values of μ_p this is not justified any more, even after perturbative subtraction of lattice artifacts. Therefore we write

$$Z^{\mathrm{RI}'\text{-MOM}}_{\mathrm{bare}}(\mu_p, a) = Z^{\mathrm{RI}'\text{-MOM}}_{\mathrm{bare}}(\mu_p, a)_{\mathrm{MC}} - A(a^2\mu_p^2), \quad \text{(E4)}$$

subtracting the (remaining) lattice artifacts A from the Monte Carlo data $Z^{\mathrm{RI}'\text{-MOM}}_{\mathrm{bare}}(\mu_p, a)_{\mathrm{MC}}$. Of course, A could be much more complicated than a simple function of $a^2\mu_p^2$, but in the end we have to restrict ourselves to a polynomial in $a^2\mu_p^2$ anyway. So we use this simplified expression already here for notational convenience and obtain

$$Z^c_\ell(\mu_p)^{\mathcal{S}\mathcal{S}'} Z^{\mathrm{RI}'\text{-MOM}}_{\mathrm{bare}}(\mu_p, a)_{\mathrm{MC}} = \frac{Z^{\mathrm{RGI}}(a)\Delta^{\mathcal{S}}_n(\mu_p)^{-1}\mathrm{e}^{-R^{\mathcal{S}}_n(\mu_p)}}{1 + R^c_\ell(\mu_p)^{\mathcal{S}\mathcal{S}'}/Z^c_\ell(\mu_p)^{\mathcal{S}\mathcal{S}'}} + Z^c_\ell(\mu_p)^{\mathcal{S}\mathcal{S}'} A(a^2\mu_p^2). \quad \text{(E5)}$$

Given that $Z^c_\ell(\mu_p)^{\mathcal{S}\mathcal{S}'} = 1 + O(g^{\mathcal{S}}(\mu_p)^2)$ we approximate this relation by

$$Z^c_\ell(\mu_p)^{\mathcal{S}\mathcal{S}'} Z^{\mathrm{RI}'\text{-MOM}}_{\mathrm{bare}}(\mu_p, a)_{\mathrm{MC}} = \frac{Z^{\mathrm{RGI}}(a)\Delta^{\mathcal{S}}_n(\mu_p)^{-1}\mathrm{e}^{-R^{\mathcal{S}}_n(\mu_p)}}{1 + R^c_\ell(\mu_p)^{\mathcal{S}\mathcal{S}'}} + A(a^2\mu_p^2). \quad \text{(E6)}$$

As we shall parametrize $(R^c_\ell)^{\mathcal{S}\mathcal{S}'}$, $R^{\mathcal{S}}_n$, and A in the following and fit the corresponding parameters, the above approximation should not be problematic. On the left-hand side we have our (possibly subtracted) Monte Carlo results for the renormalization factors, extrapolated to the chiral limit and converted to the intermediate scheme $\mathcal{S}$ using the ℓ-loop approximation. These numbers are fitted with the expression on the right-hand side, where the values of $Z^{\mathrm{RGI}}(a)$ at our four values of a are the desired numbers.

More precisely, we set

$$R^{\mathcal{S}}_n(\mu_p) = f_1 g^{\mathcal{S}}(\mu_p)^{2n} + f_2 g^{\mathcal{S}}(\mu_p)^{2n+2} + \cdots, \quad \text{(E7)}$$

$$R^c_\ell(\mu_p)^{\mathcal{S}\mathcal{S}'} = b_1 g^{\mathcal{S}'}(\mu_p)^{2\ell+2} + b_2 g^{\mathcal{S}'}(\mu_p)^{2\ell+4} + \cdots, \quad \text{(E8)}$$

$$A(a^2\mu_p^2) = g_1 a^2\mu_p^2 + g_2(a^2\mu_p^2)^2 + \cdots, \quad \text{(E9)}$$

where $b_1, f_1, \ldots$ are the (fit) parameters. Remember that in Sec. III we have argued that $O(a)$ lattice artifacts are absent. In principle, the coefficients $g_1, g_2, \ldots$ could depend on the coupling, i.e., on β. However, in the range of couplings we have at our disposal the variation of powers of a is much larger than the possible variation (logarithmic in a) of the coefficients. Therefore it seems justified to neglect this dependence and to treat $g_1, g_2, \ldots$ as constants. This might also help in disentangling lattice artifacts from truncation errors.

For the operators considered here, the $\overline{\mathrm{MS}}$ anomalous dimension is known to three loops, in some cases even to

four loops; see Appendix C. Upon combination with the four-loop β function one can thus reach at least $n = 3$. The conversion factors $Z^{\overline{\text{MS}}}_{\text{RI}'\text{-MOM}}$ and $Z^{\overline{\text{MS}}}_{\text{MOM}}$, on the other hand, are known to three loops in all cases.

There are quite a few parameters that can be varied in the analysis:

(1) the intermediate scheme $\mathcal{S}$;
(2) the scheme $\mathcal{S}'$ chosen for the coupling in which $Z^{\mathcal{S}}_{\text{RI}'\text{-MOM}}$ is expanded;
(3) the orders of the perturbative expansions used in (E6), i.e., the numbers n and ℓ;
(4) the order O_β of the perturbative expansion of the β function inserted in (49) when computing the running coupling $g^{\mathcal{S}}(M)$;
(5) the number of terms N_1, N_2, N_a taken into account in the correction terms (E7)–(E9), respectively; and
(6) the fit interval.

Ideally, the results should be independent of all these choices. Moreover, one would expect that a significant deviation from the "continuum limit" curve (obtained by setting $A = 0$) appears only for μ_p values where the data show lattice artifacts, e.g., in the form of a violation of the scaling property (89). Unfortunately, the fits of unsubtracted data do not follow this expectation, and this is the main reason why we consider the corresponding results as unreliable and do not apply our fit procedure to these data.

Our final choices are motivated by the following observations. The plateaus in Z^{RGI} look better for the choice $\mathcal{S} = \text{MOM}$ than for $\mathcal{S} = \overline{\text{MS}}$. This may be due to the above mentioned fact that the perturbative expansion of $Z^{\mathcal{S}}_{\text{RI}'\text{-MOM}}$ seems to be better behaved for $\mathcal{S} = \text{MOM}$. For the scheme $\mathcal{S}'$ the choice $\mathcal{S}' = \widetilde{\text{MOM}}\text{gg}$ seems to be favorable. For the operator $\bar{\mathcal{O}}_{h_{1,a}}$, a comparison between $\mathcal{S} = \mathcal{S}' = \overline{\text{MS}}$ and $\mathcal{S} = \text{MOM}$, $\mathcal{S}' = \widetilde{\text{MOM}}\text{gg}$ is shown in Fig. 10.

Not surprisingly, the maximal values for n and ℓ lead to the best plateaus. For the number of terms taken into account in (E7)–(E9) only 0 and 1 are reasonable choices.

As already mentioned, the perturbative behavior, i.e., the plateau starts only at rather large values of the scale, typically around $\mu_p^2 \approx 5\ \text{GeV}^2$. So the lower limit μ^2_{min} of the fit interval should be at least $5\ \text{GeV}^2$. However, the precise value does not seem to be too crucial, both $\mu^2_{\text{min}} = 5\ \text{GeV}^2$ and $\mu^2_{\text{min}} = 10\ \text{GeV}^2$ look reasonable.

So we arrive at the following choices. In the expansions originating from continuum perturbation theory which enter the fit formulas we use as many terms as are available, i.e., we take for n and ℓ the largest values possible. The same applies to O_β, so we set $O_\beta = 4$. We choose $\mathcal{S} = \text{MOM}$ and $\mathcal{S}' = \widetilde{\text{MOM}}\text{gg}$. All data for $\mu_p^2 \geq 10\ \text{GeV}^2$ are included in the fit. It is clear that the perturbative corrections (E7) and (E8) are hard to distinguish when inserted in (E6) and it does not make much sense to include both of them. So we set $N_1 = 0$ and $N_2 = 1$. Furthermore we choose $N_a = 1$. Hence we end up with six fit parameters: the four values $Z^{\text{RGI}}(a)$ along with the coefficients b_1 and g_1. The data points are weighted by their statistical errors although the deviations from the fit curves are mostly of systematic origin.

APPENDIX F: GOING FROM RGI RESULTS TO VALUES IN THE $\overline{\text{MS}}$ SCHEME

In this appendix we collect the factors by which one has to multiply Z^{RGI} in order to obtain the corresponding number in the $\overline{\text{MS}}$ scheme. They are given in Tables XI, XII, and XIII for various values of r_0 and $r_0\Lambda_{\overline{\text{MS}}}$.

TABLE XI. Factors for converting Z^{RGI} to the $\overline{\text{MS}}$ scheme obtained with $r_0 = 0.467$ fm and $r_0\Lambda_{\overline{\text{MS}}} = 0.617$.

Operator	$\mu^2 = 4\ \text{GeV}^2$	$\mu^2 = 5\ \text{GeV}^2$
$\mathcal{O}^S$, $\mathcal{O}^P$	1.40701	1.44044
$\mathcal{O}^T_{\mu\nu}$	0.91926	0.91089
Z_q	1.04534	1.04291
$\mathcal{O}_{v_{2,a}}$, $\mathcal{O}_{v_{2,b}}$, $\mathcal{O}_{r_{2,a}}$, $\mathcal{O}_{r_{2,b}}$	0.71544	0.70183
$\mathcal{O}_{h_{1,a}}$, $\mathcal{O}_{h_{1,b}}$	0.69538	0.68009
$\mathcal{O}_{v_3}$, $\mathcal{O}_{v_{3,a}}$, $\mathcal{O}_{a_2}$, $\mathcal{O}_{r_3}$	0.58648	0.56943
$\mathcal{O}_{h_{2,a}}$, $\mathcal{O}_{h_{2,b}}$, $\mathcal{O}_{h_{2,c}}$, $\mathcal{O}_{h_{2,d}}$	0.57878	0.56107
$\mathcal{O}_{v_4}$	0.50844	0.49008

TABLE XII. Factors for converting Z^{RGI} to the $\overline{\text{MS}}$ scheme obtained with $r_0 = 0.467$ fm and $r_0\Lambda_{\overline{\text{MS}}} = 0.662$.

Operator	$\mu^2 = 4\ \text{GeV}^2$	$\mu^2 = 5\ \text{GeV}^2$
$\mathcal{O}^S$, $\mathcal{O}^P$	1.38514	1.41952
$\mathcal{O}^T_{\mu\nu}$	0.92491	0.91609
Z_q	1.04704	1.04441
$\mathcal{O}_{v_{2,a}}$, $\mathcal{O}_{v_{2,b}}$, $\mathcal{O}_{r_{2,a}}$, $\mathcal{O}_{r_{2,b}}$	0.72464	0.71029
$\mathcal{O}_{h_{1,a}}$, $\mathcal{O}_{h_{1,b}}$	0.70575	0.68959
$\mathcal{O}_{v_3}$, $\mathcal{O}_{v_{3,a}}$, $\mathcal{O}_{a_2}$, $\mathcal{O}_{r_3}$	0.59809	0.58001
$\mathcal{O}_{h_{2,a}}$, $\mathcal{O}_{h_{2,b}}$, $\mathcal{O}_{h_{2,c}}$, $\mathcal{O}_{h_{2,d}}$	0.59085	0.57205
$\mathcal{O}_{v_4}$	0.52100	0.50145

TABLE XIII. Factors for converting Z^{RGI} to the $\overline{\text{MS}}$ scheme obtained with $r_0 = 0.5$ fm and $r_0\Lambda_{\overline{\text{MS}}} = 0.617$.

Operator	$\mu^2 = 4\ \text{GeV}^2$	$\mu^2 = 5\ \text{GeV}^2$
$\mathcal{O}^S$, $\mathcal{O}^P$	1.42764	1.46022
$\mathcal{O}^T_{\mu\nu}$	0.91406	0.90608
Z_q	1.04382	1.04155
$\mathcal{O}_{v_{2,a}}$, $\mathcal{O}_{v_{2,b}}$, $\mathcal{O}_{r_{2,a}}$, $\mathcal{O}_{r_{2,b}}$	0.70698	0.69402
$\mathcal{O}_{h_{1,a}}$, $\mathcal{O}_{h_{1,b}}$	0.68587	0.67134
$\mathcal{O}_{v_3}$, $\mathcal{O}_{v_{3,a}}$, $\mathcal{O}_{a_2}$, $\mathcal{O}_{r_3}$	0.57587	0.55972
$\mathcal{O}_{h_{2,a}}$, $\mathcal{O}_{h_{2,b}}$, $\mathcal{O}_{h_{2,c}}$, $\mathcal{O}_{h_{2,d}}$	0.56775	0.55100
$\mathcal{O}_{v_4}$	0.49699	0.47969

[1] S. Capitani, Phys. Rep. **382**, 113 (2003).
[2] Q. Mason, H. Trottier, and R. Horgan, Proc. Sci., LAT2005 (2006) 011.
[3] A. Skouroupathis and H. Panagopoulos, Phys. Rev. D **76**, 094514 (2007); **78**, 119901(E) (2008).
[4] A. Skouroupathis and H. Panagopoulos, Phys. Rev. D **79**, 094508 (2009).
[5] G. P. Lepage and P. B. Mackenzie, Phys. Rev. D **48**, 2250 (1993).
[6] M. Bochicchio *et al.*, Nucl. Phys. **B262**, 331 (1985).
[7] M. Lüscher, R. Narayanan, P. Weisz, and U. Wolff, Nucl. Phys. **B384**, 168 (1992).
[8] K. Jansen *et al.*, Phys. Lett. B **372**, 275 (1996).
[9] R. Sommer, arXiv:hep-ph/9711243.
[10] R. Sommer, arXiv:hep-lat/0611020.
[11] G. Martinelli *et al.*, Nucl. Phys. **B445**, 81 (1995).
[12] M. Göckeler *et al.*, Nucl. Phys. **B544**, 699 (1999).
[13] M. Göckeler *et al.* (QCDSF Collaboration), Phys. Rev. D **71**, 114511 (2005).
[14] M. Göckeler *et al.* (QCDSF/UKQCD Collaborations), Phys. Lett. B **639**, 307 (2006).
[15] P. E. L. Rakow, Nucl. Phys. B, Proc. Suppl. **140**, 34 (2005).
[16] S. Capitani and G. Rossi, Nucl. Phys. **B433**, 351 (1995).
[17] G. Beccarini, M. Bianchi, S. Capitani, and G. Rossi, Nucl. Phys. **B456**, 271 (1995).
[18] M. Göckeler *et al.*, Phys. Rev. D **54**, 5705 (1996).
[19] M. Göckeler *et al.*, Nucl. Phys. **B472**, 309 (1996).
[20] M. Göckeler, unpublished notes.
[21] J. E. Mandula and M. Ogilvie, Phys. Lett. B **185**, 127 (1987).
[22] We thank F. Niedermayer for drawing our attention to this point.
[23] B. Efron, *The Jackknife, the Bootstrap and Other Resampling Plans* (SIAM, Philadelphia, 1982).
[24] M. H. Quenouille, Biometrika **43**, 353 (1956).
[25] M. L. Paciello, S. Petrarca, B. Taglienti, and A. Vladikas, Phys. Lett. B **341**, 187 (1994).
[26] L. Giusti, S. Petrarca, B. Taglienti, and N. Tantalo, Phys. Lett. B **541**, 350 (2002).
[27] C. Gattringer, M. Göckeler, P. Huber, and C. B. Lang, Nucl. Phys. **B694**, 170 (2004).
[28] F. de Soto and C. Roiesnel, J. High Energy Phys. 09 (2007) 007.
[29] P. Boucaud *et al.*, Phys. Lett. B **575**, 256 (2003).
[30] V. Maillart and F. Niedermayer, arXiv:0807.0030.
[31] S. Capitani *et al.*, Nucl. Phys. **B593**, 183 (2001).
[32] M. Göckeler *et al.*, Phys. Rev. D **73**, 014513 (2006).
[33] J. R. Cudell, A. Le Yaouanc, and C. Pittori, Phys. Lett. B **454**, 105 (1999).
[34] K. D. Lane, Phys. Rev. D **10**, 2605 (1974).
[35] H. Pagels, Phys. Rev. D **19**, 3080 (1979).
[36] K. G. Chetyrkin and A. Rétey, arXiv:hep-ph/0007088.
[37] M. Göckeler *et al.*, Eur. Phys. J. C **48**, 523 (2006).
[38] S. Capitani (private communication).
[39] S. Capitani, Nucl. Phys. **B597**, 313 (2001).
[40] S. Capitani *et al.* (QCDSF Collaboration), Nucl. Phys. B, Proc. Suppl. **106-107**, 299 (2002).
[41] M. Lüscher and P. Weisz, Phys. Lett. B **349**, 165 (1995).
[42] A. Bode, P. Weisz, and U. Wolff (ALPHA Collaboration), Nucl. Phys. **B576**, 517 (2000); **B600**, 453(E) (2001); **B608**, 481(E) (2001).
[43] C. Christou, A. Feo, H. Panagopoulos, and E. Vicari, Nucl. Phys. **B525**, 387 (1998); **B608**, 479(E) (2001).
[44] A. Bode and H. Panagopoulos, Nucl. Phys. **B625**, 198 (2002).
[45] D. Bećirević *et al.*, J. High Energy Phys. 08 (2004) 022.
[46] P. V. Landshoff, Acta Phys. Pol. B **40**, 1967 (2009).
[47] We thank M. Stratmann for a discussion of this issue.
[48] D. Bećirević *et al.*, Phys. Rev. D **60**, 094509 (1999).
[49] D. Bećirević *et al.*, Phys. Rev. D **61**, 114508 (2000).
[50] A. Ali Khan *et al.*, Phys. Rev. D **74**, 094508 (2006).
[51] C. Aubin *et al.*, Phys. Rev. D **70**, 094505 (2004).
[52] C. T. H. Davies *et al.* (HPQCD Collaboration), Phys. Rev. D **81**, 034506 (2010).
[53] M. Della Morte *et al.* (ALPHA Collaboration), Nucl. Phys. **B713**, 378 (2005).
[54] See F. James, MINUIT Function Minimization and Error Analysis Reference Manual, http://wwwinfo.cern.ch/asdoc/minuit/minmain.html.
[55] G. Martinelli *et al.*, Nucl. Phys. **B611**, 311 (2001).
[56] S. R. Sharpe, Nucl. Phys. B, Proc. Suppl. **106-107**, 817 (2002).
[57] R. Horsley *et al.*, Phys. Rev. D **78**, 054504 (2008).
[58] A. Athenodorou, H. Panagopoulos, and A. Tsapalis, Phys. Lett. B **659**, 252 (2008).
[59] M. Della Morte, R. Sommer, and S. Takeda, Phys. Lett. B **672**, 407 (2009).
[60] T. Bakeyev *et al.* (QCDSF/UKQCD Collaborations), Phys. Lett. B **580**, 197 (2004).
[61] M. Della Morte *et al.*, J. High Energy Phys. 07 (2005) 007.
[62] M. Göckeler *et al.*, Phys. Rev. D **73**, 054508 (2006).
[63] M. Constantinou, V. Lubicz, H. Panagopoulos, and F. Stylianou, J. High Energy Phys. 10 (2009) 064.
[64] V. Giménez *et al.*, Phys. Lett. B **598**, 227 (2004).
[65] Y. Aoki *et al.*, Phys. Rev. D **78**, 054510 (2008).
[66] Y. Aoki (RBC Collaboration and UKQCD Collaboration), Proc. Sci., LATTICE2008 (2008) 222.
[67] C. Sturm *et al.*, Phys. Rev. D **80**, 014501 (2009).
[68] T. van Ritbergen, J. A. M. Vermaseren, and S. A. Larin, Phys. Lett. B **400**, 379 (1997).
[69] J. A. M. Vermaseren, S. A. Larin, and T. van Ritbergen, Phys. Lett. B **405**, 327 (1997).
[70] K. G. Chetyrkin, Phys. Lett. B **404**, 161 (1997).
[71] J. A. Gracey, Phys. Lett. B **488**, 175 (2000).
[72] S. A. Larin, T. van Ritbergen, and J. A. M. Vermaseren, Nucl. Phys. **B427**, 41 (1994).
[73] A. Rétey and J. A. M. Vermaseren, Nucl. Phys. **B604**, 281 (2001).
[74] J. A. Gracey, Nucl. Phys. **B667**, 242 (2003).
[75] J. A. Gracey, J. High Energy Phys. 10 (2006) 040.
[76] K. G. Chetyrkin and A. Rétey, Nucl. Phys. **B583**, 3 (2000).
[77] J. A. Gracey, Nucl. Phys. **B662**, 247 (2003).
[78] S. Naik, Phys. Lett. B **311**, 230 (1993).
[79] M. Lüscher and P. Weisz, Nucl. Phys. **B479**, 429 (1996).